Hernandez, Humberto., Crosstalk Between Transforming Growth Factor Beta-2 and Toll-Like Receptor 4 in the Trabecular Meshwork. Doctor of Philosophy (Visual Science), November, 2017, 166 pp., 3 tables, 31 illustrations, bibliography, 422 titles.

The trabecular meshwork (TM) is the main site of outflow resistance in primary-open angle glaucoma (POAG) patients. In these patients, aqueous humor outflow resistance increases, subsequently leading to a rise in intraocular pressure (IOP). The rise in IOP ultimately damages the optic nerve and leads to blindness. Accumulation of extracellular matrix (ECM) at the TM has been shown by our laboratory and many others to be responsible for the increase in outflow resistance. The molecular mechanisms underlying the pathology are beginning to be elucidated. The pro-fibrotic cytokine, transforming growth factor beta-2 (TGFβ2), has been shown to be elevated in the aqueous humor of POAG patients. Mice injected with adenovirus encoding active TGFβ2 develop ocular hypertension and ECM deposition at the TM. Recently, toll-like receptor 4 (TLR4) signaling has been linked to the development of fibrosis. In our studies, we evaluated the crosstalk between TGFβ2 and TLR4 in the TM. We utilized *in vitro* and *in vivo* models to evaluate the role of TLR4 on the production of ECM and development of ocular hypertension. We also utilized a conditional knockout *in vitro* and *in vivo* adenovirus delivery system to study BMP and Activin Membrane Bound Inhibitor (BAMBI), a critical molecule in the crosstalk between TGFβ2 and TLR4. Our studies reveal a novel pathway involved in the development of TM damage and potential targets to lower IOP.

CROSSTALK BETWEEN TRANSFORMING GROWTH FACTOR BETA-2 AND TOLL-LIKE RECEPTOR 4 IN THE TRABECULAR MESHWORK

Humberto Hernandez, B.S.

APPROVED:

_____

Abbot F. Clark, Ph.D., Major Professor

_____

Colleen McDowell, Ph.D., Major Professor

_____

Iok-Hou Pang, Ph.D., Committee Member

_____

Cameron Millar, Ph.D., Committee Member

_____

Weiming Mao, Ph.D., Committee Member

_____

Alakananda Basu, Ph.D., University Member

_____

Abbot F. Clark, Ph.D., Director of NTERI

_____

Johnny He, Ph.D., Dean, Graduate School of Biomedical Science

CROSSTALK BETWEEN TRANSFORMING GROWTH FACTOR BETA-2 AND TOLL-LIKE RECEPTOR 4 IN THE TRABECULAR MESHWORK

DISSERTATION

Presented to the Graduate Council of the

Graduate School of Biomedical Sciences

University of North Texas

Health Science Center at Fort Worth

in Partial Fulfillment of the Requirements

For the Degree of

DOCTOR OF PHILOSOPHY

By

Humberto Hernandez, B.S.

Fort Worth, Texas

November 2017

ACKNOWLEDGEMENTS

I would like to express my gratitude towards my mentors Dr. Abbot F. Clark and Dr. Colleen M. McDowell for their support and guidance throughout my Ph.D. training. Without your unconditional support, none of this would have been possible. Dr. Clark's student oriented personally, patience, and enthusiasm in my work have provided me with strength to complete my dissertation. Your continued presence in the laboratory bench and excitement in developing graduate students is an inspiration to me. I am very grateful for the vision screening opportunities that were readily available to me, I always felt a great reward when giving back to the community. It is these qualities and many others that make Dr. Clark a role model for graduate students. Throughout my Ph.D., Dr. McDowell has always kept an open mind. I truly appreciate those scientific conversations that lead to great discoveries. The constant reminder that I was "very close" to completing a study gave me hope and trust in myself. I will most notably remember those eureka moments we shared. The knowledge and skills you shared were indispensable to the development of my projects. I could not have found better mentors to undertake this great challenge.

I also would like to express my gratitude to my committee and university member. Dr. Iok-Hou Pang's words of wisdom and constructive criticism always left me with a strong feeling of self-assurance. The constant positive feedback and encouragement I always appreciated. Dr. Cameron Millar's sense of humor, support, experimental expertise, and love for teaching both in the bench and classroom I most truly enjoyed. Dr. Weiming Mao's guidance as a graduate adviser and availability were of the most exemplary. Dr. Alakananda Basu's exceptional support, suggestions, and interest in my work far surpassed the requirements of any committee member.

To the past and current lab members of the NTERI family, your support, knowledge and constructive criticism helped my development as a scientist. I would like to thank Dr. Clark and students (Gaurang, Avany, Dr. Silverman), Dr. McDowell and students (Steffi and Amanda), Dr. Weiming Mao and his students (Drs. Webber and Bermudez), Dr. Tara Tovar-Vidales and student (Navita), and Dr. Yang Liu and student (Elliot) for providing a nurturing working environment in the laboratory.

I also thank past teachers, coaches, and mentors for helping shape the person and scientist that I am. Specifically, I would like to thank Mr. Ibe (mathematics), Mrs. Hawkins (biology), and Mrs. Rice (athletics) for believing in my intellectual capacity. Dr. Randall Terry (plant genetics) for giving me the opportunity to fail and succeed experimentally as I developed independence in the laboratory. Dr. Ashwini Kucknoor (microbiology, immunology, and molecular biology) for being my friend, teacher, colleague, motivator and lifelong mentor. Dr. Kucknoor's support, guidance, passion and excitement for science continues to inspire me. Dr. Barry Rockx (virology) for believing in my scientific and intellectual capacities. The time spent in your laboratories was fundamental in my development both as a person and scientist. Ms. Daniella Medley (McNair Scholar's program), Dr. David Niesel (Post-Baccalaureate Research Education

Program (PREP)), and Dr. Meharvan Singh (Neurobiology of Aging Predoctoral Program) for their support in every stage of my academic and scientific career.

Lastly, I would like to thank my family and friends for their unconditional support. Most importantly, I would like to give my deepest appreciation to my loving wife Samantha. You have scarified and have endured long periods of time in my absence. You have stood next to me every step of the way, sacrificing time away from our friends and love ones. To my parents (Arturo and Maria), brothers (Arthur and Erick), sister (Reyna), in-laws (Octavio and Elvia) and brother/sister in-laws (Alex and Leslie), thank you so much for all your love and understanding. Finally, I dedicate this dissertation to my loving wife Samantha and future children, you are the reason I stand here today.

TABLE OF CONTENTS

PAGE

LIST OF ILLUSTRATRATIONS

PAGE

CHAPTER I

CHAPTER II

CHAPTER IV

LIST OF TABLES

PAGE

CHAPTER I

INTRODUCTION

Glaucoma

The glaucoma's are a heterogeneous group of optic neuropathies that ultimately lead to damage at the optic nerve head and blindness. It is estimated that approximately 70 million individuals are affected by glaucoma worldwide[1]. In the United states, the most prevalent form of glaucoma is primary open angle glaucoma (POAG), with an estimated 80% of all cases[2]. In this form of glaucoma there are defects in the conventional outflow pathway that elevates intraocular pressure (IOP) (Figure 1). The obstruction of aqueous humor outflow by excessive accumulation of ECM material at the TM is implicated to be responsible for aqueous humor outflow resistance. Recent advances in the understanding of the pathology have given insight into the molecular changes undergoing at the trabecular meshwork (TM).

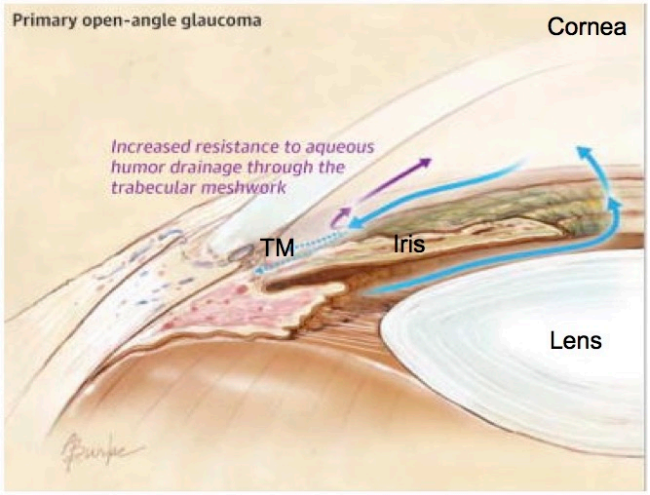

Figure 1. Primary open-angle glaucoma. Aqueous humor produced by the ciliary processes of the ciliary body travel from the posterior to the anterior chamber and exits through the TM.

Accumulation of ECM proteins increase outflow resistance and elevates IOP. **Adopted from Madeiros et al., 2014.**

Optic nerve degeneration

In the posterior segment of the eye, the optic disk is the region where retinal ganglion cell (RGCs) axons exit the eye. The rise in IOP leads to mechanical stress and strain on the lamina cribrosa (LC), leading to apoptotic degeneration of RGCs. Up to 50% of RGCs can be lost before visual field changes are detected[3, 4]. These changes at the LC are also accompanied by molecular and functional changes to resident astrocytes and microglia, and remodeling of the extracellular matrix (ECM). Activated astrocytes and microglia can also produce pro-inflammatory cytokines and proteins (TNF-α, inducible nitric oxide synthase (iNOS), interleukin-1 (IL-1), amongst others), which contribute to RGC death[5-10]. Elevation in IOP leads to remodeling of the LC ECM, which disrupts the nutritional and mechanical support to RGC axons. The LC region contains ECM proteins such as elastin and collagens[11]. Optic nerve head (ONH) astrocytes and LC cells are responsible for ECM remodeling[12-14]. Recently, Zode and colleagues demonstrated that optic nerve head astrocytes respond to transforming growth factor beta-2 (TGFβ2) by increasing ECM[15]. These findings suggest that similar pathogenic processes occurring at the trabecular meshwork (TM) are also occurring at the ONH. Future studies in the field of the ONH degeneration will likely focus on the effects of ECM and their signaling capacity on LC, ONH astrocytes, and RGCs.

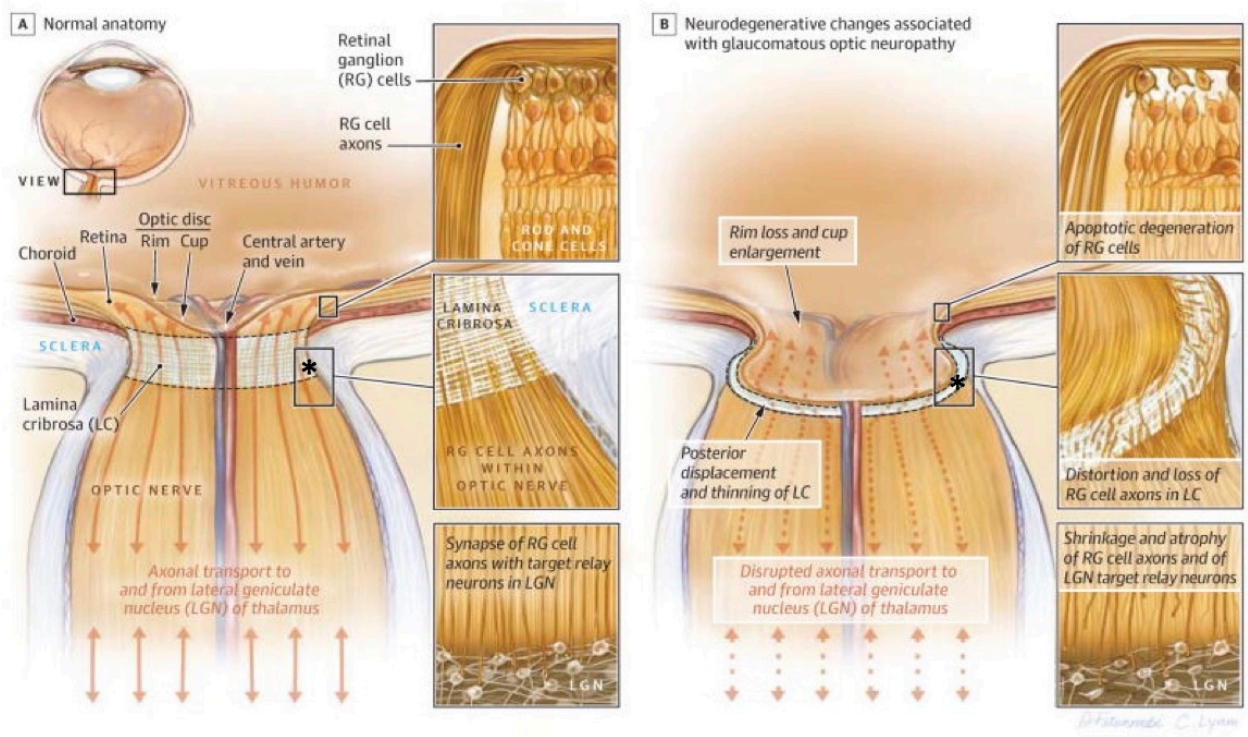

Figure 2. Normal and neurodegenerative chances at the optic nerve head. (A) RGC axons exit the eye through the lamina cribrosa, forming the optic nerve, and travel to the left and right lateral geniculate nucleus (LGN). (B) Elevation in IOP leads to damage and remodeling of the optic nerve disk. **Adopted from Weinreb et al., 2014.**

Aqueous humor

Aqueous humor is responsible for providing nutrients to the avascular structures, the cornea and lens, of the eyes. Apart from providing nutrients, it is responsible for maintaining IOP at normal physiological levels, 10 – 15 mmHg above ambient air pressure. In non-pathological conditions, aqueous humor undergoes constant turnover. The ciliary processes of the ciliary body secrete aqueous humor, reaching the anterior chamber through the pupil. Aqueous humor leaves the eye at the iridocorneal angle through a process called aqueous humor outflow. This process includes the trabecular and uveoscleral pathways, also termed conventional and nonconventional

pathways (Figure 3.). In humans, the conventional or trabecular pathway plays the greatest role in outflow. Although the unconventional pathway plays a minor role, it is the target of antiglaucoma drugs such. Drugs that target POAG usually involve either decreasing the production rate of aqueous humor in the ciliary body, or increase the uveoscleral outflow rate.

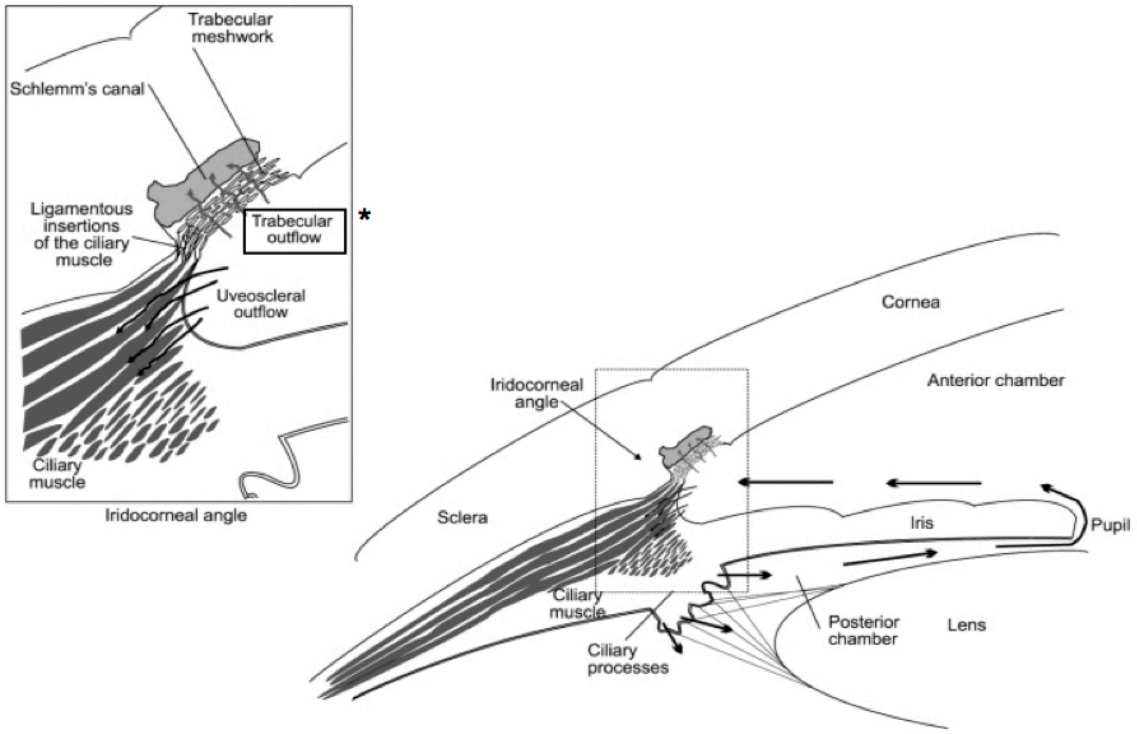

Figure 3. Schematic diagram of the aqueous humor cycle. The aqueous humor is formed in the ciliary processes from arterial blood. It is secreted to the posterior chamber and reaches the anterior chamber by crossing the pupil. The inset shows the outflow pathways. Aqueous humor exits the anterior chamber via two routes: the uveoscleral or nonconventional outflow pathway and the trabecular or conventional pathway, which comprises the trabecular meshwork (TM) and Schlemm's canal. **Figure adopted from Llobet et al., 2003.**

Trabecular meshwork

The TM is the tissue at the irido-corneal angle of the eye and is the main regulator of intraocular pressure. The structure of the trabecular meshwork is composed of beams and sheets of cell layers and is the main drainage pathway of aqueous humor from the eye. It is composed of three layers, the uveal meshwork, corneal scleral meshwork, and the juxtacanalicular tissue (JCT). The direction of aqueous humor outflow begins at the uveal meshwork intercellular spaces, followed by the corneal scleral meshwork, and finally the JCT region. The outermost region closest to the anterior chamber is the uveal meshwork. The uveal meshwork region is where the filtration system for aqueous humor begins and outflow resistance is generated. Due to its large intercellular spaces, the uveal meshwork does not offer great outflow resistance. The corneoscleral meshwork contains collagens, hyaluronic acid, and elastic fibers. Due to the high organization of the corneoscleral meshwork and narrow intercellular spaces, this region of the TM generates a certain amount of outflow resistance. The JCT region, hoever, offers the highest resistance due to its direct contact with the inner wall of endothelial cells from Schlemm's canal, the presence of dense ECM, and narrow intercellular spaces. Figure 4 illustrates the direction of aqueous humor through its TM regions and Schlemm's canal. In POAG patients, IOP is elevated and aqueous humor outflow resistance increases. Increase in aqueous humor outflow resistance at the TM has been associated with the development of ECM deposition which alters the ability of aqueous humor to leave the eye through the trabecular meshwork, leading to the necessity for higher intraocular pressure to drive aqueous humor across the TM. The development of ECM deposition has been linked to the alterations in cytokine production in the aqueous humor and trabecular meshwork.

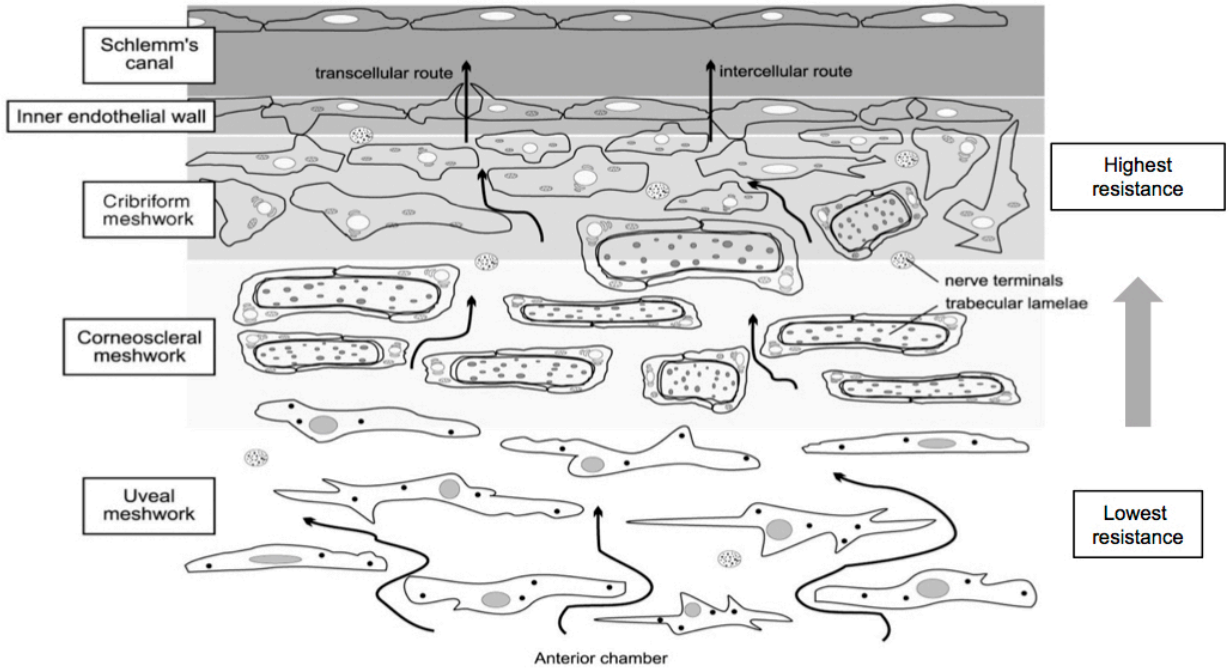

Figure 4. Direction of the aqueous humor from the anterior chamber toward Schlemm's canal. The regions of the TM are the uveal meshwork, corneoscleral meshwork, juxtacanalicular or cribriform meshwork, and Schlemm's canal. Aqueous humor flows through the intercellular spaces of the TM and crosses the inner wall of Schlemm's canal via two different mechanisms: an intercellular route and a transcellular route. Resistance to aqueous humor flow increases progressively from the anterior chamber to the inner wall of Schlemm's canal as intercellular spaces narrow. **Figure adopted from Llobet et al., 2003.**

Trabecular meshwork cells in culture

The use of TM cells to study the associated pathological signaling pathways has been invaluable to the understanding of glaucoma[16]. The first cultures were obtained from tissue culture explants[17-22]. Many TM cultures have been isolated from different species; human[17, 18, 20, 22-40], mouse[41-43], nonhuman primates[23, 44-49], porcine[50], and bovine[21, 47, 51-74]. Due to the accessibility of

bovine eyes, important discoveries of TM physiology have been made in this species. Human TM cultures have been successfully established since the 1970's[20]. A transformed human TM cell line was developed by Pang and colleagues (HTM-3), allowing for faster biochemical and pharmacological studies[75]. However, all discoveries made in TM cells from other species and transformed TM cells should be verified in primary human TM cells. With recent advances in mouse genetics, TM isolation from transgenic mice will be more readily performed. Mao and colleagues formulated a procedure by which TM cells can be isolated using intracameral injections of magnetic beads[43]. Taking advantage of the phagocytic properties of TM cells, pure cultures can be obtained. In chapter III, we utilized the magnetic bead isolation protocol to elucidate the contribution of BMP and Activin Membrane Bound Inhibitor (BAMBI) to ECM regulation in TM cells in culture.

Characterization of trabecular meshwork cells

Isolation of TM cells opened the door for *in vitro* studies. Evaluation of the function and properties of these cells could now be studied. For the first time, glaucoma associated molecules could be evaluated in conjunction with potential therapeutic drugs. After isolation, TM cell strains should be characterized. Interestingly, TM cells express protein markers that are shared by different cell types[16]. To date, few specific markers have been found that distinguish TM cells from its neighboring cell types. Instead, a panel of proteins are used to identify TM cells. The expression profile of TM cells makes them unique as they share properties similar to that of endothelium, macrophages, fibroblasts, and muscle cells[16]. For this reason, identification of TM cells has focus on a combination of markers and induction of these using glucocorticoids and TGFβ2. The characterization of TM cells has been extensively described [42, 68, 75-77]. TM cells

express matrix metalloproteases (MMPs), tenascin C, and alpha-smooth muscle actin, all of which are typically only expressed in tissues undergoing active remodeling[35, 78-82]. The presence of these proteins in the TM in a resting state indicates that the TM may have properties that allow it to undergo transient tissue repair. The first gene to be identified as a marker for TM cells was *Myocilin* (MYOC)[83]. This gene was initially termed TIGR (trabecular meshwork inducible GC response) due its inducibility with glucocorticoids. Clark and colleagues further identified the formation of cross-linked actin networks (CLANs) due to glucocorticoid treatment[38]. Soon after, changes in the ECM were observed in glucocorticoid treated TM cells in culture[84, 85] and tissue[86]. The effects of TGFβ2 on TM cells were also similar to those observed in glucocorticoid treated cells[54]. In chapter II and chapter III, all cell strains were previously characterized using the methods stated above.

Anterior segment perfusion organ culture

Development of the human anterior segment organ culture system has enabled investigators to translate the findings found on the cell culture system[87-102]. This technique was first developed by Johnson and Tschumper and allowed for the study of the TM under control experimental conditions[102]. Investigators using the organ culture system soon found changes in the ECM in dexamethasone treated eyes, confirming the observations found in the cell culture system[90, 96, 97, 101]. The development of an anterior segment organ culture system has not been limited to the human culture system, other species that have been developed and include the porcine[94, 103], bovine[90, 93] and non-human primates[87]. Using this system, novel signaling pathways and compounds can be tested for their efficacy in inducing ocular hypertension.

Animal models of ocular hypertension

There are many inducible and genetic models of ocular hypertension that investigators use to study the pathogenesis of glaucoma[104-116]. Some of these models are intraocular pressure dependent and others are intraocular pressure independent. Naturally occurring ocular hypertensive models have been observed in a Puerto Rican colony of rhesus monkey[114]. This colony was a novelty at the time it was discovered. Gaasterland and Kupfer developed an experimental monkey model using argon laser photocoagulation[117]. Using this model, IOP values could be obtained between 24 and 50 mmHg after the 4th treatment and remained elevated for 25 days. A tree shrew (*Tupaia glis belangeri*) model of ocular hypertension has been developed using the bead occlusion method[118] by Samuels and colleagues (unpublished). The IOP from these animals remains substantially elevated through eight months. The DBA/2J mouse develops progressive increase of IOP[119] due to iris abnormalities and pigment shedding related to mutations in *Gpnmb* and *Tyrp1*[120, 121]. Mutations and changes in other genes have been observed such as the *LTBP2* in feline[122], *Col1a1*[123], Y437H MYOC[124], *Sh3pxd2b*[125], and sGCalpha1 KO[126] in mice. Rats have also been used to study the development of ocular hypertension and optic nerve degeneration. In Brown Norway rats, saline injections in the episcleral vein have been shown to sustain IOP elevations after 4 weeks[127]. However, cauterization of the episcleral veins has been shown to increase IOP to 53 mmHg[128]. In Wistar rats, microbeads injections increase IOP to 29.7 mmHg and remain stable for 13 days[129]. The microbead injection method has also been shown to be effective in mice[129]. Glucocorticoids have also been used to study glucocorticoid induction of ocular hypertension (GC-OHT)[106].

Whitlock and colleagues were the first to develop a mouse model of GC-OHT[130]. This model was used to deliver DEX systemically to mice, with IOP elevation reaching only 3 to 4 mmHg by 3 weeks. Topical administration of DEX (.1%) was later shown to increase to 7.7 mmHg at 6 weeks by Zode and colleagues[131]. Patel and colleagues developed a model of GC-OHT by periocular conjunctival fornix injections of dexamethasone-21-acetate (DEX-Ac) injections[132]. Using this model, expression of fibronectin, collagen-1, and α-smooth muscle actin was observed in the TM of mouse eyes. Recently, adenovirus gene transfer has been utilized for elevating intraocular pressure in rodents[133, 134]. Using this model, the TM tissue of mice eyes can be transduced and intraocular pressure elevated. For example, over-expression of the bioactivated form of human TGFβ2 has been shown in mouse eyes to cause ocular hypertension[134-136]. Other transgenes that have also elevated IOP and include MYOC, SFRP1, DKK1, GREM1, and CD44[137]. Recently, the use of this system has been shown to increase the anterior segment pressure (ASP) using adenovirus transduction of the rhesus monkey TM with the *COCH* gene[87]. In chapter III, the adenovirus transduction system was utilized to evaluate knockdown of a regulatory protein of TGFβ2. Bouhenni and colleagues and table 1 provide an overview of animal models of glaucoma[109].

Glaucoma type	Animal	Model mode, mechanism
POAG	Monkey	Spontaneous inheritance
		Laser photocoagulation of entire TM, reduced outflow by PAS
		Intracameral injection of latex microspheres, TM blockage
		Intracameral injection of autologous fixed red blood cells, TM blockage
	Dog	Spontaneous inheritance
	Mouse	Transgenic, Myoc mutation
		Transgenic, alpha-1 subunit of collagen type I
	Rat	Topical application of dexamethasone
	Zebrafish	Transgenic, *bug eye* mutant
		Transgenic, *Irp2* mutation
		Transgenic, *wdr36* mutation
	Rabbit	Subconjunctival injection of betamethasone
		Posterior chamber injection of α-chymotrypsin, TM blockage
	Sheep	Topical application of prednisolone
	Cow	Topical application of prednisolone
	Birds	Constant Light-induced, reduced outflow facility
PACG	Dog	Spontaneous inheritance
	Turkey	Spontaneous inheritance
	Rat	Episcleral vein injection of saline, obstruction of outflow
		Injection of polystyrene microbeads or hyaluronic acid, TM blockage
		Cauterization of episcleral veins, reduced outflow by PAS
		Ligation of episcleral veins, obstruction of outflow
		Laser photocoagulation of translimbal region, reduced outflow by PAS
	Mouse	Transgenic, *Vav2/Vav3* knockout
		Laser photocoagulation of episcleral veins, reduced outflow by PAS
		Cauterization of episcleral veins, reduced outflow by PAS
	Rabbit	Water loading, decreased outflow facility
		Laser photocoagulation of TM, obstruction of outflow
PCG	Rabbit	Spontaneous inheritance
	Rat	Spontaneous inheritance, WAG strain
		Spontaneous inheritance, RCS strain
	Cat	Spontaneous inheritance
	Mouse	Transgenic, *Cyp1b1* mutation
		Transgenic, *Cyp1b1* and Tyr mutations
	Quail	Spontaneous inheritance, al mutant
Normal tension	Mouse	Transgenic, *Glast* or *Eaac1* mutation
Autoimmune	Rat	Immunization against HSP27 and HSP60, RGC loss
Pigmentary	Mouse	DBA/2J strain, Gpnmb, and Tyrp1 mutation

Table 1: Summary of the animal models commonly used for glaucoma research. **Adapted from Bouhenni et al., 2012**.

Transforming growth factor β2

TGFβ2 is a pro-fibrotic cytokine associated with the development of ocular hypertension[134-136] and fibrogenesis. The glaucomatous eye has been shown to have TGFβ2 levels as high as 2.7 ng/ml compared to 1.48 ng/ml in normal eyes[138]. POAG aqueous humor samples have been shown to have a mean concentration of bioactivated TGFβ2 higher than (pseudo) exfoliation syndrome (EXS), primary angle-closure glaucoma (PACG) and uveitis-related secondary glaucoma (SG) eyes[139]. Similarly, aqueous humor concentration of total TGFβ2 was significantly higher in glaucomatous and older eyes compared to non-glaucomatous eyes[140]. These and other studies show that TGFβ2 levels are elevated in the aqueous humor samples of POAG patients[138-143]. TGFβ2 signals both through the canonical and non-canonical SMAD signaling pathways[144-146]. The canonical SMAD pathway has been shown to be essential for TGFβ2-induced ocular hypertension in mice[147-150]. TGFβ2 binds type II receptors (TGFβRII), after which assembles, activates, and phosphorylates type I receptors (TGFβRI). Activated TGFβRI subsequently phosphorylates SMAD2/3 and leads to the association of SMAD4 into the complex. This complex interacts with coactivators or corepressors to regulate gene transcription. TGFβ2 signaling via the non-canonical SMAD signaling pathway has been shown to involve p38, ERK and JNK [144-146]. Both the canonical[151-157] and non-conical SMAD[154, 158] signaling pathways have been shown to occur in the TM[159]. Of interest, TGFβ2 has been shown to have an effect on ECM synthesis in primary NTM and GTM cell strains[54, 153, 154, 160-162]. Figure 5 shows a representation of the TGFβ signaling pathway and regulation of ECM crosslinking enzymes in the TM.

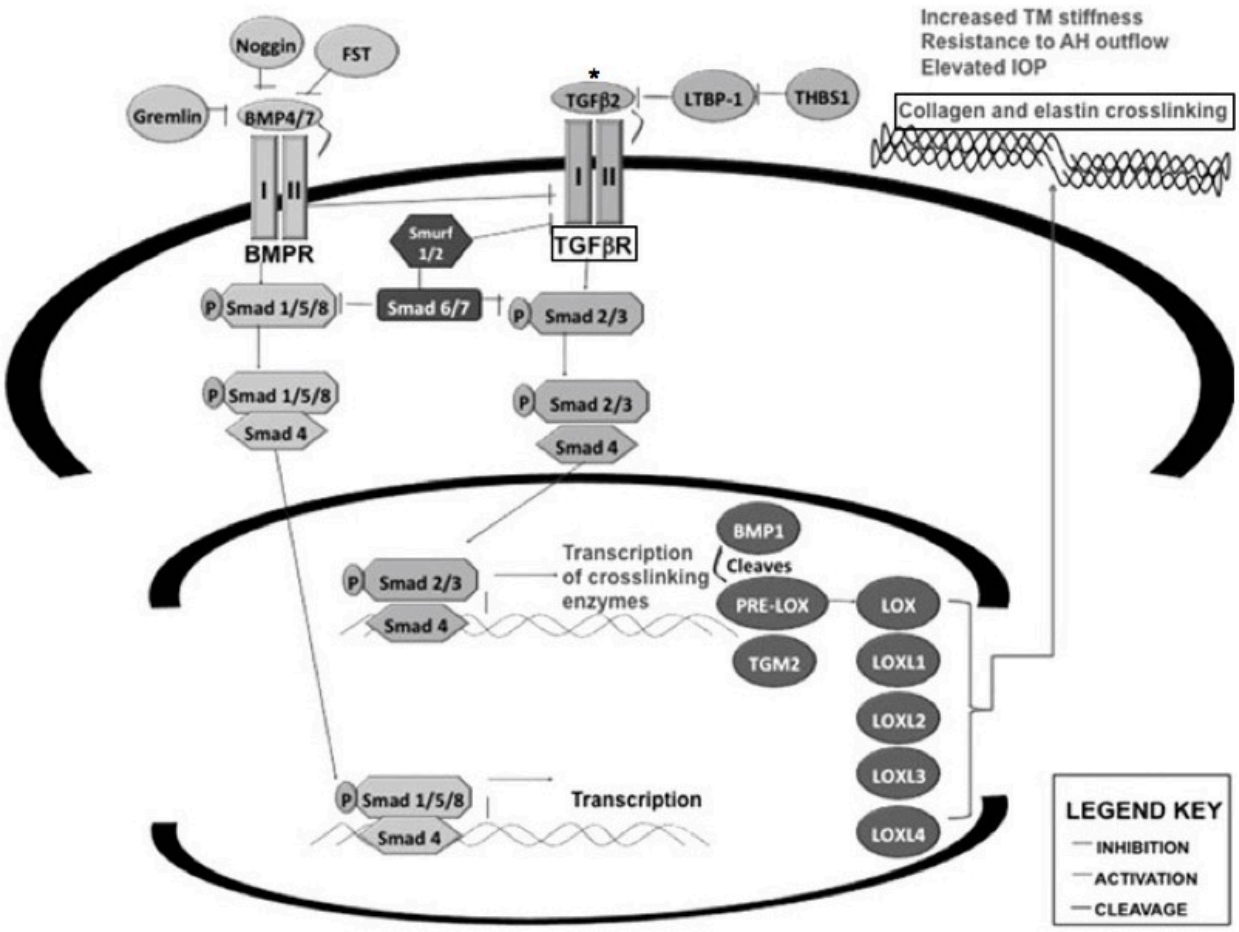

Figure 5. A schematic representation of the TGFβ signaling pathway and regulation of ECM crosslinking enzymes in the TM. The TGFβ ligand first binds the TGFβRII receptor resulting in the phosphorylation of the TGFβRII receptor. Subsequently, transcription factors SMAD2/3 are phosphorylated and bind to SMAD4. The SMAD2/3/4 complex translocates into the nucleus, and binds specific genes to activate transcription of proforms of BMP-1 and LOX family members. The proform of BMP-1 is activated by procollagen C proteinase enhancer (PCOLCE) proteins 1 and 2. BMP-1 then cleaves pro-LOX and pro-LOXL1 into their active enzymes. Activated LOX and LOXL1 subsequently crosslink collagen and elastin fibers in the ECM of the TM. **Adapted from Wordinger et al., 2014.**

Regulators of TGFβ2

Bone morphogenic proteins (BMPs) have been shown to regulate the activity of TGFβ2. BMP4 has been shown to block TGFβ2 induction of fibronectin in the TM[163]. Also in the TM, BMP7 has been shown to block TGFβ2 induction of CTGF, TSP-1, fibronectin, collagen types IV and VI, and PAI-1. In human primary keloid cells, BAMBI has been shown to inhibit TGFβ induction of collagen-1[164]. Recently, our lab has shown that TGFβ2 downregulates the expression of BAMBI[165]. These studies suggest that endogenous inhibitors of TGFβ are present in the TM, however, their expression levels are modulated by the overabundance of TGFβ2 both in the glaucomatous tissue and cells in culture.

Effects of TGFβ2 on ECM

The effects of TGFβ2 on ECM deposition and remodeling are beginning to be understood. Many fibrotic diseases have implicated TGFβ in ECM secretion and deposition[166-172]. TM cells express TGFβ2[39] and TGFβ2 receptors[37], suggesting that TM cells may be under the influence of TGFβ2 as it is present in the aqueous humor and increasing amounts in POAG patients. The increase of TGFβ2 in POAG may be the inducer of ECM deposition. Thrombospondin-1 (TSP-1), one of the most potent *in vivo* activators of TGFβ2, has been shown to be expressed in TM cells in culture and tissue. Interesting, treatment of TM cells with TGFβ2 increased the expression of TSP-1[133, 173-175]. TGFβ2 was first shown to induce fibronectin expression of the two isoforms (EDA and EDB)[176], with 0.3 ng/mL[174], 2 ng/mL[177]2.7 ng/mL[176] and 5 ng/mL[133, 178] inducing fibronectin in cell lysate and/or condition medium. The induction of ECM and associated proteins that have been documented to be increased in TM cells treated with TGFβ2 include, but are not limited to: collagen I[174, 175, 177], collagen III[175], collagen IV[133, 160, 174, 177],Collagen VI[174, 177], vimentin[160],

versican[133, 179], PAI-1[133, 174, 177, 178], and MMP-2[174]. Changes in the ECM matrix composition at the TM is considered to play a role in the development of aqueous humor outflow resistance and development of ocular hypertension. Fibronectin EDA, an isoform of fibronectin, has been linked with amplifying the deposition of ECM in the TM.

Fibronectin EDA

Fibronectin is an extracellular glycoprotein that is elevated in the aqueous humor and glaucomatous TM tissues[180-182]. Fibronectin provides structural support, signaling and regulates growth factors involved in ECM remodeling. It is a multi-domain dimer composed of combinations of domains (type I, II, and III), with over 20 alternatively spliced isoforms generated by splicing one or more of the following exon domains: extra domain A (EDA), extra domain B (EDB), and type III connecting segment domain[182-184]. Interestingly, fibronectin can bind to itself, other ECM, growth factors and receptors. Fibronectin can be found in plasma fibronectin (pFN) and cellular fibronectin (cFN), however, only the EDA and EDB domains are found in cFN isoforms[184-186]. Interesting, cFN containing the EDA domain has been shown to play important roles in tissue damage[187-190] and fibrogenesis[191-195]. Medina-Ortiz et al. 2013 showed that the human normal TM and glaucomatous TM cells and tissues express the cFN isoforms (EDA and EDB) and that the EDA isoform is elevated in the glaucomatous TM tissue[161]. The contribution of fibronectin EDA to fibrogenesis and glaucomatous TM needs further investigation. However, early reports suggested that cFN-EDA may act as an endogenous ligand for toll-like receptor 4 (TLR4)[196]. This report suggested that only the recombinant FN-EDA was able to activate TLR4 in HEK 293 cells overexpressing TLR4; these cells normally do not express TLR4. The activation of TLR4 was found to depend upon the expression of MD-2

and other TLR4 accessory proteins[196, 197]. In a recent publication, the authors concluded that FN-EDA is necessary to activate TLR4, however, other domains of fibronectin are also required for optimal activation[198].

Toll-like receptors

The toll-like receptor family is a group of receptors that recognize molecular patterns present on pathogens. They are expressed on cells as part of the innate immune system with their expression differing between cell type. In humans, TLRs 1-10 have been identified to be functional[199], where 11-13 has be reported to be expressed in the murine species (Figure 6)[200]. Humans have a nonfunctional TLR11 and do not express TLR12 and 13. The extracellular domain of each TLR is unique and has high specificity for its ligand. TLR signaling can also occur via interaction with damage-associated molecular patterns (DAMPs)[201] or pathogen-associated molecular patterns (PAMPs). Like most receptors, toll like receptors require homodimerization or heterodimerization of receptors to activate transcription factors that ultimate lead to the production of chemokine and cytokines. All mammalian TLRs have an extracellular domain that contains leucine-rich domains and an intracellular domain which is similar to the IL-1 signaling receptor that activates a signaling cascade leading to nuclear factor kB (NF-κB)[197, 202-207].

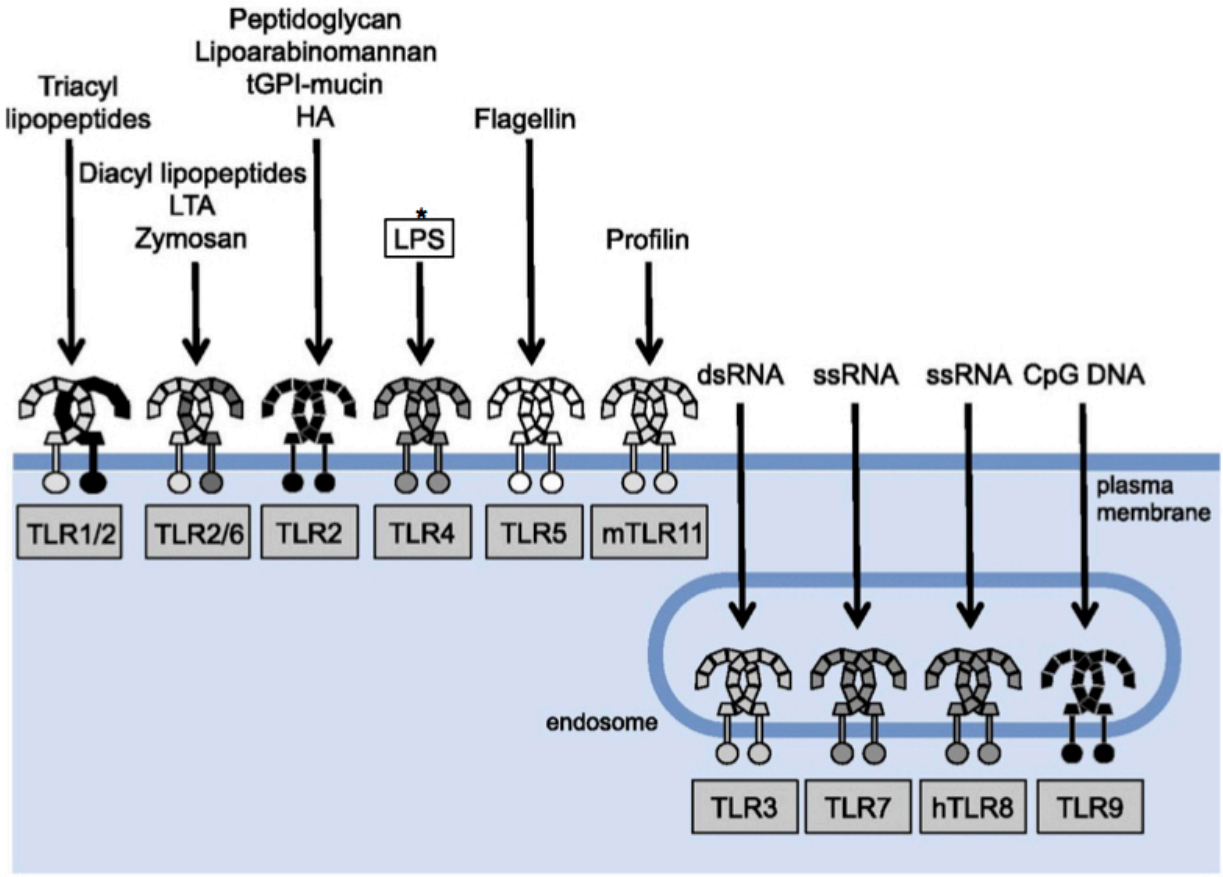

Figure 6. Cell surface and intracellular toll-like receptors (TLRs) and their ligands. TLRs are divided into two groups based on their cellular localization when sensing their respective ligands. TLRs 1, 2, 4–6, and 11 localize to the cell surface (cell surface TLRs) and TLRs 3 and 7–9 reside at endosomal compartments (intracellular TLRs). Cell surface TLRs respond to microbial membrane materials such as lipids, lipoproteins, and proteins, whereas intracellular TLRs recognize bacteria- and virus-derived nucleic acids. **Adapted from Goulopoulou et al., 2016.**

Toll-like receptor 4

TLR4 is a member of the TLR family of the innate immune system. Recent evidence suggests that endogenous ligands of cell compartments and matrix can activate TLR4, a phenomenon that can occur as a result of tissue damage or extracellular matrix remodeling. These ligands, also

known as DAMPs, have the potential to exuberate a cellular response. Endogenous DAMPs include HMGB-1, cFN-EDA, and low molecular weight hyaluronic acid, amongst others. The molecular interaction between these DAMPs and TLR4 is beginning to be elucidated. HMGB1 binds TLR4 and signals through adaptor molecules via the Toll/IL-1 receptor-domain to MyD88, IRAK, TRAF and finally to NF-κB[208]. Similar to HMGB-1, FN-EDA has been shown to activate TLR4 ultimately leading to NF-κB activation[196]. However, whether the signaling pathway is through the MyD88-dependent pathway is still not known. Hyaluronic acid and TLR4 binding interaction is still unknown, however, it is known that it requires CD14 and MD2[209]. The most known ligand of TLR4 is lipopolysaccharide (LPS). Figure 7 shows how LPS activates TLR4. Initial activation of TLR4 firsts occurs when the ligand LPS binds to circulating LPS-binding protein (LBP), three leucine rich repeats on TLR4, CD14 and MD2. This complexed is termed the LPS receptor complex. Upon TLR4 oligomerization, downstream adaptor molecules bind the TIR domain of TLR4. Interesting, TLR4 is the only TLR that requires 4 adaptor molecules to transduce signals from its TIR domain: myeloid differentiation factor 88 (**MyD88**), MyD88 adaptor like /TIR domain-containing adaptor protein (**MAL/TIRAP**), TIR domain-containing adaptor inducing interferon-β (**TRIF**), and TRIF-related adaptor molecule (**TRAM**). TLR4 signaling has been recently divided into two TLR4 responses, the MyD88-dependent responses and the MyD88-independent responses.

MyD88 dependent and independent responses

It is now widely accepted that for the MyD88-dependent pathway, assembly of a complex of proteins is necessary for the activation of NF-κB. The complex is composed of the IL-1 receptor-associated kinase 1 (**IRAK1**), **IRAK4**, tumor necrosis factor receptor associated factor

6 (**TRAF6**), and transforming growth factor β activated kinase 1 (**TAK1**). This complex can then phosphorylate and activate ikB kinase [210], mitogen-activated protein kinase (**MAPK**), and the phosphatidylinositol 3-kinase (**PI3K**) pathways. Phosphorylation of IKK and ikB lead to the release of NF-κB, which can then translocate into the nucleus and lead to gene transcription or repression. The complex can also activate PI3K, subsequently leading to AKT phosphorylation, ultimately leading to ikB activation and release of NF-κB. The complex consisting of IRAKs, TRAF6, and TAK1 can also lead to the activation of MKK, which subsequently activates mitogen-activated protein kinase (**MAPK**), **JNK**, and **ERK**. Activation of these three proteins ultimately leads to the activation of activator protein-1 (**AP-1**). In summary, both the IKK and PI3K pathways lead to NF-κB activation and the MKK pathway leads to activation of AP-1 (Figure 7). For the MyD88-independent pathway, the TIR domain activates the **TRIF/TRAM** complex, after which activates interferon regulatory factor 3 (IRF3) and induces the expression of interferon (IFN)-β and IFN-responsive genes. TLR4 downstream signaling by DAMPs in the glaucomatous TM is currently unknown. However, some DAMPs have been shown to activate NF-κB. Whether signaling of these DAMPs is through the MyD88-dependent pathway or the MyD88-independent pathway is still unknown.

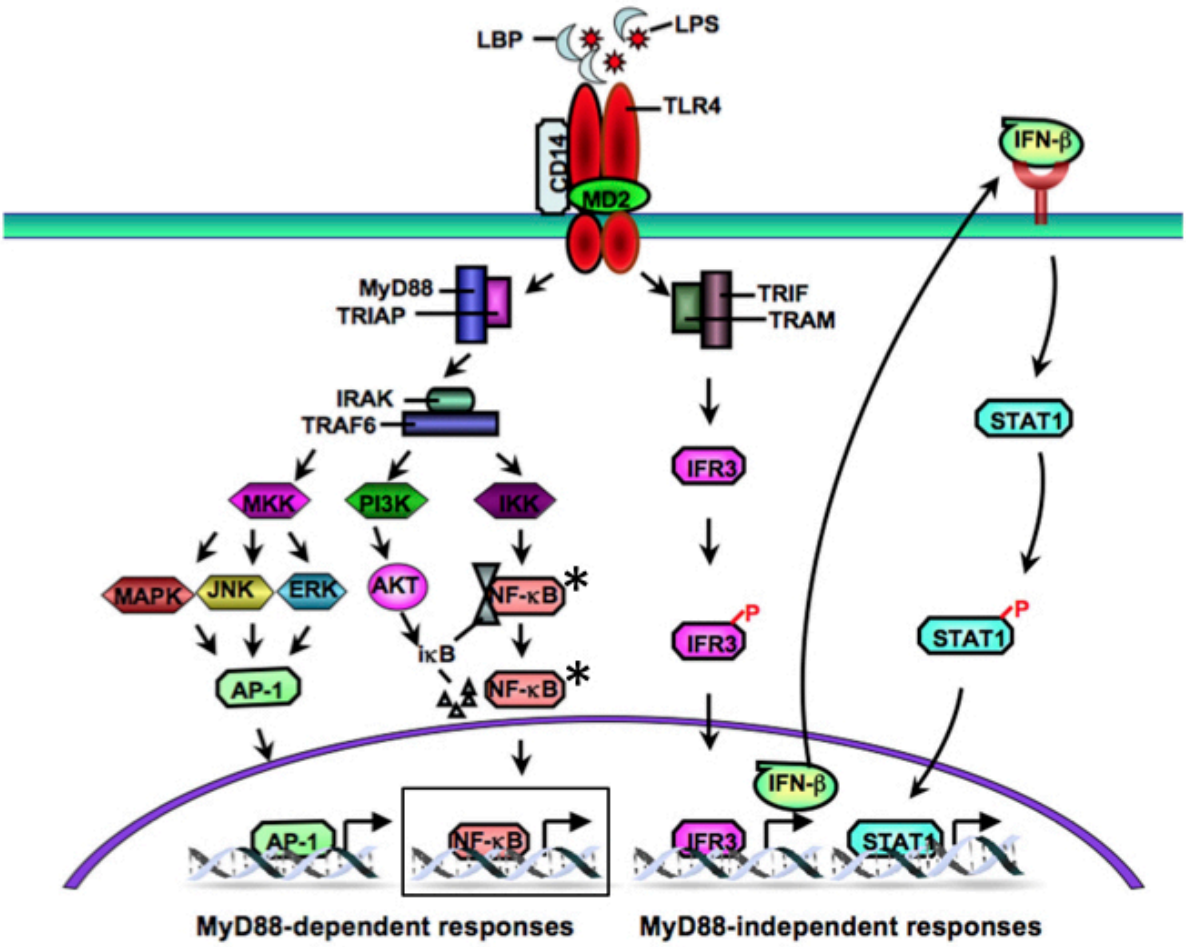

Figure 7. Schematic overview of the toll-like receptor 4 (TLR4) signaling pathway. LPS interacts with circulating LPS-binding protein (LBP) and binds to TLR4 on the cell membrane with two co-receptors, CD14 and MD2, activating MyD88-dependent and MyD88-independent TLR4 signaling via different adaptor proteins. The MyD88-dependent pathway signals through activation of ikB kinase and MAPK pathways, which in turn leads to activation of transcription factors NF-kB and AP-1, respectively, and controls the expression of pro-inflammatory cytokines and other immune related genes. In addition, PI3K and AKT are also important factors downstream of MyD88 that mediate NF-κB activation. The MyD88-independent pathway is mediated by TRIF, which activates IFR3 and induces the expression of IFN-β and IFN-responsive genes. **Adapted from Guo and Friedman, 2010.**

TLR polymorphisms in glaucoma

Polymorphisms in the TLR family have been focused on TLR2 and TLR4. There are a limited amount of studies that have evaluated polymorphisms in the genes coding for these receptors. Nakamura and colleagues were the first group to evaluate genetic differences in TLR2 in normal tension glaucoma patients. To their disappointment, they did not find single-nucleotide polymorphisms (SNPs) in the TLR2 gene in the Japanese NTG group when compared to the control group[211]. Others attempted to find a link between TLR2 and POAG. When SNP at rs5773704 was evaluated in POAG patients in the Saudi population, unfortunately for Kondkar and colleagues, no association was found in this allele[212]. These two studies suggest that there are no genetic differences in the gene coding for TLR2 in NTG and POAG patients. In relation to TLR4, Shibuya and colleagues performed SNPs on studies on NTG (n=250) and healthy patients (n=318). They found that multiple SNPs (rs10759930, rs1927914, rs1927911, rs12377632, rs2149356, and rs7037117) in the TLR4 gene were associated with the risk of NTG[213]. However, when Sun et al., 2011 evaluated the NTG Korean population for SNPs (rs10759930, rs1927914, rs1927911, rs12377632, rs2149356, rs11536889, rs7037117, and rs7045953) in the TLR4 gene, there was no statistical significance difference between the NTG patients (n=147) and controls (n=380)[214]. Interestingly, Takano and colleagues found that in Japanese individuals with POAG (n=184), NTG (n=365), and exfoliation glaucoma (XFG) (n=109), the allele frequency of rs2149356 in *Tlr4* was the most significant. Further, the SNPs at rs10759930, rs1927914, rs1927911, and rs2149356 were all significantly higher in the glaucoma groups compared to the control group[215]. Recently, Abu-Amero and colleagues evaluated the SNP at s4986790 in the *TLR4* gene of Saudi POAG patients, they found no statistical difference between the POAG (n=85) and control group (n=95)[216]. Lastly, Navarro-Partida and colleagues evaluated SNPs

Asp299Gly (rs4986790 A/G) and Thr399lle (rs4986791 C/T) in Mexican patients with POAG (n=187) and a control group (n=109). They found that the TLR4 coding SNPs Asp299Gly and Thr399lle was significantly higher in the POAG patients compared to controls, suggesting that there is a genetic susceptibility of alleles for POAG in the Mexican population[217]. These studies have many limitations, such small cohorts and are from different populations. In other diseases, the role of TLR4 in fibrogenesis has been previously studied including identification of specific SNP alleles in *TLR4* that have been associated with a delayed progression of fibrosis in liver disease and confer an overall protective effect[218, 219].

Transforming growth factor beta-2 and Toll-like receptor 4

Recent evidence has linked DAMP activated TLR4 signaling to fibrosis and the regulation and production of ECM proteins. DAMPs (FN-EDA, hyaluronan, tenascin C, amongst others) have been shown to activate TLR4 and augment TGFβ signaling and downstream fibrotic responses in other diseases such as hepatic fibrosis, renal fibrosis, lesional skin and lung in scleroderma patients, as well as in *Tlr4* mutant mice[220-224]. Activation of TLR4 downregulates BAMBI, leading to unopposed TGFβ signaling and increased ECM production[220, 221]. BAMBI downregulation by TLR4 is regulated by the MyD88-NFκB-dependent pathway[221, 225, 226]. Since the fibrotic response leads to the accumulation of endogenous TLR ligands such as FN-EDA, a feed-forward loop could develop leading to a further progression of the fibrotic response. Here we propose that a similar TGFβ-TLR4 crosstalk is involved in the production and regulation of the ECM in the glaucomatous TM.

Current problem

Although the ECM in the TM is known to be important in IOP regulation, the molecular mechanisms involved in generating a glaucomatous environment in the TM remain unknown. We propose a novel pathway that is contributing to the regulation of the ECM and fibrosis in the TM. Investigation of TGFβ2-TLR4 crosstalk in the TM will explain the mechanisms involved in the development of glaucomatous TM damage. Our data will be invaluable to the field of glaucoma and provide a framework for the development of novel therapeutic targets that could intervene and perhaps reverse glaucomatous damage to the TM.

Central Hypothesis

Elevated IOP is one of the primary risk factors in the development of glaucoma. The TM is a critical tissue involved in the outflow of aqueous humor and regulation of IOP. Changes in the ECM environment in the TM can alter the ability of aqueous humor to properly drain from the anterior chamber. The involvement of TGFβ signaling pathways in the regulation of the ECM in the TM has been extensively studied. Recent evidence has implicated TLR4 in the regulation of ECM and fibrogenesis. Here we propose that the TLR4 signaling pathway is also involved in the regulation of the ECM in the TM. Our central hypothesis is that endogenous TLR4 ligands activate TLR4 and augment TGFβ2 signaling, leading to increased ECM production in the TM and increased IOP (Figure 8).

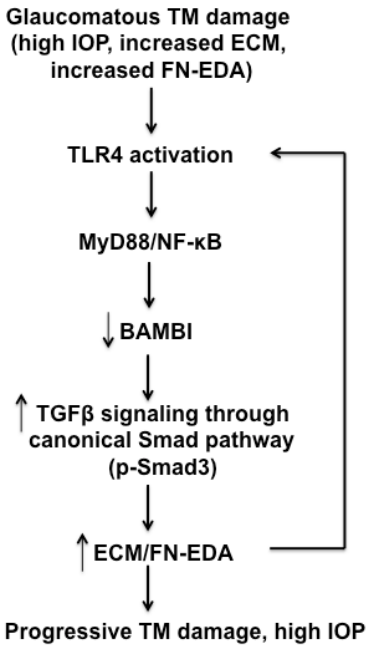

Figure 8. Crosstalk between TGFβ2 and TLR4 in the TM.

Specific Aims

Specific Aim 1: Determine the TGFβ2 – TLR4 signaling pathway regulating ECM production in transformed and primary human TM cells

1A) Evaluate the expression of TLR4 in the human and mouse TM

To evaluate the expression of TLR4 in humans, cross sections of eight individual human eyes were labeled with a TLR4 specific antibody. To validate that our cell strains and cell line expressed TLR4, RNA was isolated from primary human TM cell strains and a human transformed TM cell line, GTM3. RT-PCR was performed using primers specific to human TLR4. TM rings from C3H/HeJ, C57BL/6J, and A/J were dissected and RNA isolated for RT-PCR of *Tlr4*. Using this methodology, we ensured that our *in vivo* and *in vitro* models expressed TLR4.

1B) Block TLR4 signaling utilizing TAK-242 to decrease TGFβ2 induction of ECM molecules: fibronectin, collagen-1, and laminin

To evaluate the role of TLR4 in TGFβ2 induction of ECM, we utilized an inhibitor (TAK-242) of TLR4 signaling in cell culture. To determine the appropriate concentration of the inhibitor for our *in vitro* studies, a cell viability assay for TAK-242 was performed on GTM3 and primary NTM cells. After identifying the proper non-toxic TAK-242 concentration, GTM3 cells were pre-treated with TAK-242 for 2 hours, and subsequently treated with TGFβ2 (5ng/mL) and evaluated for fibronectin and collagen-1 expression. For western immunoblot, NTM cells were also pretreated with TAK-242 for 2 hours, and subsequently treated with TGFβ2 (5 ng/mL) for 48 hours (fibronectin). For immunocytochemistry, NTM were pretreated with TAK-242 for 2 hours followed by treatment with TGFβ2 (5 ng/mL) for 48 hours (fibronectin and laminin) and 72 hours (collagen-1).

1C) Activate TLR4 utilizing cFN-EDA and LPS in the presence or absence of TGFβ2 and/or TAK-242 to determine the effect on ECM components: fibronectin, collagen-1, and laminin

To evaluate the role of TLR4 in inducing ECM, TLR4 was activated using cFN-EDA or LPS in the presence or absence of TGFβ2 and/or TAK-242. NTM were plated on cFN-EDA–coated plates and non-coated plates with TGFβ2 in serum-free medium for 48 hours and western immunoblot performed for fibronectin changes. NTM cells (were pretreated with TAK-242 for 2 hours, and subsequently treated with TGFβ2 (5 ng/mL), TAK-242 and/or cFN-EDA for 72 hours. Western immunoblot and densitometry analysis was performed to determine total fibronectin changes in cell lysates. For immunocytochemistry, NTM cells were pretreated with

TAK-242 for 2 hours followed by treatment with TGFβ2 (5 ng/mL), cFN-EDA, and/or LPS (100 ng/mL) for 48 hours (fibronectin and laminin) and 72 hours (collagen-1).

Specific Aim 2: Determine whether knockdown of *Bambi* affects the ECM of TM cells

2A) Isolation of BAMBI flox TM cells from mice

To evaluate the role of BAMBI on TM cells, BAMBI flox TM cells were isolated from B6;129S1-Bambi^{tm1Jian}/J mice. Intracameral injections, anterior segment dissections, and magnetic bead isolation of TM cells were performed according to our established protocol[43]. To remove the pigment from the isolated cells, washing steps were performed.

2B) Characterization of BAMBI flox TM cells

MTM cells were characterized as previously described[43]. Briefly, the expression of fibronectin, collagen-1, collagen-4, laminin, and alpha-smooth muscle actin were evaluated. Confluent MTM cell cultures were stained with phalloidin-Alexa-488 for the formation of cross-linked actin networks (CLANs) after treatment with DEX for 7 days and compared to vehicle control (ETOH). Lastly, DEX induced myocilin expression was evaluated after treatment with DEX and vehicle (ETOH) for 4 days.

2C) Utilize Ad5.Cre to knockdown *Bambi* and/or challenge with Ad5.TGFβ2 and evaluate ECM changes

To determine the transduction efficiency of Adenovirus serotype 5, MTM Bambi flox cells were transduced with Ad5.GFP at 50 MOI, 100 MOI, and 200 MOI for 12 hours followed by 48 hrs incubation. Further, Ad5.Cre at 50 MOI, 100 MOI, and 200 MOI was used to evaluate BAMBI.

Changes in fibronectin and collagen-1 were evaluated. Ad5.null and Ad5.TGFβ2 at the predetermined MOI was used to determine the expression of BAMBI, fibronectin, and collagen-1.

Specific Aim 3: Determine the TGFβ2 – TLR4 signaling pathway regulating ECM production in the TM of mice and IOP

3A) Asses IOP and IOP exposure in TLR4 wildtype (C3H/OuJ), TLR4 mutant (C3H/HeJ), and BAMBI flox (B6;129S1-Bambi^{tm1Jian}/J) mice challenged with Ad5.TGFβ2 and/or Ad5.Cre

All mice were at least 3 months old at the start of the experiment. Animals were intravitreally injected with Ad5.TGFβ2, Ad5.Cre, and/or Ad5.null at 2.5 x 10^7 plaque forming units (PFU) in one eye and the contralateral uninjected eyes used as negative controls. C3H/HeJ and C3H/HeOuJ mice are genetically similar except for the genotype of *Tlr4*, while B*ambi*^{flox} mice harbor *loxP* sites flanking exon 1 of the *Bambi* locus. IOP was measured as previously described[134-136, 227]. IOP was measured on conscious mice or under isoflurane using the Tonolab tonometer. Area under the curve (AUC) was calculated as previously described[135, 136, 227].

3B) Evaluate fibronectin and/or BAMBI changes in TLR4 wildtype (C3H/OuJ), TLR4 mutant (C3H/HeJ), and BAMBI flox (B6;129S1-Bambi^{tm1Jian}/J) in the TM of mice challenged with Ad5.TGFβ2 and/or Ad5.Cre

It has been documented that TLR4 mutant mice are protected from fibrosis[228-232]. However, no study to date has evaluated BAMBI and its role in the regulation of fibrosis *in vivo*. To document the extend of ECM changes in the TM of TLR4 wildtype (C3H/OuJ), TLR4 mutant (C3H/HeJ),

and BAMBI flox mice (B6;129S1-Bambi^{tm1Jian}/J), intravitreal injections of Ad5.TGFβ2, Ad5.Cre, and/or Ad5.null was performed as described in Aim 3A. TLR4 wildtype (C3H/OuJ) and TLR4 mutant (C3H/HeJ) mice from aim 3A were harvested 5 to 8 weeks post injection and analyzed by immunohistochemistry for fibronectin. Similarly, given that adenovirus particles can reach the TM layers in 4 hours in a perfusion culture system[233] and mice TM express the transgene within 24 hours.[234], B6;129S1-*Bambi*^{tm1Jian}/J eyes were harvested 11 days post injection and analyzed by immunohistochemistry for *Bambi* knockdown and ECM expression.

3C) Assess outflow facility in BAMBI flox (B6;129S1-Bambi^{tm1Jian}/J) in the TM of mice challenged with Ad5.TGFβ2 and/or Ad5.Cre

To evaluate the effect of Ad5.TGFβ2 and/or Ad5.Cre on aqueous humor outflow rate on B6;129S1-Bambi^{tm1Jian}/J, 3 to 5 mice from aims 3A and 3B were evaluated for outflow facility determination as previously described[235, 236].

References

1. Quigley HA, Broman AT. The number of people with glaucoma worldwide in 2010 and 2020. *Br J Ophthalmol* 2006;90:262-267.

2. Friedman DS, Wolfs RC, O'Colmain BJ, et al. Prevalence of open-angle glaucoma among adults in the United States. *Arch Ophthalmol* 2004;122:532-538.

3. Harwerth RS, Wheat JL, Fredette MJ, Anderson DR. Linking structure and function in glaucoma. *Prog Retin Eye Res* 2010;29:249-271.

4. Quigley HA, Addicks EM, Green WR, Maumenee AE. Optic nerve damage in human glaucoma. II. The site of injury and susceptibility to damage. *Arch Ophthalmol* 1981;99:635-649.

5. Nutzi C, Schotzau A, Grieshaber MC. Structure and function relationship of activated retinal glia in primary open-angle glaucoma patients. *J Ophthalmol* 2017;2017:7043752.

6. Seitz R, Ohlmann A, Tamm ER. The role of Muller glia and microglia in glaucoma. *Cell Tissue Res* 2013;353:339-345.

7. Lorber B, Guidi A, Fawcett JW, Martin KR. Activated retinal glia mediated axon regeneration in experimental glaucoma. *Neurobiol Dis* 2012;45:243-252.

8. Bai Y, Shi Z, Zhuo Y, et al. In glaucoma the upregulated truncated TrkC.T1 receptor isoform in glia causes increased TNF-alpha production, leading to retinal ganglion cell death. *Invest Ophthalmol Vis Sci* 2010;51:6639-6651.

9. Feilchenfeld Z, Yucel YH, Gupta N. Oxidative injury to blood vessels and glia of the pre-laminar optic nerve head in human glaucoma. *Exp Eye Res* 2008;87:409-414.

10. Tezel G, Yang X, Luo C, Peng Y, Sun SL, Sun D. Mechanisms of immune system activation in glaucoma: oxidative stress-stimulated antigen presentation by the retina and optic nerve head glia. *Invest Ophthalmol Vis Sci* 2007;48:705-714.

11. Birch M, Brotchie D, Roberts N, Grierson I. The three-dimensional structure of the connective tissue in the lamina cribrosa of the human optic nerve head. *Ophthalmologica* 1997;211:183-191.

12. Johnson EC, Jia L, Cepurna WO, Doser TA, Morrison JC. Global changes in optic nerve head gene expression after exposure to elevated intraocular pressure in a rat glaucoma model. *Invest Ophthalmol Vis Sci* 2007;48:3161-3177.

13. Kirwan RP, Crean JK, Fenerty CH, Clark AF, O'Brien CJ. Effect of cyclical mechanical stretch and exogenous transforming growth factor-beta1 on matrix metalloproteinase-2 activity in lamina cribrosa cells from the human optic nerve head. *J Glaucoma* 2004;13:327-334.

14. Fukuchi T, Ueda J, Hanyu T, Abe H, Sawaguchi S. Distribution and expression of transforming growth factor-beta and platelet-derived growth factor in the normal and glaucomatous monkey optic nerve heads. *Jpn J Ophthalmol* 2001;45:592-599.

15. Zode GS, Sethi A, Brun-Zinkernagel A-M, Chang IF, Clark AF, Wordinger RJ. Transforming growth factor-β2 increases extracellular matrix proteins in optic nerve head cells via activation of the Smad signaling pathway. *Mol Vis* 2011;17:1745-1758.

16. Stamer WD, Clark AF. The many faces of the trabecular meshwork cell. *Exp Eye Res* 2017;158:112-123.

17. Worthen DM, Cleveland PH. Fibronectin production by cultured human trabecular meshwork cells. *Invest Ophthalmol Vis Sci* 1982;23:265-269.

18. Grierson I, Robins E, Howes RC. Preliminary observations on human trabecular meshwork cells in vitro. *Albrecht von Graefes Arch Klin Exp Ophthalmol* 1980;212:173-186.

19. Rohen JW, Schachtschabel OO, Matthiessen PF. In vitro studies on the trabecular meshwork of the primate eye. *Albrecht von Graefes Arch Klin Exp Ophthalmol* 1975;193:95-107.

20. Polansky JR, Weinreb RN, Baxter JD, Alvarado J. Human trabecular cells. I. Establishment in tissue culture and growth characteristics. *Invest Ophthalmol Vis Sci* 1979;18:1043-1049.

21. Grierson I, Robins E, Unger W, Millar L, Ahmed A. The cells of the bovine outflow system in tissue culture. *Exp Eye Res* 1985;40:35-46.

22. Steely HT, Browder SL, Julian MB, Miggans ST, Wilson KL, Clark AF. The effects of dexamethasone on fibronectin expression in cultured human trabecular meshwork cells. *Invest Ophthalmol Vis Sci* 1992;33:2242-2250.

23. Rohen JW, Schachtschabel DO, Wehrmann R. Structural changes of human and monkey trabecular meshwork following in vitro cultivation. *Graefes Arch Clin Exp Ophthalmol* 1982;218:225-232.

24. Schachtschabel DO, Rohen JW, Wever J, Sames K. Synthesis and composition of glycosaminoglycans by cultured human trabecular meshwork cells. *Graefes Arch Clin Exp Ophthalmol* 1982;218:113-117.

25. Tripathi RC, Tripathi BJ. Human trabecular endothelium, corneal endothelium, keratocytes, and scleral fibroblasts in primary cell culture. A comparative study of growth characteristics, morphology, and phagocytic activity by light and scanning electron microscopy. *Exp Eye Res* 1982;35:611-624.

26. Grierson I, Marshall J, Robins E. Human trabecular meshwork in primary culture: a morphological and autoradiographic study. *Exp Eye Res* 1983;37:349-365.

27. Polansky JR, Wood IS, Maglio MT, Alvarado JA. Trabecular meshwork cell culture in glaucoma research: evaluation of biological activity and structural properties of human trabecular cells in vitro. *Ophthalmology* 1984;91:580-595.

28. Iwamoto Y, Tamura M. Human trabecular meshwork cells in culture. *Nippon Ganka Gakkai Zasshi* 1985;89:1125-1133.

29. Hernandez MR, Weinstein BI, Schwartz J, Ritch R, Gordon GG, Southren AL. Human trabecular meshwork cells in culture: morphology and extracellular matrix components. *Invest Ophthalmol Vis Sci* 1987;28:1655-1660.

30. Kurosawa A, Elner VM, Yue BY, Elvart JL, Tso MO. Cultured trabecular-meshwork cells: immunohistochemical and lectin-binding characteristics. *Exp Eye Res* 1987;45:239-251.

31. Yue BY, Elvart JL. Biosynthesis of glycosaminoglycans by trabecular meshwork cells in vitro. *Curr Eye Res* 1987;6:959-967.

32. Higginbotham E, Yue BY, Crean E, Peace J. Effects of ascorbic acid on trabecular meshwork cells in culture. *Exp Eye Res* 1988;46:507-516.

33. Shuman MA, Polansky JR, Merkel C, Alvarado JA. Tissue plasminogen activator in cultured human trabecular meshwork cells. Predominance of enzyme over plasminogen activator inhibitor. *Invest Ophthalmol Vis Sci* 1988;29:401-405.

34. Schachtschabel DO, Binninger EA, Rohen JW. In vitro cultures of trabecular meshwork cells of the human eye as a model system for the study of cellular aging. *Arch Gerontol Geriatr* 1989;9:251-262.

35. Alexander JP, Samples JR, Van Buskirk EM, Acott TS. Expression of matrix metalloproteinases and inhibitor by human trabecular meshwork. *Invest Ophthalmol Vis Sci* 1991;32:172-180.

36. Hoya T. Effects of elastase on cultured human trabecular meshwork. *Ophthalmologica* 1992;204:156-161.

37. Tripathi RC, Borisuth NS, Kolli SP, Tripathi BJ. Trabecular cells express receptors that bind TGF-beta 1 and TGF-beta 2: a qualitative and quantitative characterization. *Invest Ophthalmol Vis Sci* 1993;34:260-263.

38. Clark AF, Wilson K, McCartney MD, Miggans ST, Kunkle M, Howe W. Glucocorticoid-induced formation of cross-linked actin networks in cultured human trabecular meshwork cells. *Invest Ophthalmol Vis Sci* 1994;35:281-294.

39. Tripathi RC, Chan WF, Li J, Tripathi BJ. Trabecular cells express the TGF-beta 2 gene and secrete the cytokine. *Experimental Eye Research* 1994;58:523-528.

40. Tripathi RC, Li J, Tripathi BJ. Immunolocalization of bFGF in the trabecular meshwork and detection of its mRNA in trabecular cells. *Exp Eye Res* 1994;58:503-507.

41. Begley CG, Yue BY, Hendricks RL. Murine trabecular meshwork cells in tissue culture. *Curr Eye Res* 1991;10:1015-1030.

42. Tamm ER, Russell P, Piatigorsky J. Development of characterization of a immortal and differentiated murine trabecular meshwork cell line. *Invest Ophthalmol Vis Sci* 1999;40:1392-1403.

43. Mao W, Liu Y, Wordinger RJ, Clark AF. A magnetic bead-based method for mouse trabecular meshwork cell isolation. *Invest Ophthalmol Vis Sci* 2013;54:3600-3606.

44. Dannheim R, Barany EH. Attempts at reverse perfusion of the trabecular meshwork in different monkey species (*Cercopithecus ethiops*, *Macaca mulatta*, and *Macaca speciosa*). *Invest Ophthalmol* 1968;7:305-318.

45. Schachtshabel DO, Bigalke B, Rohen JW. Production of glycosaminoglycans by cell cultures of the trabecular meshwork of the primate eye. *Exp Eye Res* 1977;24:71-80.

46. Engelbrecht-Schnur S, Siegner A, Prehm P, Lütjen-Drecoll E. Dexamethasone treatment decreases hyaluronan-formation by primate trabecular meshwork cells in vitro. *Exp Eye Res* 1997;64:539-543.

47. Tamm ER, Russell P, Johnson DH, Piatigorsky J. Human and monkey trabecular meshwork accumulate alpha B-crystallin in response to heat shock and oxidative stress. *Invest Ophthalmol Vis Sci* 1996;37:2402-2413.

48. Weinreb RN, Mitchell MD. Prostaglandin production by cultured cynomolgus monkey trabecular meshwork cells. *Prostaglandins Leukot Essent Fatty Acids* 1989;36:97-100.

49. Clark AF, Steely HT, Dickerson JE, Jr., et al. Glucocorticoid induction of the glaucoma gene MYOC in human and monkey trabecular meshwork cells and tissues. *Invest Ophthalmol Vis Sci* 2001;42:1769-1780.

50. Zhou Q, Zhao JL, Liu YQ. The effect of endothelial leukocyte-adhesion molecule-1 on the shape and cytoskeleton of porcine trabecular meshwork cells. *Zhonghua Yan Ke Za Zhi* 2004;40:614-619.

51. Xue W, Du S, Li Y, Yang Y, Sun J. Effects of nitric oxide on proliferation and apoptosis of cultured bovine trabecular meshwork cells. *J Huazhong Univ Sci Technolog Med Sci* 2002;22:73-76.

52. Nakamura Y, Hirano S, Suzuki K, Seki K, Sagara T, Nishida T. Signaling mechanism of TGF-beta1-induced collagen contraction mediated by bovine trabecular meshwork cells. *Invest Ophthalmol Vis Sci* 2002;43:3465-3472.

53. Gu Y, Zeng S, Qiu P, Peng D, Yan G. Apoptosis of bovine trabecular meshwork cells induced by dexamethasone. *Zhonghua Yan Ke Za Zhi* 2002;38:302-304.

54. Cao Y, Wei H, Zhang Y, Da B, Lu Y. Effect of transforming growth factor-beta(2) on extracellular matrix synthesis in bovine trabecular meshwork cells. *Zhonghua Yan Ke Za Zhi* 2002;38:429-432.

55. Cao Y, Wei H, Da B, Pfaffl M, Li Z. Insulin-like growth factor-I gene cloning and protein expression in bovine trabecular meshwork tissue and cells. *J Huazhong Univ Sci Technolog Med Sci* 2002;22:69-72.

56. Cao Y, Pfaffl MW, Da B, Wei H. Insulin-like growth factor 1 (IGF-1) mRNA and IGF-1 protein. Expression in cells of the trabecular meshwork of the bovine eye. *Ophthalmologe* 2002;99:555-558.

57. Cao Y, Dong J, Wei H. Expression of insulin-like growth factor-I in bovine trabecular meshwork cells in vitro. *Zhonghua Yan Ke Za Zhi* 2002;38:305-307.

58. Shen F, Zhang L, Liu T. Effects of angiotensin II on the 3H-TdR incorporation and synthesis of collagen in cultured bovine trabecular meshwork cells. *Yan Ke Xue Bao* 2001;17:209-212.

59. Jiang F, Wei H, Lu Y. A study of toxicity of 5-fluorouracil on bovine trabecular meshwork cells in vitro. *J Tongji Med Univ* 2001;21:82-85.

60. Cao Y, Wei H, Da B, Huang Y. Effect of transforming growth factor-beta 2 on phagocytosis in cultured bovine trabecular meshwork cells. *J Tongji Med Univ* 2001;21:318-320.

61. Yang X, Li M. Establishment of in vitro culture of bovine trabecular meshwork cells and their phagocytosis. *Zhonghua Yan Ke Za Zhi* 1996;32:136-139.

62. Kawa JE, Higginbotham EJ, Chang IL, Yue BY. Effects of antiglaucoma medications on bovine trabecular meshwork cells in vitro. *Exp Eye Res* 1993;57:557-565.

63. Coroneo MT, Korbmacher C, Flugel C, Stiemer B, Lütjen-Drecoll E, Wiederholt M. Electrical and morphological evidence for heterogeneous populations of cultured bovine trabecular meshwork cells. *Exp Eye Res* 1991;52:375-388.

64. Srinivas SP, Maertens C, Goon LH, et al. Cell volume response to hyposmotic shock and elevated cAMP in bovine trabecular meshwork cells. *Exp Eye Res* 2004;78:15-26.

65. Nakamura Y, Sagara T, Seki K, Hirano S, Nishida T. Permissive effect of fibronectin on collagen gel contraction mediated by bovine trabecular meshwork cells. *Invest Ophthalmol Vis Sci* 2003;44:4331-4336.

66. Cao Y, Wei H, Pfaffl MW, Da B. Effect of transforming growth factor beta 2 on phagocytosis in cultured bovine trabecular meshwork cells. *Ophthalmologe* 2003;100:535-538.

67. Bermudez JY, Webber HC, Brown B, Braun TA, Clark AF, Mao W. A comparison of gene expression profiles between glucocorticoid responder and non-responder bovine trabecular meshwork cells using RNA sequencing. *PLoS One* 2017;12:e0169671.

68. Mao W, Liu Y, Mody A, Montecchi-Palmer M, Wordinger RJ, Clark AF. Characterization of a spontaneously immortalized bovine trabecular meshwork cell line. *Exp Eye Res* 2012;105:53-59.

69. Wade NC, Grierson I, O'Reilly S, et al. Cross-linked actin networks (CLANs) in bovine trabecular meshwork cells. *Exp Eye Res* 2009;89:648-659.

70. Bertazolli-Filho R, Laicine EM, Haddad A. Synthesis and secretion of transferrin by a bovine trabecular meshwork cell line. *Braz J Med Biol Res* 2007;40:1345-1351.

71. Gu Y, Zeng S, Qiu P, Wu Y, Peng D, Yan G. Molecular mechanism of bovine trabecular meshwork cells apoptosis induced by dexamethasone and protection by pilocarpine. *Yan Ke Xue Bao* 2005;21:44-51, 61.

72. Choritz L, Rosenthal R, Fromm M, Foerster MH, Thieme H. Pharmacological and functional characterization of endothelin receptors in bovine trabecular meshwork and ciliary muscle. *Ophthalmic Res* 2005;37:179-187.

73. Crean EV, Sherwood ME, Casey R, Miller MW, Richardson TM. Establishment of calf trabecular meshwork cell cultures. *Exp Eye Res* 1986;43:503-517.

74. Crean EV, Tyson SL, Richardson TM. Factors influencing glycosaminoglycan synthesis by calf trabecular meshwork cell cultures. *Exp Eye Res* 1986;43:365-374.

75. Pang IH, Shade DL, Clark AF, Steely HT, DeSantis L. Preliminary characterization of a transformed cell strain derived from human trabecular meshwork. *Curr Eye Res* 1994;13:51-63.

76. Lin S, Lee OT, Minasi P, Wong J. Isolation, culture, and characterization of human fetal trabecular meshwork cells. *Curr Eye Res* 2007;32:43-50.

77. Gonzalez P, Epstein DL, Borras T. Characterization of gene expression in human trabecular meshwork using single-pass sequencing of 1060 clones. *Invest Ophthalmol Vis Sci* 2000;41:3678-3693.

78. Keller KE, Acott TS. The juxtacanalicular region of ocular trabecular meshwork: a tissue with a unique extracellular matrix and specialized function. *J Ocul Biol* 2013;1:3.

79. Keller KE, Vranka JA, Haddadin RI, et al. The effects of tenascin C knockdown on trabecular meshwork outflow resistance. *Invest Ophthalmol Vis Sci* 2013;54:5613-5623.

80. Bradley JM, Kelley MJ, Zhu X, Anderssohn AM, Alexander JP, Acott TS. Effects of mechanical stretching on trabecular matrix metalloproteinases. *Invest Ophthalmol Vis Sci* 2001;42:1505-1513.

81. Midwood KS, Hussenet T, Langlois B, Orend G. Advances in tenascin-C biology. *Cell Mol Life Sci* 2011;68:3175-3199.

82. Vittal V, Rose A, Gregory KE, Kelley MJ, Acott TS. Changes in gene expression by trabecular meshwork cells in response to mechanical stretching. *Invest Ophthalmol Vis Sci* 2005;46:2857-2868.

83. Polansky JR, Fauss DJ, Chen P, et al. Cellular pharmacology and molecular biology of the trabecular meshwork inducible glucocorticoid response gene product. *Ophthalmologica* 1997;211:126-139.

84. Liu X, Wu Z, Sheibani N, Brandt CR, Polansky JR, Kaufman PL. Low dose latrunculin-A inhibits dexamethasone-induced changes in the actin cytoskeleton and alters extracellular matrix protein expression in cultured human trabecular meshwork cells. *Exp Eye Res* 2003;77:181-188.

85. Zhou L, Li Y, Yue BY. Glucocorticoid effects on extracellular matrix proteins and integrins in bovine trabecular meshwork cells in relation to glaucoma. *Int J Mol Med* 1998;1:339-346.

86. Tawara A, Tou N, Kubota T, Harada Y, Yokota K. Immunohistochemical evaluation of the extracellular matrix in trabecular meshwork in steroid-induced glaucoma. *Graefes Arch Clin Exp Ophthalmol* 2008;246:1021-1028.

87. Lee ES, Gabelt BT, Faralli JA, et al. COCH transgene expression in cultured human trabecular meshwork cells and its effect on outflow facility in monkey organ cultured anterior segments. *Invest Ophthalmol Vis Sci* 2010;51:2060-2066.

88. Comes N, Borrás T. Functional delivery of synthetic naked siRNA to the human trabecular meshwork in perfused organ cultures. *Mol Vis* 2007;13:1363-1374.

89. Liu X, Hu Y, Filla MS, et al. The effect of C3 transgene expression on actin and cellular adhesions in cultured human trabecular meshwork cells and on outflow facility in organ cultured monkey eyes. *Mol Vis* 2005;11:1112-1121.

90. Zhou L, Higginbotham EJ, Yue BY. Effects of ascorbic acid on levels of fibronectin, laminin and collagen type 1 in bovine trabecular meshwork in organ culture. *Curr Eye Res* 1998;17:211-217.

91. Johnson DH. The effect of cytochalasin D on outflow facility and the trabecular meshwork of the human eye in perfusion organ culture. *Invest Ophthalmol Vis Sci* 1997;38:2790-2799.

92. Snyder RW, Stamer WD, Kramer TR, Seftor RE. Corticosteroid treatment and trabecular meshwork proteases in cell and organ culture supernatants. *Exp Eye Res* 1993;57:461-468.

93. Sawaguchi S, Lam TT, Yue BY, Tso MO. Effects of glycosaminoglycan-degrading enzymes on bovine trabecular meshwork in organ culture. *J Glaucoma* 1993;2:80-86.

94. Miyanaga K. Porcine trabecular meshwork organ culture. *Nippon Ganka Gakkai Zasshi* 1993;97:1151-1156.

95. Johnson DH, Tschumper RC. Ethacrynic acid: outflow effects and toxicity in human trabecular meshwork in perfusion organ culture. *Curr Eye Res* 1993;12:385-396.

96. Tschumper RC, Johnson DH, Bradley JM, Acott TS. Glycosaminoglycans of human trabecular meshwork in perfusion organ culture. *Curr Eye Res* 1990;9:363-369.

97. Johnson DH, Bradley JM, Acott TS. The effect of dexamethasone on glycosaminoglycans of human trabecular meshwork in perfusion organ culture. *Invest Ophthalmol Vis Sci* 1990;31:2568-2571.

98. Buller C, Johnson DH, Tschumper RC. Human trabecular meshwork phagocytosis. Observations in an organ culture system. *Invest Ophthalmol Vis Sci* 1990;31:2156-2163.

99. Johnson DH, Tschumper RC. The effect of organ culture on human trabecular meshwork. *Exp Eye Res* 1989;49:113-127.

100. Urakawa Y, Miyazaki M, Ishihara A, Segawa K, Watanabe S, Shimizu Y. Human trabecular meshwork organ culture. *Jpn J Ophthalmol* 1988;32:401-411.

101. Acott TS, Kingsley PD, Samples JR, Van Buskirk EM. Human trabecular meshwork organ culture: morphology and glycosaminoglycan synthesis. *Invest Ophthalmol Vis Sci* 1988;29:90-100.

102. Johnson DH, Tschumper RC. Human trabecular meshwork organ culture. A new method. *Invest Ophthalmol Vis Sci* 1987;28:945-953.

103. Loewen RT, Roy P, Park DB, et al. A Porcine Anterior Segment Perfusion and Transduction Model With Direct Visualization of the Trabecular Meshwork. *Invest Ophthalmol Vis Sci* 2016;57:1338-1344.

104. Almasieh M, Levin LA. Neuroprotection in glaucoma: animal models and clinical trials. *Annu Rev Vis Sci* 2017;3:91-120.

105. Struebing FL, Geisert EE. What animal models can tell us about glaucoma. *Prog Mol Biol Transl Sci* 2015;134:365-380.

106. Overby DR, Clark AF. Animal models of glucocorticoid-induced glaucoma. *Exp Eye Res* 2015;141:15-22.

107. Iglesias AI, Springelkamp H, Ramdas WD, Klaver CC, Willemsen R, van Duijn CM. Genes, pathways, and animal models in primary open-angle glaucoma. *Eye (Lond)* 2015;29:1285-1298.

108. Akaishi T, Shimazaki A, Tonouchi A, Ueda K, Miyawaki N, Kawazu K. Benefits of tafluprost and timolol fixed-dose combination for the treatment of glaucoma are confirmed by studies on experimental animal models. *J Ocul Pharmacol Ther* 2015;31:518-524.

109. Bouhenni RA, Dunmire J, Sewell A, Edward DP. Animal models of glaucoma. *J Biomed Biotechnol* 2012;2012:692609.

110. Stewart WC, Magrath GN, Demos CM, Nelson LA, Stewart JA. Predictive value of the efficacy of glaucoma medications in animal models: preclinical to regulatory studies. *Br J Ophthalmol* 2011;95:1355-1360.

111. Vecino E. Animal models in the study of the glaucoma: past, present and future. *Arch Soc Esp Oftalmol* 2008;83:517-519.

112. Albrecht May C. Comparative anatomy of the optic nerve head and inner retina in non-primate animal models used for glaucoma research. *Open Ophthalmol J* 2008;2:94-101.

113. Levin LA. Animal and culture models of glaucoma for studying neuroprotection. *Eur J Ophthalmol* 2001;11 Suppl 2:S23-29.

114. Dawson WW, Brooks DE, Hope GM, et al. Primary open angle glaucomas in the rhesus monkey. *Br J Ophthalmol* 1993;77:302-310.

115. Gelatt KN. Animal models for glaucoma. *Invest Ophthalmol Vis Sci* 1977;16:592-596.

116. Podos SM. Animal models of human glaucoma. *Trans Sect Ophthalmol Am Acad Ophthalmol Otolaryngol* 1976;81:OP632-635.

117. Gaasterland D, Kupfer C. Experimental glaucoma in the rhesus monkey. *Invest Ophthalmol* 1974;13:455-457.

118. Samsel PA, Kisiswa L, Erichsen JT, Cross SD, Morgan JE. A novel method for the induction of experimental glaucoma using magnetic microspheres. *Invest Ophthalmol Vis Sci* 2011;52:1671-1675.

119. John SW, Smith RS, Savinova OV, et al. Essential iris atrophy, pigment dispersion, and glaucoma in DBA/2J mice. *Invest Ophthalmol Vis Sci* 1998;39:951-962.

120. Chang B, Smith RS, Hawes NL, et al. Interacting loci cause severe iris atrophy and glaucoma in DBA/2J mice. *Nat Genet* 1999;21:405-409.

121. Anderson MG, Smith RS, Hawes NL, et al. Mutations in genes encoding melanosomal proteins cause pigmentary glaucoma in DBA/2J mice. *Nat Genet* 2002;30:81-85.

122. Kuehn MH, Lipsett KA, Menotti-Raymond M, et al. A mutation in LTBP2 causes congenital glaucoma in domestic cats (*Felis catus*). *PLoS One* 2016;11:e0154412.

123. Mabuchi F, Lindsey JD, Aihara M, Mackey MR, Weinreb RN. Optic nerve damage in mice with a targeted type I collagen mutation. *Invest Ophthalmol Vis Sci* 2004;45:1841-1845.

124. Zode GS, Kuehn MH, Nishimura DY, et al. Reduction of ER stress via a chemical chaperone prevents disease phenotypes in a mouse model of primary open angle glaucoma. *J Clin Invest* 2011;121:3542-3553.

125. Mao M, Hedberg-Buenz A, Koehn D, John SW, Anderson MG. Anterior segment dysgenesis and early-onset glaucoma in nee mice with mutation of Sh3pxd2b. *Invest Ophthalmol Vis Sci* 2011;52:2679-2688.

126. Buys ES, Ko YC, Alt C, et al. Soluble guanylate cyclase alpha1-deficient mice: a novel murine model for primary open angle glaucoma. *PLoS One* 2013;8:e60156.

127. Morrison JC, Moore CG, Deppmeier LM, Gold BG, Meshul CK, Johnson EC. A rat model of chronic pressure-induced optic nerve damage. *Exp Eye Res* 1997;64:85-96.

128. Shareef SR, Garcia-Valenzuela E, Salierno A, Walsh J, Sharma SC. Chronic ocular hypertension following episcleral venous occlusion in rats. *Exp Eye Res* 1995;61:379-382.

129. Sappington RM, Carlson BJ, Crish SD, Calkins DJ. The microbead occlusion model: a paradigm for induced ocular hypertension in rats and mice. *Invest Ophthalmol Vis Sci* 2010;51:207-216.

130. Whitlock NA, McKnight B, Corcoran KN, Rodriguez LA, Rice DS. Increased intraocular pressure in mice treated with dexamethasone. *Invest Ophthalmol Vis Sci* 2010;51:6496-6503.

131. Zode GS, Sharma AB, Lin X, et al. Ocular-specific ER stress reduction rescues glaucoma in murine glucocorticoid-induced glaucoma. *J Clin Invest* 2014;124:1956-1965.

132. Patel GC, Phan TN, Maddineni P, et al. Dexamethasone-induced ocular hypertension in mice: effects of myocilin and route of administration. *Am J Pathol* 2017;187:713-723.

133. Fleenor DL, Shepard AR, Hellberg PE, Jacobson N, Pang IH, Clark AF. TGFbeta2-induced changes in human trabecular meshwork: implications for intraocular pressure. *Invest Ophthalmol Vis Sci* 2006;47:226-234.

134. Shepard AR, Millar JC, Pang IH, Jacobson N, Wang WH, Clark AF. Adenoviral gene transfer of active human transforming growth factor-beta2 elevates intraocular pressure and reduces outflow facility in rodent eyes. *Invest Ophthalmol Vis Sci* 2010;51:2067-2076.

135. McDowell CM, Hernandez H, Mao W, Clark AF. Gremlin Induces Ocular Hypertension in Mice Through Smad3-Dependent Signaling. *Invest Ophthalmol Vis Sci* 2015;56:5485-5492.

136. McDowell CM, Tebow HE, Wordinger RJ, Clark AF. Smad3 is necessary for transforming growth factor-beta2 induced ocular hypertension in mice. *Exp Eye Res* 2013;116:419-423.

137. Pang IH, Millar JC, Clark AF. Elevation of intraocular pressure in rodents using viral vectors targeting the trabecular meshwork. *Exp Eye Res* 2015;141:33-41.

138. Tripathi RC, Li J, Chan WF, Tripathi BJ. Aqueous humor in glaucomatous eyes contains an increased level of TGF-beta 2. *Exp Eye Res* 1994;59:723-727.

139. Inatani M, Tanihara H, Katsuta H, Honjo M, Kido N, Honda Y. Transforming growth factor-beta 2 levels in aqueous humor of glaucomatous eyes. *Graefes Arch Clin Exp Ophthalmol* 2001;239:109-113.

140. Trivedi RH, Nutaitis M, Vroman D, Crosson CE. Influence of race and age on aqueous humor levels of transforming growth factor-beta 2 in glaucomatous and nonglaucomatous eyes. *J Ocul Pharmacol Ther* 2011;27:477-480.

141. Ochiai Y, Ochiai H. Higher concentration of transforming growth factor-beta in aqueous humor of glaucomatous eyes and diabetic eyes. *Jpn J Ophthalmol* 2002;46:249-253.

142. Ozcan AA, Ozdemir N, Canataroglu A. The aqueous levels of TGF-beta2 in patients with glaucoma. *Int Ophthalmol* 2004;25:19-22.

143. Min SH, Lee TI, Chung YS, Kim HK. Transforming growth factor-beta levels in human aqueous humor of glaucomatous, diabetic and uveitic eyes. *Korean J Ophthalmol* 2006;20:162-165.

144. Javelaud D, Mauviel A. Mammalian transforming growth factor-betas: Smad signaling and physio-pathological roles. *Int J Biochem Cell Biol* 2004;36:1161-1165.

145. Javelaud D, Mauviel A. Crosstalk mechanisms between the mitogen-activated protein kinase pathways and Smad signaling downstream of TGF-beta: implications for carcinogenesis. *Oncogene* 2005;24:5742-5750.

146. Massague J. How cells read TGF-beta signals. *Nat Rev Mol Cell Biol* 2000;1:169-178.

147. McDowell CMT, H. E.; Wodinger, R.J.; Clark, A.F. Smad3 is necessary for transforming growth factor-beta2 induced ocular hypertension in mice. *Exp Eye Res* 2013;in press.

148. Tovar-Vidales T, Clark AF, Wordinger RJ. Transforming growth factor-beta2 utilizes the canonical Smad-signaling pathway to regulate tissue transglutaminase expression in human trabecular meshwork cells. *Exp Eye Res* 2011;93:442-451.

149. Sethi A, Jain A, Zode GS, Wordinger RJ, Clark AF. Role of TGFbeta/Smad signaling in gremlin induction of human trabecular meshwork extracellular matrix proteins. *Invest Ophthalmol Vis Sci* 2011;52:5251-5259.

150. Zode GS, Sethi A, Brun-Zinkernagel AM, Chang IF, Clark AF, Wordinger RJ. Transforming growth factor-beta2 increases extracellular matrix proteins in optic nerve head cells via activation of the Smad signaling pathway. *Mol Vis* 2011;17:1745-1758.

151. Webber HC, Bermudez JY, Sethi A, Clark AF, Mao W. Crosstalk between TGFbeta and Wnt signaling pathways in the human trabecular meshwork. *Exp Eye Res* 2016;148:97-102.

152. McDowell CM, Tebow HE, Wordinger RJ, Clark AF. Smad3 is necessary for transforming growth factor-beta2 induced ocular hypertension in mice. *Experimental Eye Research* 2013;116:419-423.

153. Tovar-Vidales T, Clark AF, Wordinger RJ. Transforming growth factor-beta2 utilizes the canonical smad-signaling pathway to regulate tissue transglutaminase expression in human trabecular meshwork cells. *Experimental Eye Research* 2011;93:442-451.

154. Sethi A, Mao W, Wordinger RJ, Clark AF. Transforming growth factor-beta induces extracellular matrix protein cross-linking lysyl oxidase (LOX) genes in human trabecular meshwork cells. *Invest Ophthalmol Vis Sci* 2011;52:5240-5250.

155. Sethi A, Jain A, Zode GS, Wordinger RJ, Clark AF. Role of TGFbeta/Smad signaling in gremlin induction of human trabecular meshwork extracellular matrix proteins. *IOVS* 2011;52:5251-5259.

156. Su Y, Yang C-YC, Li Z, et al. Smad7 siRNA inhibit expression of extracellular matrix in trabecular meshwork cells treated with TGF-β2. *Mol Vis* 2012;18:1881-1884.

157. Fuchshofer R, Stephan DA, Russell P, Tamm ER. Gene expression profiling of TGFbeta2- and/or BMP7-treated trabecular meshwork cells: Identification of Smad7 as a critical inhibitor of TGF-beta2 signaling. *Exp Eye Res* 2009;88:1020-1032.

158. Pervan CL. Smad-independent TGF-beta2 signaling pathways in human trabecular meshwork cells. *Exp Eye Res* 2016.

159. Montecchi-Palmer M, Bermudez JY, Webber HC, Patel GC, Clark AF, Mao W. TGFbeta2 induces the formation of cross-linked actin networks (CLANs) in human trabecular meshwork cells through the smad and non-smad dependent pathways. *Invest Ophthalmol Vis Sci* 2017;58:1288-1295.

160. Zhao X, Ramsey KE, Stephan DA, Russell P. Gene and protein expression changes in human trabecular meshwork cells treated with transforming growth factor-beta. *Invest Ophthalmol Vis Sci* 2004;45:4023-4034.

161. Medina-Ortiz WE, Belmares R, Neubauer S, Wordinger RJ, Clark AF. Cellular fibronectin expression in human trabecular meshwork and induction by transforming growth factor-β2. *IOVS* 2013;54:6779-6788.

162. Hernandez H, Medina-Ortiz WE, Luan T, Clark AF, McDowell CM. Crosstalk between transforming growth factor beta-2 and toll-like receptor 4 in the trabecular meshwork. *Invest Ophthalmol Vis Sci* 2017;58:1811-1823.

163. Wordinger RJ, Fleenor DL, Hellberg PE, et al. Effects of TGF-beta2, BMP-4, and gremlin in the trabecular meshwork: implications for glaucoma. *IOVS* 2007;48:1191-1200.

164. Lin L, Wang Y, Liu W, Huang Y. BAMBI inhibits skin fibrosis in keloid through suppressing TGF-beta1-induced hypernomic fibroblast cell proliferation and excessive accumulation of collagen I. *Int J Clin Exp Med* 2015;8:13227-13234.

165. Tovar-Vidales T, Fitzgerald AM, Clark AF. Human trabecular meshwork cells express BMP antagonist mRNAs and proteins. *Exp Eye Res* 2016;147:156-160.

166. Willis BC, Borok Z. TGF-beta-induced EMT: mechanisms and implications for fibrotic lung disease. *Am J Physiol Lung Cell Mol Physiol* 2007;293:L525-534.

167. Liu Y. Renal fibrosis: new insights into the pathogenesis and therapeutics. *Kidney Int* 2006;69:213-217.

168. Gressner AM, Weiskirchen R. Modern pathogenetic concepts of liver fibrosis suggest stellate cells and TGF-beta as major players and therapeutic targets. *J Cell Mol Med* 2006;10:76-99.

169. Bataller R, Brenner DA. Liver fibrosis. *J Clin Invest* 2005;115:209-218.

170. Huggins JT, Sahn SA. Causes and management of pleural fibrosis. *Respirology* 2004;9:441-447.

171. Schnaper HW, Hayashida T, Hubchak SC, Poncelet AC. TGF-beta signal transduction and mesangial cell fibrogenesis. *Am J Physiol Renal Physiol* 2003;284:F243-252.

172. Ihn H. The role of TGF-beta signaling in the pathogenesis of fibrosis in scleroderma. *Arch Immunol Ther Exp (Warsz)* 2002;50:325-331.

173. Flügel-Koch C, Ohlmann A, Fuchshofer R, Welge-Lussen U, Tamm ER. Thrombospondin-1 in the trabecular meshwork: localization in normal and glaucomatous eyes, and induction by TGF-beta1 and dexamethasone in vitro. *Exp Eye Res* 2004;79:649-663.

174. Fuchshofer R, Yu AH, Welge-Lussen U, Tamm ER. Bone morphogenetic protein-7 is an antagonist of transforming growth factor-beta2 in human trabecular meshwork cells. *Invest Ophthalmol Vis Sci* 2007;48:715-726.

175. Bollinger KE, Crabb JS, Yuan X, Putliwala T, Clark AF, Crabb JW. Quantitative proteomics: TGFbeta(2) signaling in trabecular meshwork cells. *Invest Ophthalmol Vis Sci* 2011;52:8287-8294.

176. Li J, Tripathi BJ, Tripathi RC. Modulation of pre-mRNA splicing and protein production of fibronectin by TGF-beta2 in porcine trabecular cells. *Invest Ophthalmol Vis Sci* 2000;41:3437-3443.

177. Han H, Wecker T, Grehn F, Schlunck G. Elasticity-dependent modulation of TGF-beta responses in human trabecular meshwork cells. *Invest Ophthalmol Vis Sci* 2011;52:2889-2896.

178. Mody AA, Wordinger RJ, Clark AF. Role of ID proteins in BMP4 inhibition of profibrotic effects of TGF-beta2 in human TM cells. *Invest Ophthalmol Vis Sci* 2017;58:849-859.

179. Zhao X, Russell P. Versican splice variants in human trabecular meshwork and ciliary muscle. *Mol Vis* 2005;11:603-608.

180. Acott TS, Kelley MJ. Extracellular matrix in the trabecular meshwork. *Experimental Eye Research* 2008;86:543-561.

181. Faralli JA, Schwinn MK, Gonzalez JM, Filla MS, Peters DM. Functional properties of fibronectin in the trabecular meshwork. *Experimental Eye Research* 2009;88:689-693.

182. White ES, Baralle FE, Muro AF. New insights into form and function of fibronectin splice variants. *J Pathol* 2008;216:1-14.

183. White ES, Muro AF. Fibronectin splice variants: understanding their multiple roles in health and disease using engineered mouse models. *IUBMB Life* 2011;63:538-546.

184. To WS, Midwood KS. Plasma and cellular fibronectin: distinct and independent functions during tissue repair. *Fibrogenesis Tissue Repair* 2011;4:21.

185. Wierzbicka-Patynowski I, Schwarzbauer JE. The ins and outs of fibronectin matrix assembly. *J Cell Sci* 2003;116:3269-3276.

186. Mao Y, Schwarzbauer JE. Fibronectin fibrillogenesis, a cell-mediated matrix assembly process. *Matrix Biol* 2005;24:389-399.

187. Jarnagin WR, Rockey DC, Koteliansky VE, Wang SS, Bissell DM. Expression of variant fibronectins in wound healing: cellular source and biological activity of the EIIIA segment in rat hepatic fibrogenesis. *J Cell Biol* 1994;127:2037-2048.

188. George J, Wang SS, Sevcsik AM, et al. Transforming growth factor-beta initiates wound repair in rat liver through induction of the EIIIA-fibronectin splice isoform. *Am J Pathol* 2000;156:115-124.

189. Saito S, Yamaji N, Yasunaga K, et al. The fibronectin extra domain A activates matrix metalloproteinase gene expression by an interleukin-1-dependent mechanism. *J Biol Chem* 1999;274:30756-30763.

190. Hino K, Shiozawa S, Kuroki Y, et al. EDA-containing fibronectin is synthesized from rheumatoid synovial fibroblast-like cells. *Arthritis Rheum* 1995;38:678-683.

191. Kelsh RM, McKeown-Longo PJ, Clark RA. EDA fibronectin in keloids create a vicious cycle of fibrotic tumor formation. *J Invest Dermatol* 2015;135:1714-1718.

192. Andrews JP, Marttala J, Macarak E, Rosenbloom J, Uitto J. Keloid Pathogenesis: Potential Role of Cellular Fibronectin with the EDA Domain. *J Invest Dermatol* 2015;135:1921-1924.

193. Booth AJ, Wood SC, Cornett AM, et al. Recipient-derived EDA fibronectin promotes cardiac allograft fibrosis. *J Pathol* 2012;226:609-618.

194. He M, Yu S, Xue AM, et al. Expression of EDA-fibronectin in injured human skin fibroblast and its potential application in estimation of wound healing. *Fa Yi Xue Za Zhi* 2007;23:94-96.

195. Muro AF, Chauhan AK, Gajovic S, et al. Regulated splicing of the fibronectin EDA exon is essential for proper skin wound healing and normal lifespan. *J Cell Biol* 2003;162:149-160.

196. Okamura Y, Watari M, Jerud ES, et al. The extra domain A of fibronectin activates Toll-like receptor 4. *J Biol Chem* 2001;276:10229-10233.

197. Yang H, Young DW, Gusovsky F, Chow JC. Cellular events mediated by lipopolysaccharide-stimulated toll-like receptor 4. MD-2 is required for activation of mitogen-activated protein kinases and Elk-1. *J Biol Chem* 2000;275:20861-20866.

198. Julier Z, Martino MM, de Titta A, Jeanbart L, Hubbell JA. The TLR4 agonist fibronectin extra domain A is cryptic, exposed by elastase-2; use in a fibrin matrix cancer vaccine. *Scientific reports* 2015;5:8569.

199. Szabo G, Dolganiuc A, Mandrekar P. Pattern recognition receptors: a contemporary view on liver diseases. *Hepatology* 2006;44:287-298.

200. Yarovinsky F. Innate immunity to *Toxoplasma gondii* infection. *Nat Rev Immunol* 2014;14:109-121.

201. Miller RE, Belmadani A, Ishihara S, et al. Damage-associated molecular patterns generated in osteoarthritis directly excite murine nociceptive neurons through Toll-like receptor 4. *Arthritis Rheumatol* 2015;67:2933-2943.

202. Medzhitov R, Preston-Hurlburt P, Janeway CA, Jr. A human homologue of the *Drosophila* Toll protein signals activation of adaptive immunity. *Nature* 1997;388:394-397.

203. Janeway CA, Jr., Medzhitov R. Lipoproteins take their toll on the host. *Curr Biol* 1999;9:R879-882.

204. Chaudhary PM, Ferguson C, Nguyen V, et al. Cloning and characterization of two Toll/Interleukin-1 receptor-like genes TIL3 and TIL4: evidence for a multi-gene receptor family in humans. *Blood* 1998;91:4020-4027.

205. Chow JC, Young DW, Golenbock DT, Christ WJ, Gusovsky F. Toll-like receptor-4 mediates lipopolysaccharide-induced signal transduction. *J Biol Chem* 1999;274:10689-10692.

206. Medzhitov R, Preston-Hurlburt P, Kopp E, et al. MyD88 is an adaptor protein in the hToll/IL-1 receptor family signaling pathways. *Mol Cell* 1998;2:253-258.

207. Rock FL, Hardiman G, Timans JC, Kastelein RA, Bazan JF. A family of human receptors structurally related to *Drosophila* Toll. *Proc Natl Acad Sci U S A* 1998;95:588-593.

208. Yang QW, Xiang J, Zhou Y, Zhong Q, Li JC. Targeting HMGB1/TLR4 signaling as a novel approach to treatment of cerebral ischemia. *Front Biosci (Schol Ed)* 2010;2:1081-1091.

209. Jiang D, Liang J, Noble PW. Hyaluronan as an immune regulator in human diseases. *Physiol Rev* 2011;91:221-264.

210. Gingery A, Bradley EW, Pederson L, Ruan M, Horwood NJ, Oursler MJ. TGF-beta coordinately activates TAK1/MEK/AKT/NFkB and SMAD pathways to promote osteoclast survival. *Exp Cell Res* 2008;314:2725-2738.

211. Nakamura J, Meguro A, Ota M, et al. Association of toll-like receptor 2 gene polymorphisms with normal tension glaucoma. *Mol Vis* 2009;15:2905-2910.

212. Kondkar AA, Mousa A, Azad TA, et al. Analysis of toll-like receptor 2 polymorphism (rs5743704) in saudi patients with primary open-angle glaucoma. *Genet Test Mol Biomarkers* 2016;20:216-219.

213. Shibuya E, Meguro A, Ota M, et al. Association of Toll-like receptor 4 gene polymorphisms with normal tension glaucoma. *Invest Ophthalmol Vis Sci* 2008;49:4453-4457.

214. Suh W, Kim S, Ki CS, Kee C. Toll-like receptor 4 gene polymorphisms do not associate with normal tension glaucoma in a Korean population. *Mol Vis* 2011;17:2343-2348.

215. Takano Y, Shi D, Shimizu A, et al. Association of Toll-like receptor 4 gene polymorphisms in Japanese subjects with primary open-angle, normal-tension, and exfoliation glaucoma. *Am J Ophthalmol* 2012;154:825-832 e821.

216. Abu-Amero KK, Kondkar AA, Mousa A, et al. Analysis of toll-like receptor rs4986790 polymorphism in Saudi patients with primary open angle glaucoma. *Ophthalmic Genet* 2017;38:133-137.

217. Navarro-Partida J, Martinez-Rizo AB, Ramirez-Barrera P, et al. Association of Toll-like receptor 4 single-nucleotide polymorphisms Asp299Gly and Thr399Ile with the risk of primary open angle glaucoma. *Graefes Arch Clin Exp Ophthalmol* 2017;255:995-1001.

218. Huang H, Shiffman ML, Friedman S, et al. A 7 gene signature identifies the risk of developing cirrhosis in patients with chronic hepatitis C. *Hepatology* 2007;46:297-306.

219. Li Y, Chang M, Abar O, et al. Multiple variants in toll-like receptor 4 gene modulate risk of liver fibrosis in caucasians with chronic hepatitis C infection. *J Hepatol* 2009;51:750-757.

220. Bhattacharyya S, Kelley K, Melichian DS, et al. Toll-like receptor 4 signaling augments transforming growth factor-beta responses: a novel mechanism for maintaining and amplifying fibrosis in scleroderma. *Am J Pathol* 2013;182:192-205.

221. Seki E, De Minicis S, Osterreicher CH, et al. TLR4 enhances TGF-beta signaling and hepatic fibrosis. *Nat Med* 2007;13:1324-1332.

222. Pulskens WP, Rampanelli E, Teske GJ, et al. TLR4 promotes fibrosis but attenuates tubular damage in progressive renal injury. *J Am Soc Nephrol* 2010;21:1299-1308.

223. Campbell MT, Hile KL, Zhang H, et al. Toll-like receptor 4: a novel signaling pathway during renal fibrogenesis. *J Surg Res* 2011;168:e61-69.

224. Poltorak A, He X, Smirnova I, et al. Defective LPS signaling in C3H/HeJ and C57BL/10ScCr mice: mutations in Tlr4 gene. *Science* 1998;282:2085-2088.

225. Yang L, Seki E. Toll-like receptors in liver fibrosis: cellular crosstalk and mechanisms. *Front Physiol* 2012;3:138.

226. Guo J, Friedman SL. Toll-like receptor 4 signaling in liver injury and hepatic fibrogenesis. *Fibrogenesis Tissue Repair* 2010;3:21.

227. McDowell CM, Luan T, Zhang Z, et al. Mutant human myocilin induces strain specific differences in ocular hypertension and optic nerve damage in mice. *Exp Eye Res* 2012;100:65-72.

228. Franko AJ, Sharplin J, Ward WF, Taylor JM. Evidence for two patterns of inheritance of sensitivity to induction of lung fibrosis in mice by radiation, one of which involves two genes. *Radiat Res* 1996;146:68-74.

229. Johnston CJ, Piedboeuf B, Baggs R, Rubin P, Finkelstein JN. Differences in correlation of mRNA gene expression in mice sensitive and resistant to radiation-induced pulmonary fibrosis. *Radiat Res* 1995;142:197-203.

230. Johnston CJ, Piedboeuf B, Rubin P, Williams JP, Baggs R, Finkelstein JN. Early and persistent alterations in the expression of interleukin-1 alpha, interleukin-1 beta and tumor necrosis factor alpha mRNA levels in fibrosis-resistant and sensitive mice after thoracic irradiation. *Radiat Res* 1996;145:762-767.

231. Souza AC, Tsuji T, Baranova IN, et al. TLR4 mutant mice are protected from renal fibrosis and chronic kidney disease progression. *Physiol Rep* 2015;3.

232. Margetts PJ, Hoff C, Liu L, et al. Transforming growth factor beta-induced peritoneal fibrosis is mouse strain dependent. *Nephrol Dial Transplant* 2013;28:2015-2027.

233. Borrás T, Rowlette LL, Erzurum SC, Epstein DL. Adenoviral reporter gene transfer to the human trabecular meshwork does not alter aqueous humor outflow. Relevance for potential gene therapy of glaucoma. *Gene Ther* 1999;6:515-524.

234. Ueyama K, Mori K, Shoji T, et al. Ocular localization and transduction by adenoviral vectors are serotype-dependent and can be modified by inclusion of RGD fiber modifications. *PLoS One* 2014;9:e108071.

235. Millar JC, Phan TN, Pang IH, Clark AF. Strain and age effects on aqueous humor dynamics in the mouse. *Invest Ophthalmol Vis Sci* 2015;56:5764-5776.

236. Millar JC, Clark AF, Pang IH. Assessment of aqueous humor dynamics in the mouse by a novel method of constant-flow infusion. *Invest Ophthalmol Vis Sci* 2011;52:685-694.

CHAPTER II

CROSSTALK BETWEEN TRANSFORMING GROWTH FACTOR BETA-2 AND TOLL-LIKE RECEPTOR 4 IN THE TRABECULAR MESHWORK

Humberto Hernandez, Wanda E. Medina-Ortiz, Tomi Luan, Abbot F. Clark, and Colleen M. McDowell

IOVS February 2017

ABSTRACT

Purpose

The trabecular meshwork (TM) is involved in the outflow of aqueous humor and intraocular pressure (IOP) regulation. Regulation of the ECM by TGFβ2 signaling pathways in the TM has been extensively studied. Recent evidence has implicated toll-like receptor 4 (TLR4) in the regulation of ECM and fibrogenesis in liver, kidney, lung, and skin. Here, we investigate the role of TGFβ2-TLR4 signaling crosstalk in the regulation of the ECM in the TM and ocular hypertension.

Methods

Cross-sections of human donor eyes, primary human TM cells in culture, and dissected mouse TM rings were used to determine *Tlr4* expression in the TM. TM cells in culture were treated with TGFβ2 (5ng/ml), TLR4 inhibitor (TAK-242, 15μM), and a TLR4 ligand (cFN-EDA). A/J (n=13), AKR/J (n=7), BALBc/J (n=8), C3H/HeJ (n=20), and C3H/HeOuJ (n=10) mice were injected intravitreally with Ad5.hTGFβ2$^{c226s/c228s}$ in one eye, with the uninjected contralateral eye serving as a control. Conscious IOP measurements were taken using a TonoLab rebound tonometer.

Results

TLR4 is expressed in the human and mouse TM. Inhibition of TLR4 signaling in the presence of TGFβ2 decreases fibronectin expression. Activation of TLR4 by cFN-EDA in the presence of TGFβ2 further increases fibronectin, laminin, and collagen-1 expression, and TLR4 signaling inhibition blocks this effect. Ad5.hTGFβ2$^{c226s/c228s}$ induces ocular hypertension in wild-type mice but has no effect in *Tlr4* mutant (C3H/HeJ) mice.

Conclusions

These studies identify TGFβ2–TLR4 crosstalk as a novel pathway involved in ECM regulation in the TM and ocular hypertension. These data further explain the complex mechanisms involved in the development of glaucomatous TM damage.

Keywords**:** TGFβ2, TLR4, trabecular meshwork

Grant support: Bright Focus Foundation G2014063 (CMM), R01EY026529 (CMM), and Neurobiology of Aging training grant T32AG020494 (HH).

Introduction

The glaucomas are a heterogeneous group of optic neuropathies with clinical features that include cupping of the optic disc, thinning and loss of the retinal nerve fiber layer, and characteristic visual field defects[1]. A variety of risk factors have been identified for the development of glaucoma including elevated intraocular pressure (IOP), age, family history, central corneal thickness, and steroid responsiveness. IOP is the most significant causative risk factor for both the development and progression of glaucoma. Not all ocular hypertensive individuals develop glaucoma, but lowering IOP decreases the risk for developing glaucoma[2] and decreases glaucoma progression both early[3] and late[4] in the disease.

IOP is regulated by aqueous humor (AH) production and drainage from the eye. The trabecular meshwork (TM) is well known to be a critical tissue in aqueous humor drainage. The TM is a porous structure consisting of a series of fenestrated beams and sheets of extracellular matrix (ECM) covered with TM cells[5, 6]. The ECM of the TM is important in forming an outflow pathway for aqueous humor drainage[7, 8]. The TM imparts a normal resistance to AH outflow that becomes abnormally increased in glaucoma. The ECM composition of the TM plays a major role in the regulation of IOP. The ability of the TM to respond to the dynamic changes in IOP in a homeostatic state relies on the ECM remodeling capabilities of the TM[9]. Even in a resting normal state, the TM cells express matrix metalloproteases (MMPs), tenascin C, and alpha-smooth muscle actin, all of which are typically only expressed in tissues undergoing active remodeling[10-15]. The presence of these proteins in the TM in a resting state indicates the TM may have properties that allow it to undergo transient tissue repair as part of normal maintenance, allowing proper aqueous humor drainage from the eye and IOP regulation. There is also a great deal of evidence demonstrating changes to the TM ECM in glaucoma. Increased deposition of

ECM proteins in the TM, increased aqueous humor outflow resistance, and increased IOP are all associated with primary open angle glaucoma (POAG)[16, 17]. The glaucomatous TM also has increased deposition of fibronectin[18, 19], fine fibrillar material[20, 21] and altered glycosaminoglycan composition[22]. These data demonstrate that the ECM architecture of the TM is important in regulating aqueous humor outflow and IOP.

It is well established that aqueous humor levels of transforming growth factor-β2 (TGFβ2) are elevated in POAG patients[23-26]. We and others have shown that TGFβ2 treatment of TM cells alters the ECM composition[27-29] and induces ECM cross-linking[30-32]. The addition of TGFβ2 elevates IOP in the anterior segment perfusion organ culture models[27, 33] and over-expression of a bioactivated form of TGFβ2 in mouse eyes causes ocular hypertension[34-36]. TGFβ2 is known to regulate the expression of ECM proteins through the canonical SMAD pathway as well as non-canonical signaling pathways[37-40]. We have previously demonstrated that TGFβ2 signals through the canonical SMAD and non-SMAD pathways and alters the ECM in human TM cells[30, 31]. We have also demonstrated that TGFβ2 signaling through the canonical SMAD pathway is essential for TGFβ2-induced ocular hypertension in mice[36]. Additionally, the cellular fibronectin isoform EDA (cFN-EDA) is present, and induced by TGFβ2, in human TM cells and tissues, and cFN-EDA protein expression is elevated in glaucomatous TM tissues[19]. In summary, these data suggest that TGFβ2 regulates the expression of ECM proteins in the TM, and the effects of TGFβ2 signaling are a major component in the development of ocular hypertension.

TLR4 is a member of the toll-like receptor family. TLR4 was originally identified as the specific receptor for lipopolysaccharide (LPS)[41, 42]. TLR4 can also be activated by endogenous ligands, known as DAMPs (damage-associated molecular patterns), which are generated *in situ*

as a result of injury, cell damage, ECM remodeling, and oxidative stress[43, 44]. Recent evidence has linked DAMP activated TLR4 signaling to fibrosis and the regulation and production of ECM proteins. DAMPs (cFN-EDA, low molecular weight hyaluronan, tenascin C, amongst others) have been shown to activate TLR4 and augment TGFβ signaling and downstream fibrotic responses in other diseases such as hepatic fibrosis, renal fibrosis, lesional skin and lung in scleroderma patients, as well as in *Tlr4* mutant mice[41, 45-48]. The role of TLR4 in fibrogenesis has been previously studied including identification of specific SNP alleles in *TLR4* that have been associated with a delayed progression of fibrosis in liver disease and confer an overall protective effect[49, 50]. Here we demonstrate that a similar TGFβ-TLR4 crosstalk is involved in the production and regulation of the ECM in the TM as well as regulation of IOP.

MATERIALS AND METHODS

Human TM cell culture

Primary normal human TM cell strains, NTM cells, (NTM1022-02, NTM115-01, NTM210-05, and NTM176-04) were isolated from normal (non-glaucomatous) donor eyes and characterized as previously described[19, 28, 51]. All donor tissues were obtained and managed according to the guidelines in the Declaration of Helsinki for research involving human tissue. The transformed GTM3 cell line has previously been described[52]. Cells were cultured and maintained in Dulbecco's modified Eagle's medium (DMEM; Invitrogen-Gibco Life Technologies, Grand Island, NY) containing 10% fetal bovine serum (FBS; Atlas Biologicals Products, Fort Collins, CO) and supplemented with penicillin (100 units/ml), streptomycin (0.1 mg/ml) and L-glutamine (0.292 mg/ml) (Gibco BRL Life Technologies).

TLR4 inhibition and activation

Primary NTM cells and GTM3 cells were grown to confluency and pre-treated with a TLR4 selective inhibitor TAK-242 (also known as CLI-095, InvivoGen, San Diego, CA) at 15 μM for 2 hrs. TAK-242 selectively inhibits the interaction between TLR4 and its adaptor molecules, TIRAP and TRAM, via the TLR4 intracellular Cys747 residue, thereby inhibiting TLR4 downstream signaling events[53]. Cells were then incubated with TGFβ2 (5 ng/ml) and/or TAK-242 (15 μM) for 24, 48, or 72 hours in serum free medium. For TLR4 activation studies, cellular fibronectin (cFN) containing FN-EDA was isolated from human foreskin fibroblast (F2518; Sigma-Aldrich, St. Louis, MO) and reconstituted with sterile phosphate-buffered saline solution (PBS) to a stock concentration of 1 mg/ml. Precautions were taken to avoid repeated thaw/freezing steps. NTM cells were grown to confluency and pre-treated with TAK-242 and then subsequently incubated with serum free medium containing TGFβ2 (5 ng/ml), and/or TAK-242 (15 μM), and/or cFN-EDA (10 μg/ml), and/or LPS (100 ng/ml) for 24, 48, or 72 hours. Western blot and qPCR experiments were performed as described below.

Cellular FN coating

The initial analysis with cFN-EDA was done on coated surfaces (Figure 4A, 4B). Wells from a 24-well plate were coated with 180 μl of cFN-EDA (10 μg/ml), and air-dried under sterile conditions (1-2 hours). The same volume of sterile PBS was applied to control surfaces. NTM cells were seeded ($5.5x10^4$ cells) on cFN-EDA coated or uncoated surfaces. TGFβ2 (5 ng/ml) was added and cultured for 48 hrs. Western blot was performed as described below with the following exceptions, Super Signal West Dura ECL Chemiluminescence Detection kit (Pierce Biotechnology, Rockford, IL) was used to develop the immunolabled signals and blots were imaged using the FluorChem 8900 Image System (Alpha Innotech, San Leandro, CA).

Immunocytochemistry

Primary NTM cells were seeded on 24 well plates on coverslips and allowed to reach confluency. After completing the treatment time course of 48 (to assess fibronectin and laminin) or 72 (to assess collagen-1) hours, cells were washed with PBS, fixed with 4% paraformaldehyde (PFA), permeabilized with 0.05% Triton X-100 in PBS and blocked using Superblock Blocking Buffer in PBS (Thermo Fisher Scientific; Rockford, IL) for 60 minutes at room temperature. Cells were labeled overnight at 4°C with rabbit anti-fibronectin (EMD Millipore; Billerica, MA) 1:1000 dilution, anti-laminin (Novus Biologicals, LL; Littleton, CO) 1:250 dilution, and anti-collagen-1 (Novus Biologicals, LL; Littleton, CO) 1:250 dilution in Superblock Blocking Buffer in PBS. Treatment without the primary antibody was used as a negative control. Coverslips were incubated for 2 hours using Alexa-Fluor-labeled anti-rabbit (Life Technologies; Carlsbad, CA) 1:1000 dilution. Coverslips were mounted to slides with Prolong Gold mounting medium containing DAPI (Invitrogen-Molecular Probes; Carlsbad, CA). Image acquisition was performed using the Keyence BZ-X700 fluorescence microscope (Keyence Corporation of America; Itasca, IL). All images were taken at 200x magnification, scale bar represents 100 μm.

RT-PCR and Quantitative (q)PCR

For the human TM cell strain and GTM3 samples, cells were washed with PBS and RNA was extracted using Isol-RNA Lysis Reagent (5PRIME, Gaithersburg, MD). For the mouse samples, TM rings were carefully dissected taking extra care to remove as much of the sclera and cornea as possible, and RNA was extracted using Isol-RNA Lysis Reagent (5PRIME, Gaithersburg, MD). Samples were reverse-transcribed to cDNA (Bio-Rad iScript cDNA

synthesis Kit; Bio-Rad, Hercules, CA). Each PCR reaction contained: 10 µl of 2X iQ SYBR Green Supermix (Bio-Rad, Hercules, CA), 0.25 µl of forward primer (100 µM), 0.25 µl reverse primer (100 µM), 8.5 µl dH2O, and 1.0 µl of cDNA template (25 ng/ul). Primer used in the PCR reactions: mouse *Tlr4* (5'- AGTGGGTCAAGGAACAGAAGCA-3', 5'-CTTTACCAGCTCATTTCTCACC-3')[54], human *TLR4* (5'- AGATGGGGCATATCAGAGC-3', 5'- GTCCATCGTTTGGTTCTGG-3')[55], *FN* (5'GGTGACACTTATGAGCGCCCTA-3', 5'-AACATGTAGCCACCAGTCTCAT-3'), *COL1* (5'-GGAATGAAAGG GACACAGAGG-3', 5'-TAGCACCATCATTTCCACGA-3'), and *GAPDH* (5'-ACTCCACTCACGGCAAATTC-3', 5'-TCTCCATGGT GGTGAAGAACA-3'). For RT-PCR experiments, samples were run on a 3% agarose gel. For qPCR, samples were run on a BioRad CFX96 Real-Time System C1000 Touch Thermal Cycler and fold change calculated using the ΔΔCt method comparing expression to *Gapdh* and untreated control cells. Statistical significance was calculated by one-way ANOVA and Tukey post-hoc analysis.

Western blot analysis

All western blot studies were performed as stated unless otherwise noted. Briefly, NTM cell strains were treated as stated above for 48 or 72 hrs. Whole cell lysate and conditioned medium [56] were collected from each condition. Cell lysates were extracted using lysis buffer (M-PER, Thermo Fisher Scientific Inc., Rockford, IL; EDTA and protease inhibitor cocktail, Pierce Biotechnology, Inc., Rockford, IL), and Bio-Rad Dc protein Lowry assay (Bio-Rad Laboratories, Hercules, CA) was used to estimate total protein concentrations. Each loading sample contained 35 µg of lysate and 4x Laemmli Buffer (Bio-Rad Laboratories, Hercules, CA), for a total volume of 40 µL. Samples were boiled for 10 minutes followed by separation using 8% SDS-PAGE. To

verify equal loading for CM samples, gels were stained with Gel Code Blue Stain Reagent (Thermo Fisher Scientific Inc., Rockford, IL). Proteins from electrophoresed gels were transferred to PVDF membranes (Millipore, Bedford, MA), and membranes were blocked with Superblock Blocking Buffer in TBS (Thermo Fisher Scientific; Rockford, IL). Membranes were immunolabeled overnight at 4°C with primary antibodies: rabbit anti-fibronectin (EMD Millipore; Billerica, MA) dilution 1:1000 and rabbit anti-GAPDH (Cell Signaling, Danvers, MA) dilution 1:1000. Blots were incubated for 1 hour with horseradish peroxidase (HRP) conjugated goat anti-rabbit secondary antibody (1:1,000; Pierce Biotechnology, Inc., Rockford, IL) diluted in Superblock Blocking Buffer in TBS. Immunolabeled signals were developed using Clarity™ Western ECL Substrate, and blot images were acquired using ChemiDoc Touch Imaging System (Bio-Rad Laboratories, Hercules, CA). Each experiment was repeated 2-3 times in each individual NTM cell strain and a total of four independent NTM cell strains were tested. Densitometry analysis of Western immunoblot images was used to determine changes in protein content after treatment. Band intensity for fibronectin and GAPDH (loading control) was measured using Image Lab Software (Bio-Rad Laboratories). Each target protein densitometry value was normalized against its corresponding GAPDH value, and fold change was compared to control and represented as the mean ± SEM. Statistical significance was determined by one-way ANOVA and Tukey post-hoc analysis comparing all treatments.

Cell viability assay

GTM3 and primary human TM cells were plated at 5000 cells/well in a 96 well opaque walled plate with 100 ul of complete medium. After 24 hours, cells were treated (8 wells/treatment). Cells were treated with TAK-242 (0.5, 1.0, 5.0, 15.0, or 50.0 μM) or vehicle

control for 24 hours. Cell viability was then assessed using the CellTiter-Glo® Luminescent Cell Viability Assay (Promega, Madison, WI). Briefly, CellTiter-Glo® Reagent was added equal to the volume of cell culture medium present (100µl of reagent to 100µl of medium containing cells). Contents were mixed for 2 minutes on an orbital shaker to induce cell lysis. The plate was incubated at room temperature for 10 minutes to stabilize luminescent signal and luminescence was recorded.

Animals and adenovirus injection

All experiments were conducted in compliance with the ARVO Statement of the Use of Animals in Opththalmic and Vision Research and the University of North Texas Health Science Center (UNTHSC; Fort Worth, TX, USA) Institutional Animal Care and Use Committee (IACUC) Guidelines and Regulations. We used A/J (n=13), AKR/J (n=7), BALBc/J (n=8), C3H/HeJ (n=20), and C3H/HeOuJ (n=10) mouse strains obtained from The Jackson Laboratory. All mice were 5-8 months old at the start of the experiment. All animals were housed in the UNTHSC vivarium. Adenovirus 5 (Ad5) viral vector expressing human $TGF\beta^{c226s/c228s}$ (hereafter referred to as Ad5.TGFβ2) (University of Iowa, Iowa City, IA) was used to over-express TGFβ2 as previously described[34-36]. Ad5.null vector (Vector Biolabs, Malvern, PA) was used as a negative control. Briefly, 2 µl of 2.5×10^7 plaque forming units (pfu) were intravitreally injected into one eye, and the contralateral eyes were used as negative controls.

Intraocular pressure measurements

IOP was measured as previously described[34-36, 57]. Briefly, IOP was measured on conscious mice using the Tonolab tonometer (Colonial Medical Supply, Franconia, NH). All IOP measurements were performed during the same time period of the light-on phase. IOP exposure was calculated by subtracting the area under the curve (AUC) of the uninjected control eyes from the AUC of injected eyes for each individual animal's IOP readings over time as previously described[35, 36, 57]. Statistical significance was determined by Student's paired t-test at each time point comparing the injected eye to the contralateral uninjected control eye for A/J, BALBc/J and AKR/J mice. Since the C3H/HeJ and C3H/HeOuJ strains were compared to each other, statistical significance was determined by one way ANOVA at each time point comparing the injected eye to the contralateral uninjected control eye between each strain. All mice were 5-8 months old at the start of the experiment.

Immunohistochemistry of mouse eyes

After completion of the IOP time course, mouse eyes were enucleated and fixed in 4% paraformaldehyde overnight. Eyes were embedded in paraffin, cut into 5 μm sections, and transferred to glass slides. Deparaffinization was performed by washing two times with xylene, 100% ethanol, 95% ethanol, and 50% ethanol for 2 minutes each. Slides were then soaked in PBS for 5 minutes. Tissues were blocked using Superblock Blocking Buffer in PBS (Thermo Fisher Scientific; Rockford, IL) for 30-60 minutes. Rabbit anti-fibronectin (EMD Millipore; Billerica, MA) 1:1000 dilution was used to label fibronectin, followed by Alexa-Fluor-labeled anti-rabbit Ig (Life Technologies; Carlsbad, CA) 1:1000 dilution. Prolong Gold mounting medium containing DAPI (Invitrogen-Molecular Probes; Carlsbad, CA) was used to mount the

slides and imaged using fluorescent microscope Nikon ECLIPSE Ti-U (Nikon Instruments Inc.; Melville, NY) equipped with a CRi Nuance FX Camera System (Perkin-Elmer, Waltham, MA). All images were taken at 400x magnification; scale bar represents 50 μm.

Immunohistochemistry of human eyes

Human donor eyes were obtained formalin fixed within 6 hours of death from regional eye banks, and were paraffin embedded and sectioned (two 5-μm sagittal sections per slide; n = 8 donors). Sections were deparaffinized, rehydrated, and processed for citrate/heat antigen retrieval, 15 minutes in 100°C citrate buffer (pH 6.0) followed by 15 minutes in room temperature citrate buffer (pH 6.0). Nonspecific staining was blocked by incubation for 15 minutes with 0.05 M glycine/PBS followed by 30 minutes with 5% normal goat serum/PBS. Sections were immunolabeled overnight at 4°C with rabbit anti-TLR4 antibody (1:1000) (Abcam, Cambridge, United Kingdom), washed, and incubated for an hour with secondary antibody. Secondary antibody used was donkey anti-rabbit Alexa Fluor 488 (1:500). Slides were mounted and images acquired using a Nikon Eclipse Ti inverted fluorescence microscope (Nikon, Inc., Melville, NY) equipped with the Cri Nuance FX Camera System (Perkin-Elmer, Inc., Waltham, MA). All images were taken at 400x magnification, scale bar represents 50 μm.

RESULTS

TLR4 is expressed in the mouse and human TM

TLR4 has been well studied in other tissues of the eye such as the retina, iris, and cornea. In addition, TLR4 was recently reported to be expressed in the TM[58]. Here we confirm these data and demonstrate that TLR4 is expressed in the human TM (Figure 1A,1B), in primary human

TM cell cultures (Figure 1C), as well as in the TM of several inbred mouse strains (Figure 1D).

Inhibition of TLR4 signaling blocks TGFβ2 induced ECM production in primary human TM cells

It is well established that TGFβ2 induces ECM protein production in the TM. Here, we demonstrate that inhibition of TLR4 signaling by a selective inhibitor, TAK-242, blocks the effect of TGFβ2 on ECM production. A cell viability assay and dose response assay was performed using GTM3 cells (Figure 2A) and a primary human cell strain (Figure 2B) to determine the inhibitor toxicity and efficacy in TM cells. Cell viability significantly decreased at 50 μM in both GTM3 cells and the primary human TM cells (Figure 2A, 2B). In addition, TAK-242 significantly decreased TGFβ2 (5ng/mL) induced fibronectin [59] and collagen-1 (COL1) mRNA expression at 5 μM and 15 μM (Figure 2C, 2D). TAK-242 (15 μM) also significantly decreased TGFβ2 induced FN protein expression (Figure 2E, 2F). Therefore, a 15 μM concentration of TAK-242 was determined to be the optimal concentration for maximum inhibition of TGFβ2 induced ECM production in TM cells.

Primary TM cells were treated with TGFβ2 (5ng/mL) and 15 μM of the TLR4 signaling inhibitor TAK-242 for 48 hours. As previously reported, TGFβ2 induced the expression of FN in both cell lysates (Figure 3A, 3B) and in conditioned medium (Figure 3C, 3D). However, TLR4 signaling inhibition significantly blocked TGFβ2-induced FN expression, and FN levels remained similar to control levels in both cell lysates and conditioned medium (Figure 3) (n=4 primary TM cell strains, each repeated in 3 independent experiments). We also demonstrated this effect at the RNA level (data not shown): TGFβ2 significantly increased fibronectin mRNA expression 4.69 +/- 0.99 fold, while TGFβ2 in the presence of TAK-242 blocked this effect with

a fibronectin mRNA expression of 1.42 +/- 0.61 fold (n=3 primary human TM cells strains, fold change calculated to untreated controls cells and *Gapdh* expression, $p<0.05$ by one-way ANOVA). There was no significant difference between untreated control cells and TGFβ2 + TAK-242 treated cells. These data suggest the TLR4 signaling plays a major role in the TGFβ2 signaling pathway affecting the ECM in TM cells.

Activation of TLR4 enhances TGFβ2 induced ECM production in human TM cells

cFN-EDA is an isoform of FN and is a known ligand of TLR4. Previous studies have demonstrated that cFN-EDA can activate TLR4 signaling[60]. In addition, we have previously shown that cFN-EDA is significantly elevated in the glaucomatous human TM compared to normal eyes[19]. Therefore, we utilized cellular FN (cFN) containing FN-EDA as a TLR4 activator (cFN-EDA). The role of cFN-EDA in TM cells was tested using cFN (10 μg/ml) coated surfaces compared to uncoated control treated cells and uncoated TGFβ2 treated cells for 48 hours (Figure 4A, 4B). Using this methodology, we demonstrate that both TGFβ2 and cFN-EDA significantly increase FN expression in cell lysates (n=3 primary human TM cell strains, $p<0.05$). These data show that cFN-EDA is able to induce the expression of FN to the same degree as TGFβ2.

We also demonstrate that cFN-EDA is able to enhance the effects of TGFβ2 in primary human TM cells by adding cFN to the culture medium. TM cells were grown to confluency and then treated with cFN-EDA (10 μg/ml), TGFβ2 (5 ng/ml), and/or TAK-242 (15 μM) for 72 hours (n=4 primary TM cell strains, each repeated in 2 independent experiments). As expected, TGFβ2 significantly induced FN expression compared to control cells ($p<0.001$) (Figure 4C, 4D). There was no significant difference between TGFβ2 treated cells and cFN-EDA treated

cells, indicating they equally induce expression of FN in the cell lysates. cFN-EDA further enhanced the TGFβ2 induction of FN protein expression (Figure 4C, 4D). The TLR4 signaling inhibitor TAK-242 was able to block both TGFβ2 and cFN-EDA induced expression of FN, $p<0.01$ (Figure 4C, 4D).

In addition to western blotting techniques, we also tested the effect of TGFβ2 and TLR4 on ECM proteins using immunocytochemistry. TM cells were grown to confluency and then treated with cFN-EDA (10 μg/ml), TGFβ2 (5 ng/ml), and/or TAK-242 (15 μM) for 48 or 72 hours. As a positive control we utilized the known TLR4 ligand, LPS (100 ng/ml), to independently activate TLR4 in our culture system. As expected, TGFβ2 induced FN (Figure 5B), COL1 (Figure 6B), and Laminin (Figure 7B) expression compared to untreated control cells (Figure 5A, 6A, 7A). TAK-242 blocked the TGFβ2 induction of each of these proteins, FN (Figure 5D), COL1 (Figure 6D), and Laminin (Figure 7D). In addition, cFN-EDA was able to independently induce expression of FN (Figure 5E), COL1 (Figure 6E), and Laminin (Figure 7E). Moreover, cFN-EDA in the presence of TGFβ2 enhanced the effect of TGFβ2 alone and cFN-EDA alone on FN (Figure 5F), COL1 (Figure 6F), and Laminin (Figure 7F). TAK-242 completely blocked the effect of both cFN-EDA and TGFβ2 on FN (Figure 5G, 5H), COL1 (Figure 6G, 6H), and Laminin (Figure 7G, 7H). Similar to cFN-EDA, LPS induced expression of FN (Figure 5I), COL1 (Figure 6I), and Laminin (Figure 7I) compared to untreated control cells, and the addition of LPS + TGFβ2 amplified the effect on FN (Figure 5J), COL1 (Figure 6J), and Laminin (Figure 7J). TAK-242 was also able to block the effect of both LPS and TGFβ2 on FN (Figure 5K, 5L), COL1 (Figure 6K, 6L), and Laminin (Figure 7K, 7L). Each experiment was repeated in 3 primary human TM cell strains. These data suggest a TGFβ2-TLR4 signaling crosstalk in the TM.

Mutation in TLR4 blocks TGFβ2 induced ocular hypertension in mice

To further test the relationship between TGFβ2 and TLR4, we utilized our established mouse model of ocular hypertension using an Ad5.TGFβ2 virus containing a bioactivated form of TGFβ2[34-36]. Ad5.TGFβ2 was injected intravitreally into one eye of each animal and the contralateral uninjected eye was used as a negative control. In order to determine specific mouse strain susceptibility to Ad5.TGFβ2 induced ocular hypertension, we tested several genetically distinct inbred strains of mice. A/J (n=13), Balbc/J (n=8), and AKR/J (n=7) all developed a significant IOP elevation for the duration of the 8 week time course in the Ad5.TGFβ2 injected eye, with no significant change in IOP in the contralateral uninjected eye (Figure 8A, 8B, 8C). Ad5.null (n=5) had no effect on IOP at any time point (Figure 8D). The C3H/HeJ mouse strain has a spontaneous missense mutation in the *Tlr4* gene, which leads to a single amino acid change of a highly conserved proline to histidine at codon 712 in the cytoplasmic portion of TLR4[41]. This mutation in TLR4 impedes downstream signal transduction and produces a phenotype similar to that of *Tlr4* knockout mice[41, 42, 61]. Interestingly, when the C3H/HeJ mice (*Tlr4* mutant) are injected intravitreally with Ad5.TGFβ2, no biologically significant IOP elevation developed (Figure 9A). However, the founder strain, C3H/HeOuJ (*Tlr4* wildtype), which contains the wildtype *Tlr4* gene, developed significant IOP elevation after injection with Ad5.TGFβ2 (Figure 9A), similar to what we observed in the other inbred mouse strains that also harbor a wild-type *Tlr4* allele (Figure 8). There was no significant difference in IOP between the uninjected control eyes from C3H/HeJ and C3H/HeOuJ mice at any time point. C3H/HeJ and C3H/HeOuJ IOP data are a combination of three independent experiments (C3H/HeJ n=20 (n=15 days 0-47, n=5 days 0-22); C3H/HeOuJ n=10 (n=5 days 0-47, n=5 days 0-22)). IOP exposure was also calculated and

Tlr4 wildtype mice had an increased IOP exposure both early (Days 0-22, $p<0.05$) and throughout the complete time course (Days 0-47, $p<0.01$) compared to *Tlr4* mutant mice (Figure 9B). *Tlr4* wildtype mice (n=13 mice 5-8 weeks post-injection) also demonstrated increased FN expression in the TM after IOP elevation compared to *Tlr4* mutant mice (n=7 mice 5-8 weeks post-injection) (Figure 10). These data suggest that the TGFβ2 and TLR4 signaling pathways are involved in the development of ocular hypertension in mice.

DISCUSSION

We present a novel pathway that is contributing to the regulation of the ECM and fibrosis in TM cells (Figure 11). Although the ECM in TM cells is known to be important in IOP regulation, the molecular mechanisms involved in generating a glaucomatous environment in the TM remain unknown. Investigation of TGFβ2-TLR4 crosstalk in the TM further explains the mechanisms involved in the development of glaucomatous TM damage. Our data will be invaluable to the field of glaucoma and provide a framework for the development of novel therapeutic targets that could intervene and perhaps reverse glaucomatous damage to the TM. We and others have previously published the importance of the TGFβ signaling pathway in the regulation of ECM proteins in the glaucomatous TM and the effect on intraocular pressure[23, 25, 27-31, 33, 34, 36]. In glaucoma there are vast changes to the ECM of the TM and the disease is progressive in nature, which is similar to the changes described in other fibrotic diseases. We demonstrate that the ECM composition in the TM is regulated by crosstalk between the TGFβ signaling pathway and the TLR4 signaling pathway. Published literature supports these findings in other fibrotic diseased tissues such as the liver, kidney, lung, and skin [45-48].

Upon TLR4 activation, TLR4 forms a complex with myeolid differentiation factor-2 allowing for TLR4 adaptor proteins TIRAP and TRAM to be recruited, which functions to further recruit additional adaptor proteins TRIF and MyD88[62]. Activation of the MyD88 dependent pathway ultimately leads to translocation of NFκB into the nucleus which then functions in the regulation of many genes including cytokines, chemokines, proteins that regulate cell cycle and cell survival, amongst others[62, 63]. Abnormal TLR4 signaling has been linked to several inflammatory and autoimmune diseases[64, 65]. In addition, DAMPs (cFN-EDA, low molecular weight hyaluronan, tenascin C, amongst others) have been shown to activate TLR4 and augment TGFβ signaling and downstream fibrotic responses in other diseases[45, 63, 66].

TLR4 activation downregulates the TGFβ pseudoreceptor BMP and the activin membrane-bound inhibitor (BAMBI), which enhances TGFβ signaling leading to increased ECM production[45, 46]. We have recently shown that BAMBI is expressed in the TM and BAMBI expression is downregulated by the presence of TGFβ2 (5ng/ml) for 24 hours[67]. BAMBI downregulation by TLR4 is regulated by the MyD88-NFκB-dependent pathway[46, 63, 66]. BAMBI functions to inhibit TGFβ signaling by cooperating with SMAD7 and impairing SMAD3 activation, while knockdown of *Bambi* expression enhances TGFβ signaling[68]. BAMBI can also interact with bone morphogenic protein (BMP) receptors directly and antagonize BMP signaling as well as interact directly with TGFβ receptors and anatagonize TGFβ signaling[69]. BMPs can suppress the TGFβ2 induced ECM deposition[28, 29], the BMP antagonist gremlin elevates IOP in perfusion cultured anterior segments[28], and over-expression of gremlin in mouse eyes causes ocular hypertension[35], suggesting that BMP signaling is required for regulating normal outflow. Further experiments are needed to determine the exact mechanistic role of BAMBI in TGFβ2-TLR4 signaling in the TM; however, these data suggest that activation of TLR4 downregulates

BAMBI leading to unopposed TGFβ signaling and fibrogenesis. Since the fibrotic response leads to the accumulation of endogenous TLR4 ligands such as cFN-EDA, a feed-forward loop could develop, leading to a further progression of the fibrotic response.

In summary, we demonstrate that a profibrotic TGFβ-TLR4 crosstalk is involved in the production and regulation of the ECM in the TM. These data illustrate a novel pathway involved in the development of TM damage which could provide new targets to lower IOP and further explain the mechanisms involved in the development of glaucomatous TM damage.

Figure Legends

Figure 1

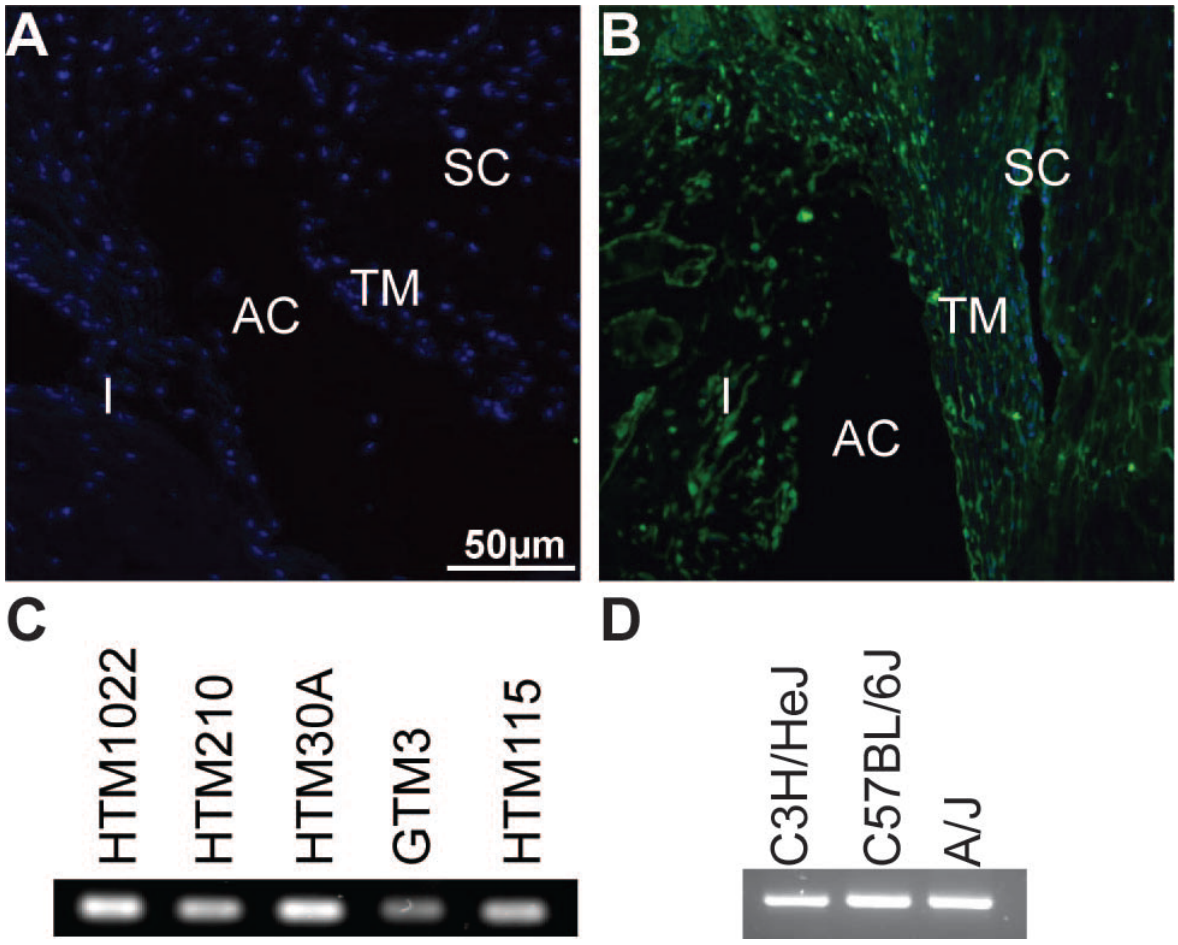

Figure 1. TLR4 is expressed in the human and mouse TM. Cross-sections of 8 individual human eyes were labeled with a TLR4 specific antibody. (A) No primary antibody control. (B) TLR4 expression in the human TM (TM, trabecular meshwork; SC, Schlemm's canal; AC, anterior chamber; I, iris). (C) RNA was isolated from primary human TM cell strains and a human transformed TM cell line, GTM3. Using primers specific to human *TLR4*, RT-PCR was performed. *TLR4* is expressed in human TM cells. (D) The TM ring from mice was carefully dissected and RNA isolated. Using primers specific to mouse *Tlr4*, RT-PCR was performed. *Tlr4* is expressed in the TM ring of C3H/HeJ, C57BL/6J, and A/J mice.

Figure 2

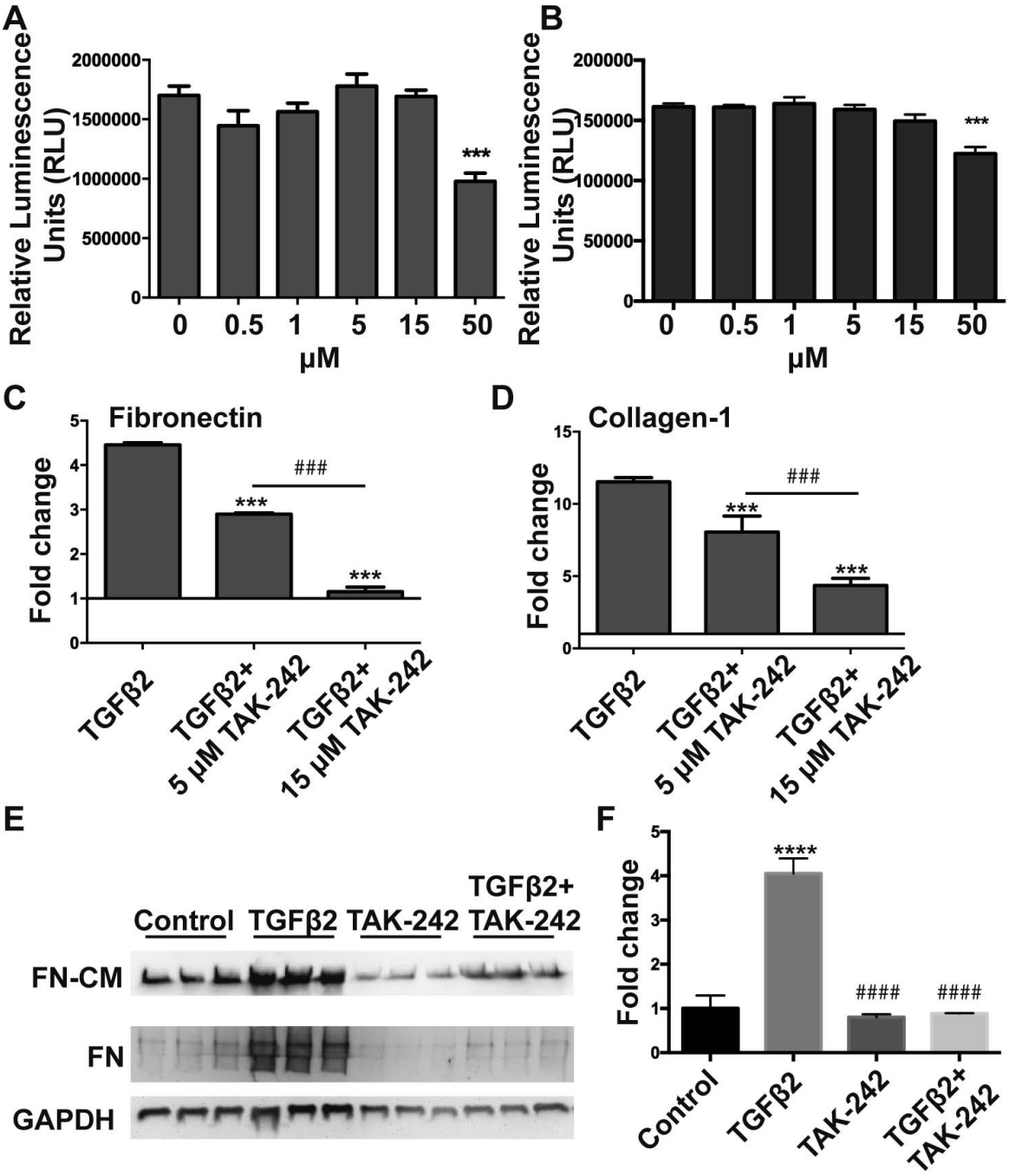
A
Relative Luminescence Units (RLU)
2000000
1500000
1000000
500000
0
***
0 0.5 1 5 15 50
μM
B
Relative Luminescence Units (RLU)
200000
150000
100000
50000
0
***
0 0.5 1 5 15 50
μM
C
Fibronectin
Fold change
5
4
3
2
1
0
###
***
***
TGFβ2
TGFβ2+ 5 μM TAK-242
TGFβ2+ 15 μM TAK-242
D
Collagen-1
Fold change
15
10
5
0
###
***
***
TGFβ2
TGFβ2+ 5 μM TAK-242
TGFβ2+ 15 μM TAK-242
E
Control
TGFβ2
TAK-242
TGFβ2+ TAK-242
FN-CM
FN
GAPDH
F
Fold change
5
4
3
2
1
0
****
####
Control
TGFβ2
TAK-242
TGFβ2+ TAK-242

Figure 2. Inhibition of TLR4 signaling in the presence or absence of TGFβ2 decreases fibronectin and collagen-1 expression. (A,B) TM cell viability after dose response with selective TLR4 signaling inhibitor (TAK-242). The cell viability assay revealed that 50 μM TAK-242 decreased cell viability compared to untreated cells in both transformed GTM3 cells (A) and a primary human TM cell strain (B), (n=8 technical replicates/cell strain). (C-F) GTM3 cells were pre-treated with 5 μM or 15 μM TAK-242 for 2 hours, and subsequently treated with TGFβ2 for 24 hours (RNA analysis) or 48 hours (protein analysis). (C, D) TLR4 signaling inhibition decreased mRNA expression of fibronectin and collagen-1. Data represented as mean +/- SEM, n=3, * = compared to TGFβ2 treated cells, # = compared to treatment. (E) Western immunoblots of fibronectin conditioned medium (FN-CM) and cell lysates. (F) Densitometric analysis of cell lysates show that TLR4 signaling inhibition decreased fibronectin protein levels compared to cells treated with TGFβ2. For cell lysates, expression of fibronectin was normalized to GAPDH (loading control) and fold change was compared to control treated cells (n=3). Statistical significance was determined by one-way ANOVA and Tukey post-hoc analysis, *** $p<0.001$, ****$p<0.0001$, ### $p<0.001$, #### $p<0.0001$, * compared to untreated control cells, # compared to TGFβ2 treated cells.

Figure 3

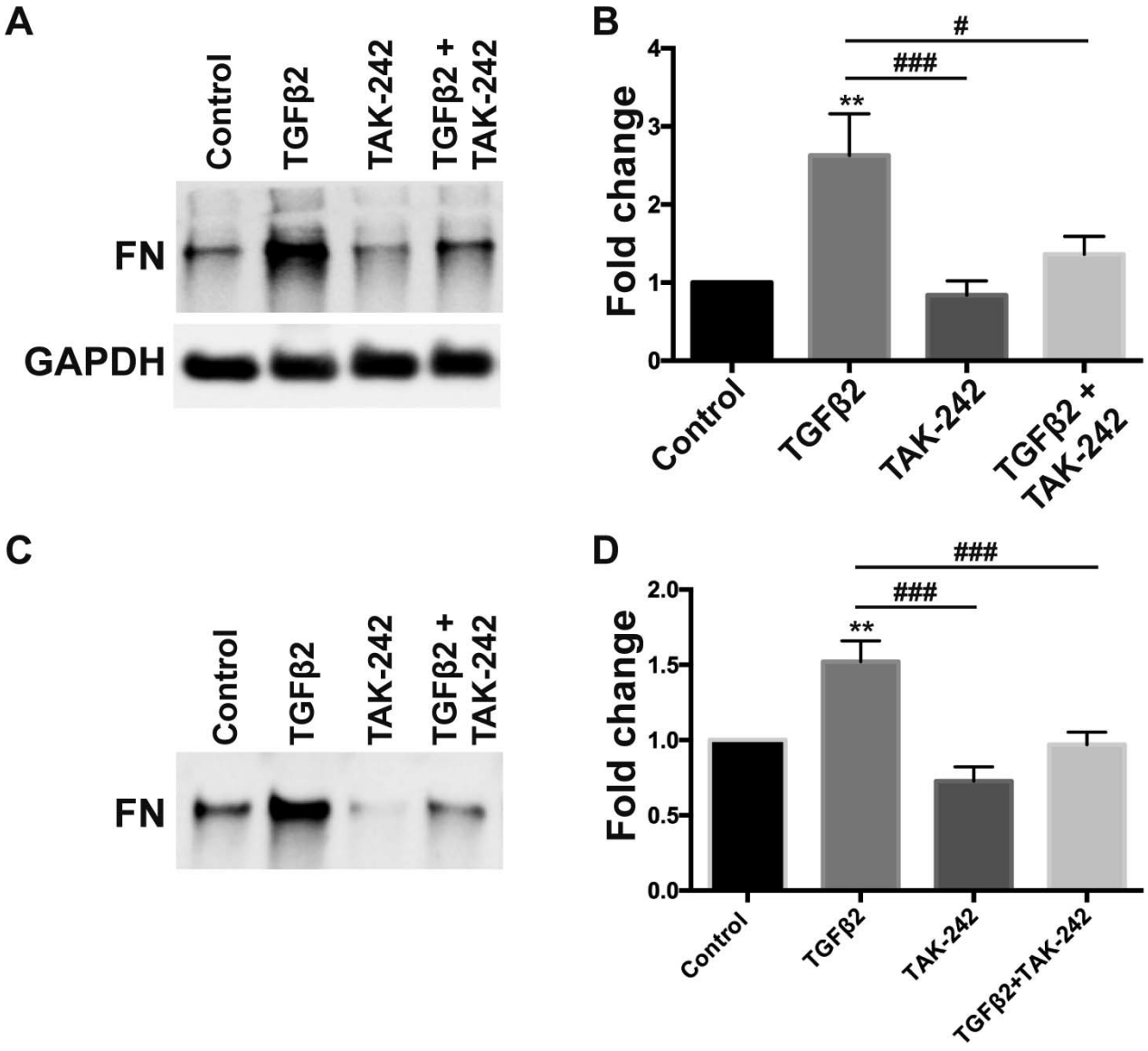
A
Control
TGFβ2
TAK-242
TGFβ2 + TAK-242
FN
GAPDH
B
Fold change
#
###
**
Control
TGFβ2
TAK-242
TGFβ2 + TAK-242
C
Control
TGFβ2
TAK-242
TGFβ2 + TAK-242
FN
D
Fold change
###
###
**
Control
TGFβ2
TAK-242
TGFβ2+TAK-242

Figure 3. Inhibition of TLR4 signaling decreases TGFβ2-induced FN expression in primary TM cells. Human primary TM cells (n=4 cell strains, 3 independent experiments) were pre-treated with TAK-242 (15 μM) for 2 hours, and subsequently treated with TGFβ2 (5 ng/mL) for 48 hrs. (A) Western immunoblot and (B) densitometric analysis of cell lysates show that TGFβ2 increases total fibronectin expression, while inhibition of TLR4 signaling with TAK-242 blocks the effect of TGFβ2. (C) Western immunoblot and (D) densitometric analysis of conditioned medium show that TGFβ2 increases total fibronectin and inhibition of TLR4 signaling with TAK-242 blocks the effect of TGFβ2. For cell lysates, expression of fibronectin was normalized to GAPDH (loading control) and fold change was compared to control treated cells. Statistical significance was determined by one-way ANOVA and Tukey post-hoc analysis, ** $p<0.01$, # $p<0.01$, ### $p<0.001$ (* = compared to untreated control cells, # = compare to treatment).

Figure 4

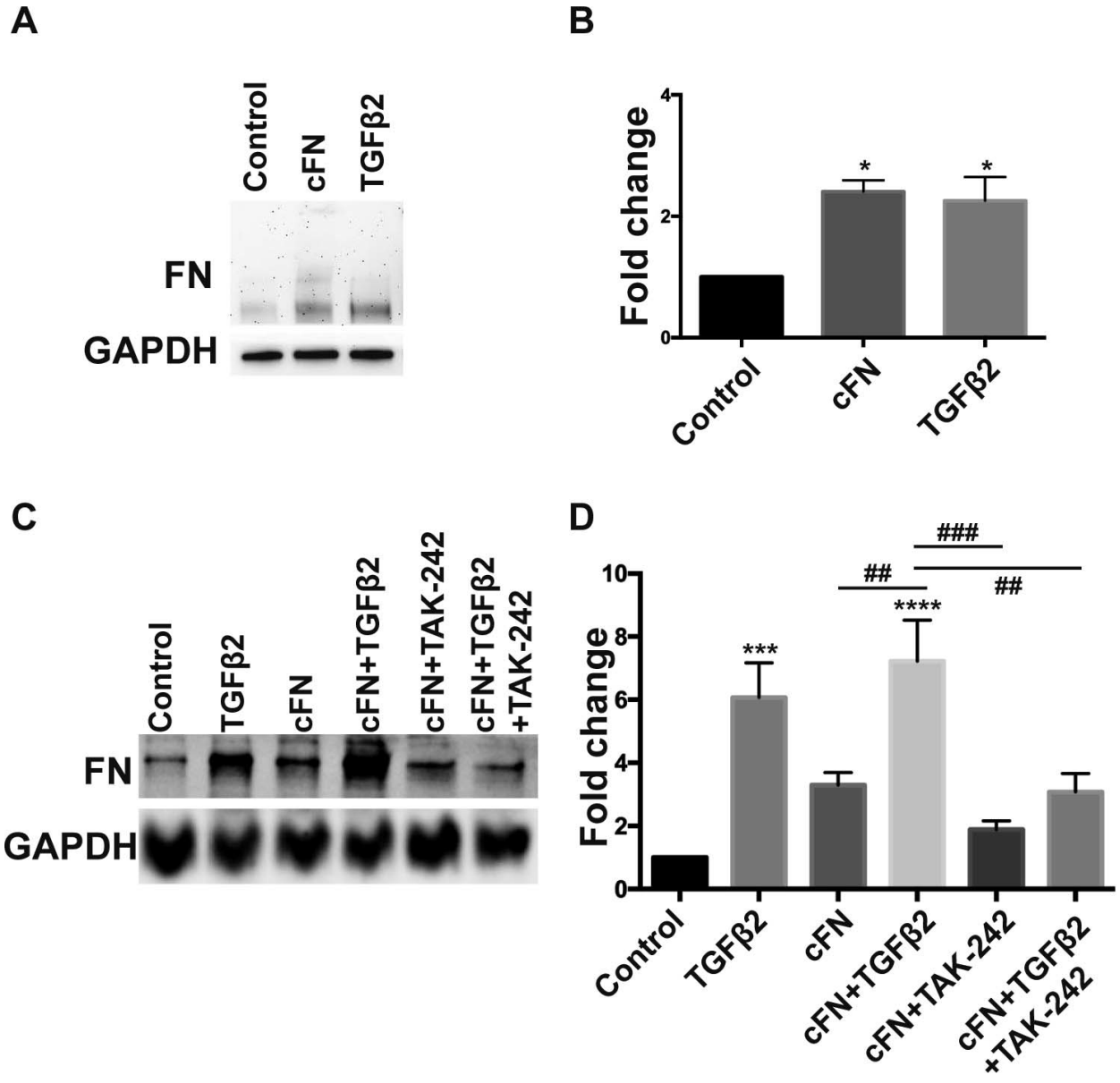
A
Control
cFN
TGFβ2
FN
GAPDH
B
Fold change
0
2
4
*
*
Control
cFN
TGFβ2
C
Control
TGFβ2
cFN
cFN+TGFβ2
cFN+TAK-242
cFN+TGFβ2
+TAK-242
FN
GAPDH
D
Fold change
0
2
4
6
8
10
***
****
##
##
###
Control
TGFβ2
cFN
cFN+TGFβ2
cFN+TAK-242
cFN+TGFβ2
+TAK-242

Figure 4. Activation of TLR4 by cFN containing the EDA isoform increases fibronectin expression in primary TM cells. (A,B) NTM (n=3 primary human TM cells strains) were plated on cFN-EDA coated plates and non-coated plates with TGFβ2 in serum free medium for 48 hrs. (A) Western immunoblot and (B) densitometric analysis show that cFN-EDA increases total fibronectin in cell lysates to significant comparable levels as TGFβ2. (C,D) NTM cells (n=4 primary human TM cells strains, each repeated in 2 independent experiments) were pre-treated with TAK-242 for 2 hours, and subsequently treated with TGFβ2 (5ng/mL), TAK-242 (15 μM), and/or cFN-EDA for 72 hrs. (C) Western immunoblot and (D) densitometric analysis show that TGFβ2 and cFN-EDA independently increase total levels of fibronectin in the cell lysates, and together amplify the total fibronectin expression. Inhibition of TLR4 signaling via TAK-242 blocks the effect of cFN-EDA and TGFβ2. Statistical significance determined by one-way ANOVA and tukey post-hoc analysis, * $p< 0.05$, *** $p<0.001$, **** $p<0.0001$, ## $p<0.01$, ### $p<0.001$ (* = compared to control, # = compare to treatment).

Figure 5

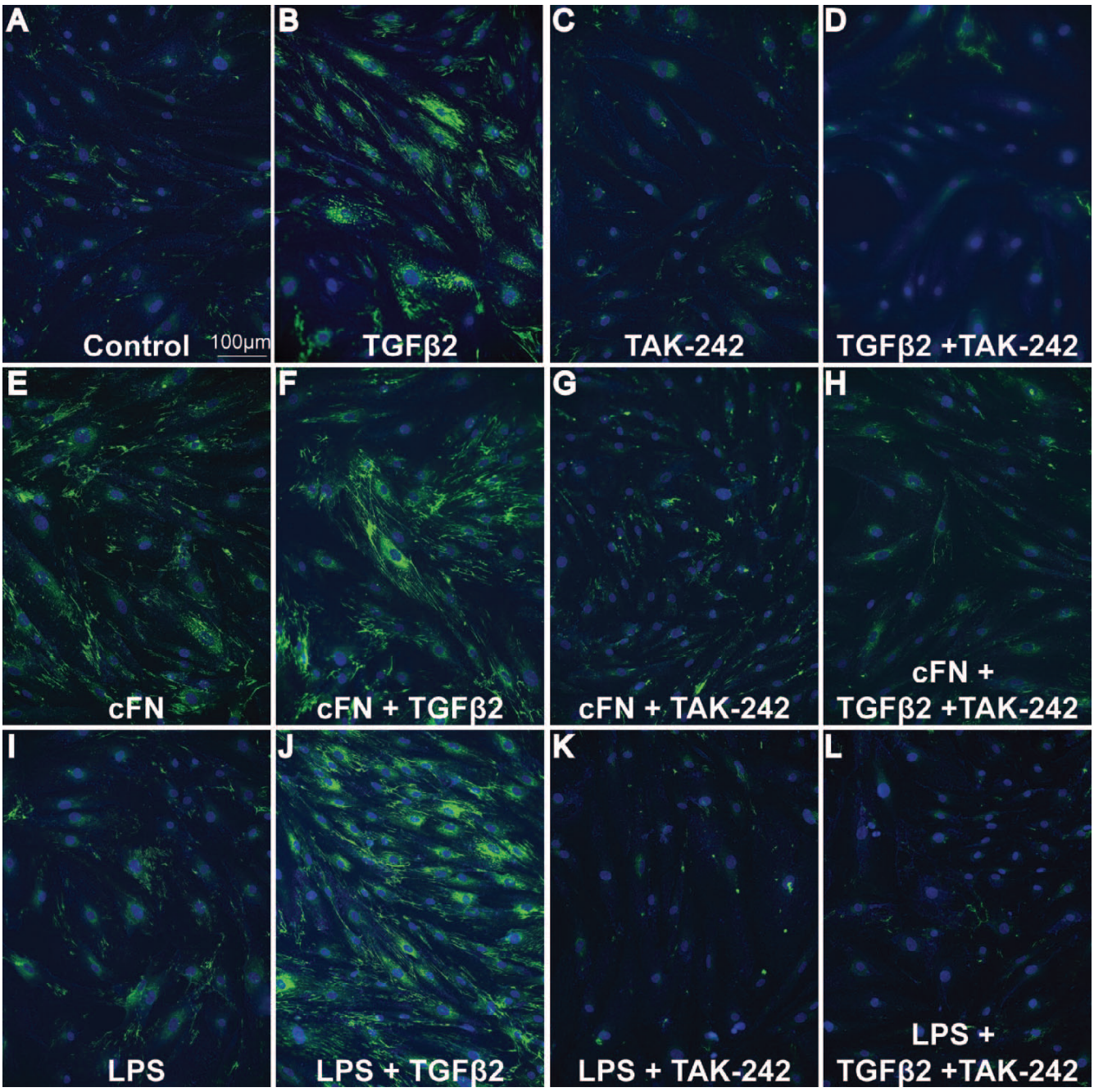
A
Control
100μm
B
TGFβ2
C
TAK-242
D
TGFβ2 +TAK-242
E
cFN
F
cFN + TGFβ2
G
cFN + TAK-242
H
cFN +
TGFβ2 +TAK-242
I
LPS
J
LPS + TGFβ2
K
LPS + TAK-242
L
LPS +
TGFβ2 +TAK-242

Figure 5. Effect of TGFβ2, cFN-EDA, LPS, and TLR4 signaling inhibition on FN expression in primary human TM cells. NTM cells (n=3 primary human cell strains) were grown to confluency, treated with (B,D,F,H,J,L) TGFβ2 (5 ng/mL), (E-H) cFN-EDA (10 μg/mL), or [70] LPS (100 ng/mL). NTM cells involving TLR4 signaling inhibition were pre-treated with TAK-242 (15 μM) for 2 hours (C, D, G, H, K, L), followed by treatment with (D,H,L) TGFβ2 (5ng/mL), (G, H) cFN-EDA (10 μg/mL), and/or (K, L) LPS (100ng/mL) in serum free medium with TAK-242 (15 μM) for 48 hrs. Immunocytochemistry studies revealed that TGFβ2, cFN-EDA, and LPS increases total FN expression compared to controls. Treatment with TGFβ2 and activation of TLR4 with cFN-EDA or LPS increased the staining signal when compared to TGFβ2 alone. Inhibition of TLR4 signaling via TAK-242 blocked the effect of all treatments. Scale bar represents 100 μm.

Figure 6

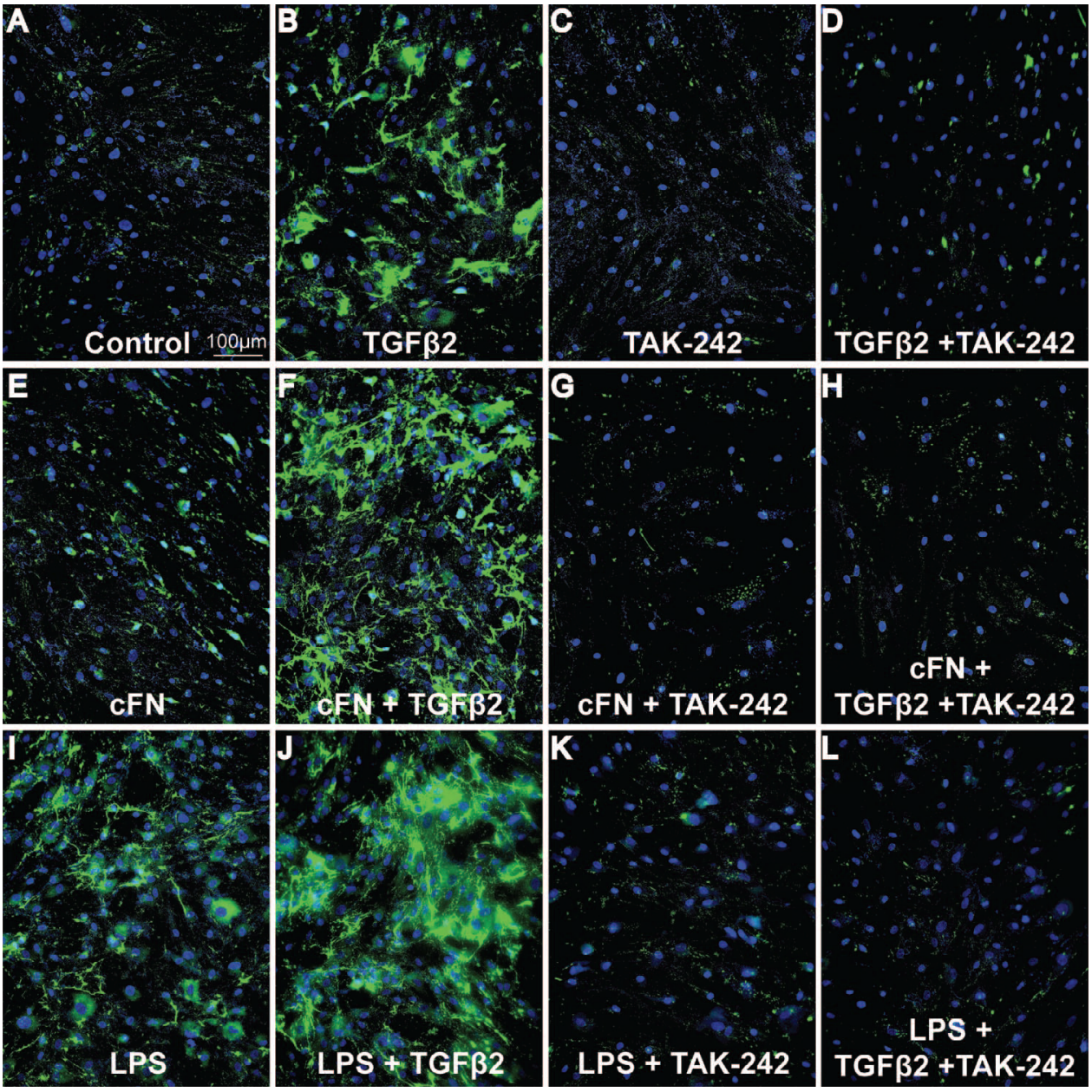
A
Control
100μm
B
TGFβ2
C
TAK-242
D
TGFβ2 +TAK-242
E
cFN
F
cFN + TGFβ2
G
cFN + TAK-242
H
cFN +
TGFβ2 +TAK-242
I
LPS
J
LPS + TGFβ2
K
LPS + TAK-242
L
LPS +
TGFβ2 +TAK-242

Figure 6. Effect of TGFβ2, cFN-EDA, LPS, and TLR4 signaling inhibition on COL-1 expression in primary human TM cells. NTM cells (n=3 cell strains) were grown to confluency, treated with (B,D,F,H,J,L) TGFβ2 (5 ng/mL), (E-H) cFN-EDA (10 μg/mL), or [70] LPS (100 ng/mL). NTM cells involving TLR4 signaling inhibition were pre-treated with TAK-242 (15 μM) for 2 hrs. (C, D, G, H, K, L), followed by treatment with (D,H,L) TGF-β2 (5ng/mL), (G, H) cFN-EDA (10 μg/mL), and/or (K, L) LPS (100ng/mL) in serum free medium with TAK-242 (15 μM) for 72 hrs. Immunocytochemistry studies revealed that TGFβ2, cFN-EDA, and LPS increases COL-1 expression compared to controls. Treatment with TGFβ2 and activation of TLR4 with cFN-EDA or LPS increased the staining signal when compared to TGFβ2 alone. Inhibition of TLR4 signaling via TAK-242 blocked the effect of all treatments. Scale bar represents 100 μm.

Figure 7

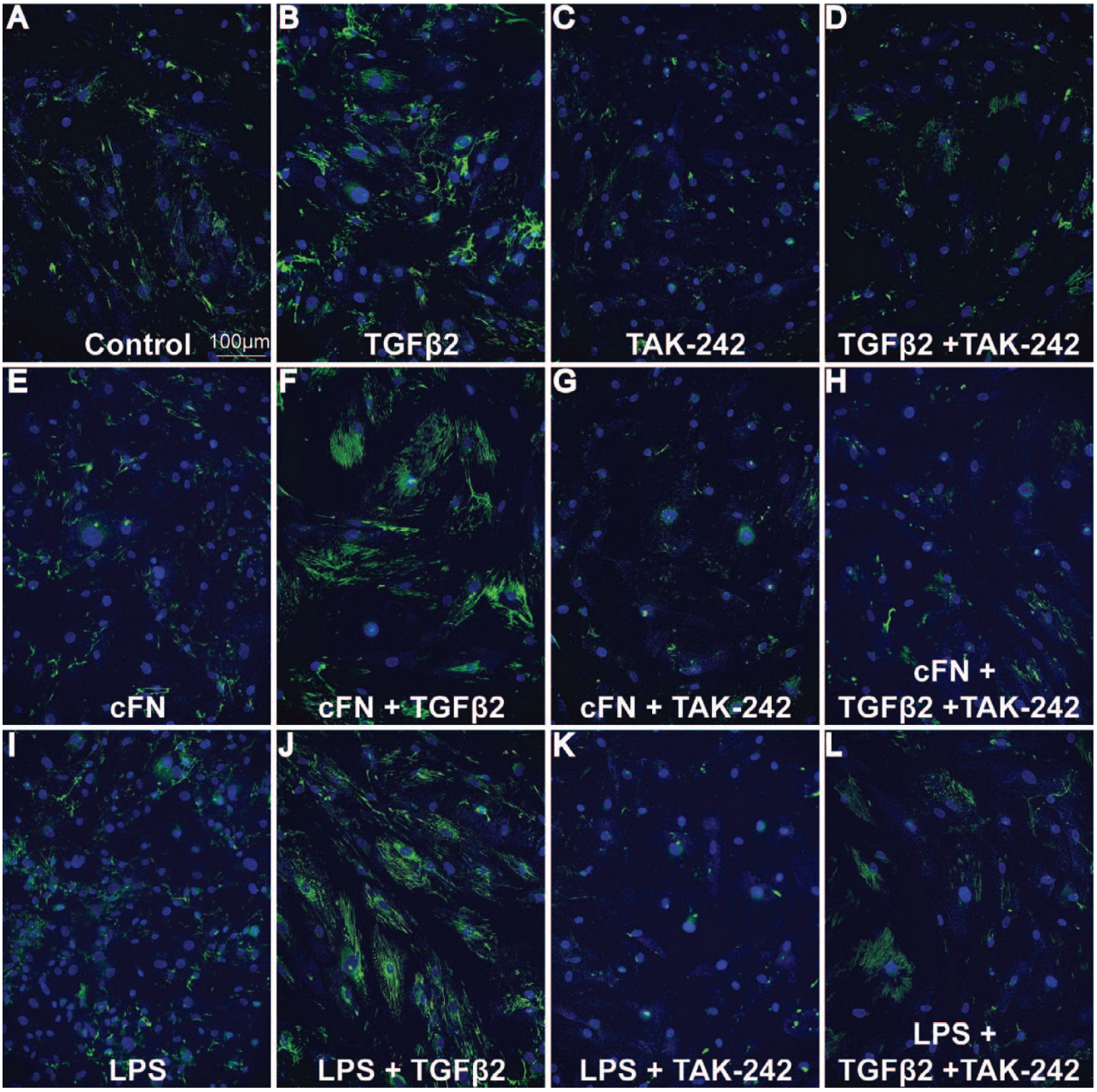
A
Control
100μm
B
TGFβ2
C
TAK-242
D
TGFβ2 +TAK-242
E
cFN
F
cFN + TGFβ2
G
cFN + TAK-242
H
cFN +
TGFβ2 +TAK-242
I
LPS
J
LPS + TGFβ2
K
LPS + TAK-242
L
LPS +
TGFβ2 +TAK-242

Figure 7. Effect of TGFβ2, cFN-EDA, LPS, and TLR4 signaling inhibition on laminin expression in primary human TM cells. NTM cells (n=3 cell strains) were grown to confluency, treated with (B,D,F,H,J,L) TGFβ2 (5 ng/mL), (E-H) cFN-EDA (10 μg/mL), or [70] LPS (100 ng/mL). NTM cells involving TLR4 signaling inhibition were pre-treated with TAK-242 (15 μM) for 2 hrs. (C, D, G, H, K, L), followed by treatment with (D,H,L) TGFβ2 (5ng/mL), (G, H) cFN-EDA (10 μg/mL), and/or (K, L) LPS (100ng/mL) in serum free medium with TAK-242 (15 μM) for 48 hrs. Immunocytochemistry studies revealed that TGFβ2, cFN-EDA, and LPS increases laminin expressiom compared to controls. Treatment with TGFβ2 and activation of TLR4 with cFN-EDA or LPS increased the staining signal when compared to TGFβ2 alone. Inhibition of TLR4 signaling via TAK-242 blocked the effect of all treatments. Scale bar represents 100 μm.

Figure 8

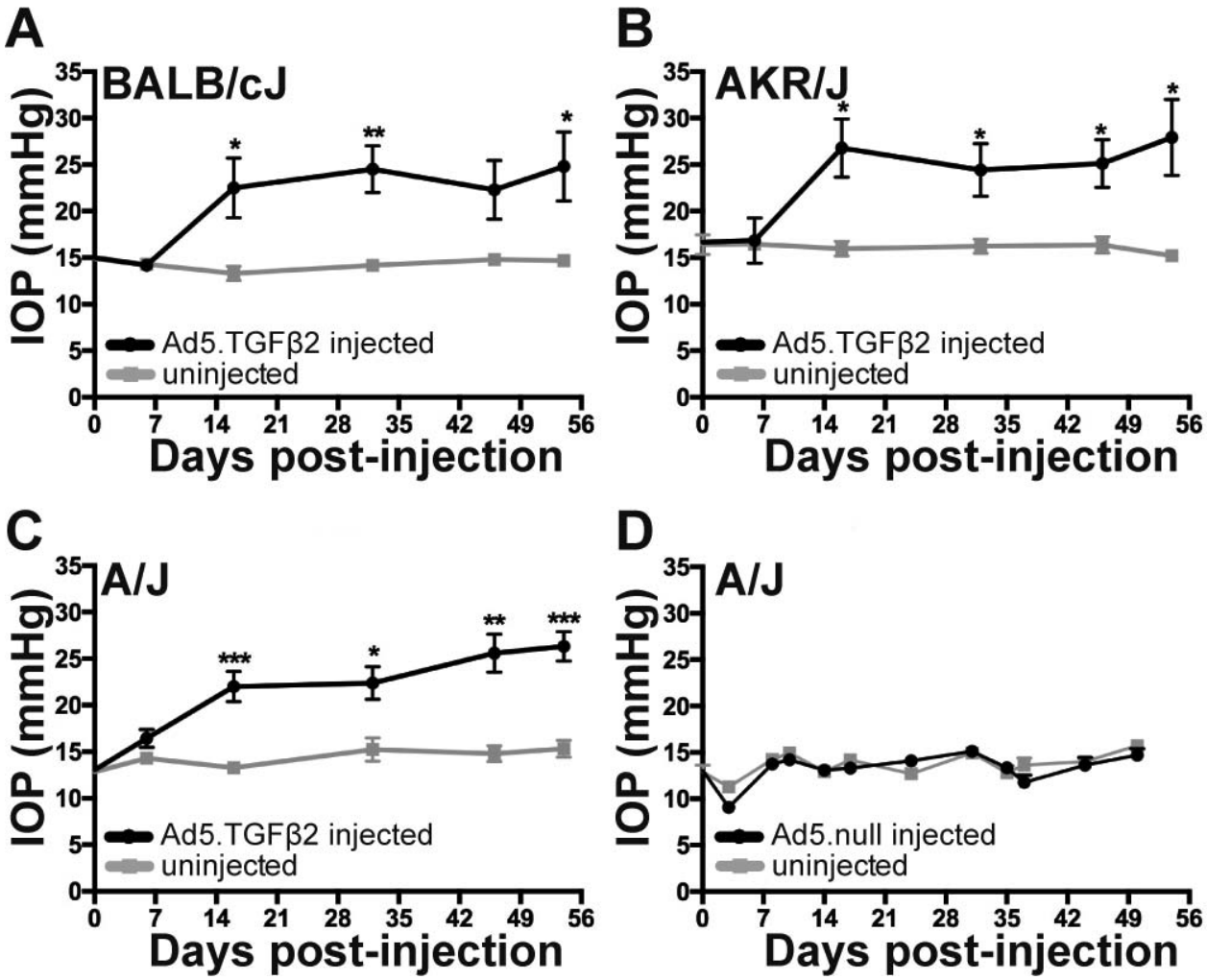
A
BALB/cJ
IOP (mmHg)
Days post-injection
Ad5.TGFβ2 injected
uninjected
B
AKR/J
IOP (mmHg)
Days post-injection
Ad5.TGFβ2 injected
uninjected
C
A/J
IOP (mmHg)
Days post-injection
Ad5.TGFβ2 injected
uninjected
D
A/J
IOP (mmHg)
Days post-injection
Ad5.null injected
uninjected

Figure 8. Ad5.TGFβ2 induces ocular hypertension in mice. Ad5.TGFβ2 ($2.5x10^7$ pfu) was intravitreally injected in one eye of each animal and the contralateral uninjected eyes were used as negative controls. IOP was significantly elevated in (A) BALBc/J (n=8), (B) AKR/J (n=7), and (C) A/J (n=13) mice throughout an eight week time course. (D) Administration of Ad5.null (n=5) had no effect on IOP. These data suggest that overexpression of bioactivated TGFβ2 in the TM of mice induces ocular hypertension. Statistical significance determined by Student's paired t-test at each time point, *$p<0.05$, ** $p<0.01$, ***$p<0.001$.

Figure 9

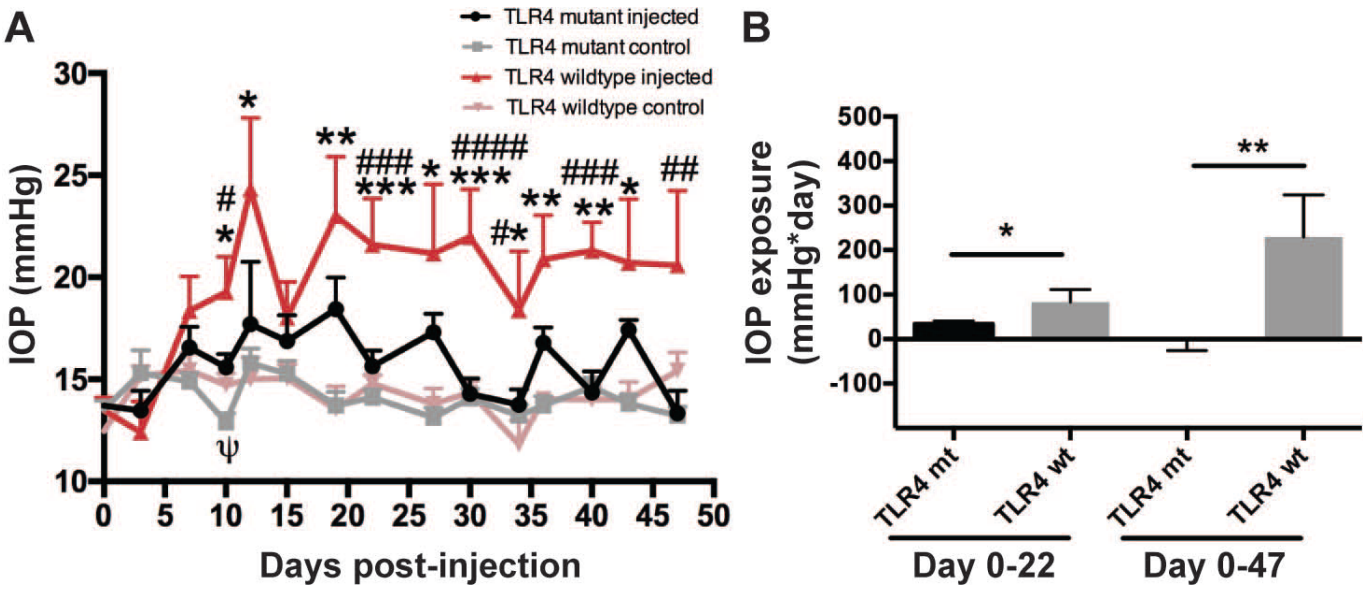
A
TLR4 mutant injected
TLR4 mutant control
TLR4 wildtype injected
TLR4 wildtype control
IOP (mmHg)
Days post-injection
B
IOP exposure (mmHg*day)
TLR4 mt
TLR4 wt
TLR4 mt
TLR4 wt
Day 0-22
Day 0-47

Figure 9. Ad5.TGFβ2 does not induce ocular hypertension in *Tlr4* mutant mice. Ad5.TGFβ2 ($2.5x10^7$ pfu) was intravitreally injected in one eye of each animal and the contralateral uninjected eyes were used as negative controls. C3H/HeJ and C3H/HeOuJ mice are genetically similar except for the genotype of *Tlr4*. (A) The *Tlr4* mutant strain of mice (C3H/HeJ, n=20) had no biologically significant IOP elevation at any time point throughout the 6 week time course. However, Ad5.TGFβ2 induced ocular hypertension in C3H/HeOuJ (n=10) which are wild-type for *Tlr4*. (B) *Tlr4* wildtype mice had a higher IOP exposure than *Tlr4* mutant mice both early (22 days) and throughout (47 days) the time course, statistical significance determined by Student's t test. For IOP measurements, statistical significance determined by one way ANOVA at each time point, *p<0.05, ** p<0.01, ***p<0.001, **** p<0.0001, #p<0.05, ## p<0.01, ###p<0.001, #### p<0.0001. * = *Tlr4* wildtype injected vs *Tlr4* wildtype control, # = *Tlr4* wildtype injected vs. *Tlr4* mutant injected, Ψ = *Tlr4* mutant injected vs *Tlr4* mutant control.

Figure 10

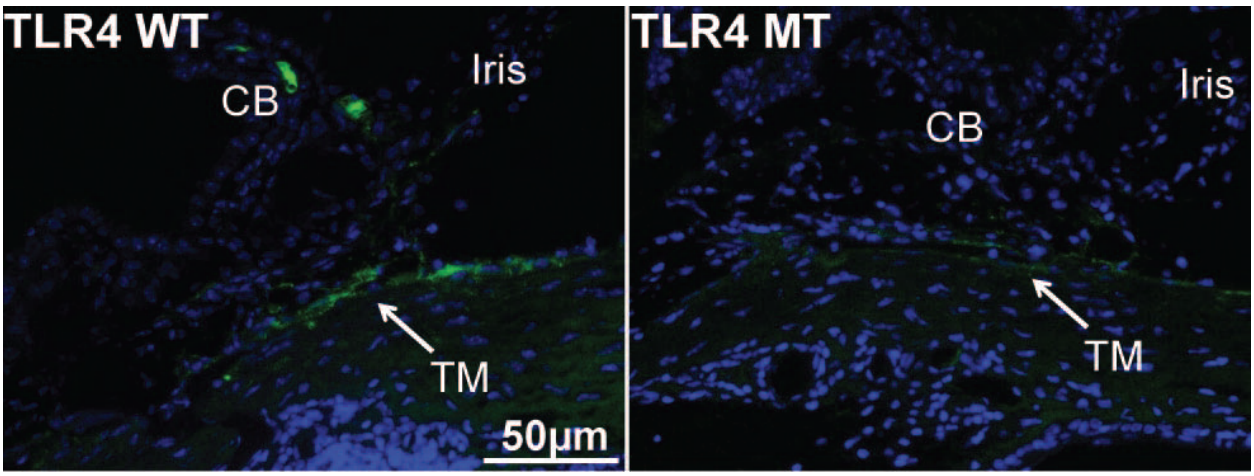

Figure 10. Fibronectin expression is increased in the TM of *Tlr4* wildtype but not *Tlr4* mutant mice treated with Ad5.TGFβ2. Mice were injected with Ad5.TGFβ2 ($2.5x10^7$ pfu) intravitreally in one eye of each animal and the contralateral uninjected eyes were used as negative controls. Mice were harvested 5-8 weeks post-injection and analyzed by immunohistochemistry. (A) *Tlr4* wildtype mice (n=8) had increased FN expression compared to (B) *Tlr4* mutant mice (n=12). Scale bar represents 50 μm.

Figure 11

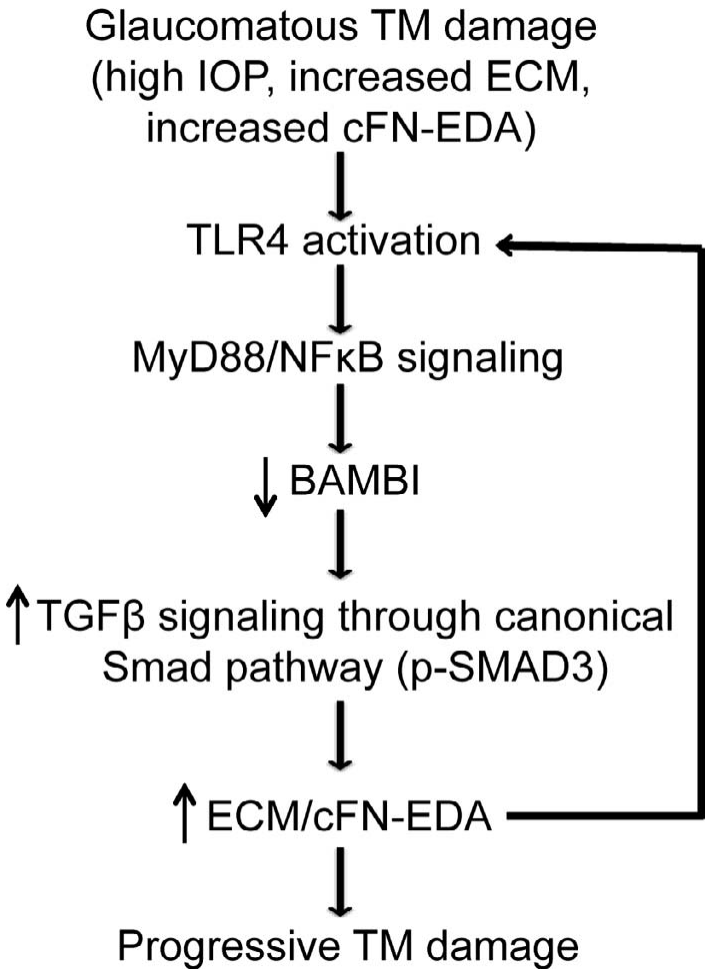
Glaucomatous TM damage
(high IOP, increased ECM,
increased cFN-EDA)
TLR4 activation
MyD88/NFκB signaling
↓ BAMBI
↑TGFβ signaling through canonical
Smad pathway (p-SMAD3)
↑ECM/cFN-EDA
Progressive TM damage

Figure 11. Proposed pathway of TGFβ2-TLR4 signaling crosstalk in the glaucomatous TM. TLR4 is activated by endogenous ligands known as DAMPs, which are produced in response to cell damage and increased ECM production and accumulation. TLR4 signals through the MyD88/ NFκB signaling pathway, leading to downregulation of BAMBI and uninhibited TGFβ2 signaling. The increased TGFβ2 signaling leads to an increase in DAMP and ECM production, which can further activate TLR4. The feed-forward loop produced by TGFβ2-TLR4 signaling leads to progressive fibrosis in the TM.

Reference

1. Quigley HA. Open-angle glaucoma. *N Engl J Med* 1993;328:1097-1106.

2. Kass MA, Heuer DK, Higginbotham EJ, et al. The Ocular Hypertension Treatment Study: a randomized trial determines that topical ocular hypotensive medication delays or prevents the onset of primary open-angle glaucoma. *Arch Ophthalmol* 2002;120:701-713; discussion 829-730.

3. Leske MC, Heijl A, Hussein M, Bengtsson B, Hyman L, Komaroff E. Factors for glaucoma progression and the effect of treatment: the early manifest glaucoma trial. *Arch Ophthalmol* 2003;121:48-56.

4. The Advanced Glaucoma Intervention Study (AGIS): 7. The relationship between control of intraocular pressure and visual field deterioration.The AGIS Investigators. *Am J Ophthalmol* 2000;130:429-440.

5. Vranka JA, Kelley MJ, Acott TS, Keller KE. Extracellular matrix in the trabecular meshwork: intraocular pressure regulation and dysregulation in glaucoma. *Exp Eye Res* 2015;133:112-125.

6. Hogan MJ, Alvarado, J., Weddell, J.E. *Histology of the Human Ey: an Atlas and Textbook*. The University of Michigan: Saunders; 1971.

7. Gong H, Tripathi RC, Tripathi BJ. Morphology of the aqueous outflow pathway. *Microscopy research and technique* 1996;33:336-367.

8. Morrison JC, Acott, T.S. Anatomy and Physiology of Aqueous Humor Outflow. In: Gumpert E (ed), *Glaucoma: Science and Practice*: Thieme Medical Publishers; 2003:24-41.

9. Keller KE, Aga M, Bradley JM, Kelley MJ, Acott TS. Extracellular matrix turnover and outflow resistance. *Exp Eye Res* 2009;88:676-682.

10. Keller KE, Acott TS. The Juxtacanalicular Region of Ocular Trabecular Meshwork: A Tissue with a Unique Extracellular Matrix and Specialized Function. *J Ocul Biol* 2013;1:3.

11. Keller KE, Vranka JA, Haddadin RI, et al. The effects of tenascin C knockdown on trabecular meshwork outflow resistance. *Invest Ophthalmol Vis Sci* 2013;54:5613-5623.

12. Bradley JM, Kelley MJ, Zhu X, Anderssohn AM, Alexander JP, Acott TS. Effects of mechanical stretching on trabecular matrix metalloproteinases. *Invest Ophthalmol Vis Sci* 2001;42:1505-1513.

13. Alexander JP, Samples JR, Van Buskirk EM, Acott TS. Expression of matrix metalloproteinases and inhibitor by human trabecular meshwork. *Invest Ophthalmol Vis Sci* 1991;32:172-180.

14. Midwood KS, Hussenet T, Langlois B, Orend G. Advances in tenascin-C biology. *Cell Mol Life Sci* 2011;68:3175-3199.

15. Vittal V, Rose A, Gregory KE, Kelley MJ, Acott TS. Changes in gene expression by trabecular meshwork cells in response to mechanical stretching. *Invest Ophthalmol Vis Sci* 2005;46:2857-2868.

16. Lutjen-Drecoll E. Functional morphology of the trabecular meshwork in primate eyes. *Prog Retin Eye Res* 1999;18:91-119.

17. Rohen JW, Witmer R. Electrn microscopic studies on the trabecular meshwork in glaucoma simplex. *Albrecht Von Graefes Arch Klin Exp Ophthalmol* 1972;183:251-266.

18. Babizhayev MA, Brodskaya MW. Immunohistochemical monitoring of the effect of a synthetic fibronectin-like peptide (Arg-Gly-Asp) on the age-related changes in the isolated human corneoscleral tissue of glaucomatous eyes. *Mech Ageing Dev* 1993;72:1-12.

19. Medina-Ortiz WE, Belmares R, Neubauer S, Wordinger RJ, Clark AF. Cellular fibronectin expression in human trabecular meshwork and induction by transforming growth factor-beta2. *Invest Ophthalmol Vis Sci* 2013;54:6779-6788.

20. Lutjen-Drecoll E, Shimizu T, Rohrbach M, Rohen JW. Quantitative analysis of 'plaque material' in the inner- and outer wall of Schlemm's canal in normal- and glaucomatous eyes. *Exp Eye Res* 1986;42:443-455.

21. Rohen JW, Lutjen-Drecoll E, Flugel C, Meyer M, Grierson I. Ultrastructure of the trabecular meshwork in untreated cases of primary open-angle glaucoma (POAG). *Exp Eye Res* 1993;56:683-692.

22. Knepper PA, Goossens W, Hvizd M, Palmberg PF. Glycosaminoglycans of the human trabecular meshwork in primary open-angle glaucoma. *Invest Ophthalmol Vis Sci* 1996;37:1360-1367.

23. Inatani M, Tanihara H, Katsuta H, Honjo M, Kido N, Honda Y. Transforming growth factor-beta 2 levels in aqueous humor of glaucomatous eyes. *Graefes Arch Clin Exp Ophthalmol* 2001;239:109-113.

24. Ochiai Y, Ochiai H. Higher concentration of transforming growth factor-beta in aqueous humor of glaucomatous eyes and diabetic eyes. *Jpn J Ophthalmol* 2002;46:249-253.

25. Ozcan AA, Ozdemir N, Canataroglu A. The aqueous levels of TGF-beta2 in patients with glaucoma. *Int Ophthalmol* 2004;25:19-22.

26. Tripathi RC, Li J, Chan WF, Tripathi BJ. Aqueous humor in glaucomatous eyes contains an increased level of TGF-beta 2. *Exp Eye Res* 1994;59:723-727.

27. Fleenor DL, Shepard AR, Hellberg PE, Jacobson N, Pang IH, Clark AF. TGFbeta2-induced changes in human trabecular meshwork: implications for intraocular pressure. *Invest Ophthalmol Vis Sci* 2006;47:226-234.

28. Wordinger RJ, Fleenor DL, Hellberg PE, et al. Effects of TGF-beta2, BMP-4, and gremlin in the trabecular meshwork: implications for glaucoma. *Invest Ophthalmol Vis Sci* 2007;48:1191-1200.

29. Fuchshofer R, Yu AH, Welge-Lussen U, Tamm ER. Bone morphogenetic protein-7 is an antagonist of transforming growth factor-beta2 in human trabecular meshwork cells. *Invest Ophthalmol Vis Sci* 2007;48:715-726.

30. Sethi A, Jain A, Zode GS, Wordinger RJ, Clark AF. Role of TGFbeta/Smad signaling in gremlin induction of human trabecular meshwork extracellular matrix proteins. *Invest Ophthalmol Vis Sci* 2011;52:5251-5259.

31. Tovar-Vidales T, Clark AF, Wordinger RJ. Transforming growth factor-beta2 utilizes the canonical Smad-signaling pathway to regulate tissue transglutaminase expression in human trabecular meshwork cells. *Exp Eye Res* 2011;93:442-451.

32. Welge-Lussen U, May CA, Lutjen-Drecoll E. Induction of tissue transglutaminase in the trabecular meshwork by TGF-beta1 and TGF-beta2. *Invest Ophthalmol Vis Sci* 2000;41:2229-2238.

33. Gottanka J, Chan D, Eichhorn M, Lutjen-Drecoll E, Ethier CR. Effects of TGF-beta2 in perfused human eyes. *Invest Ophthalmol Vis Sci* 2004;45:153-158.

34. Shepard AR, Millar JC, Pang IH, Jacobson N, Wang WH, Clark AF. Adenoviral gene transfer of active human transforming growth factor-{beta}2 elevates intraocular pressure and reduces outflow facility in rodent eyes. *Invest Ophthalmol Vis Sci* 2010;51:2067-2076.

35. McDowell CM, Hernandez H, Mao W, Clark AF. Gremlin Induces Ocular Hypertension in Mice Through Smad3-Dependent Signaling. *Invest Ophthalmol Vis Sci* 2015;56:5485-5492.

36. McDowell CM, Tebow HE, Wordinger RJ, Clark AF. Smad3 is necessary for transforming growth factor-beta2 induced ocular hypertension in mice. *Exp Eye Res* 2013;116:419-423.

37. Javelaud D, Mauviel A. Crosstalk mechanisms between the mitogen-activated protein kinase pathways and Smad signaling downstream of TGF-beta: implications for carcinogenesis. *Oncogene* 2005;24:5742-5750.

38. Javelaud D, Mauviel A. [Transforming growth factor-betas: smad signaling and roles in physiopathology]. *Pathol Biol (Paris)* 2004;52:50-54.

39. Javelaud D, Mauviel A. Mammalian transforming growth factor-betas: Smad signaling and physio-pathological roles. *Int J Biochem Cell Biol* 2004;36:1161-1165.

40. Massague J, Chen YG. Controlling TGF-beta signaling. *Genes Dev* 2000;14:627-644.

41. Poltorak A, He X, Smirnova I, et al. Defective LPS signaling in C3H/HeJ and C57BL/10ScCr mice: mutations in Tlr4 gene. *Science* 1998;282:2085-2088.

42. Hoshino K, Takeuchi O, Kawai T, et al. Cutting edge: Toll-like receptor 4 (TLR4)-deficient mice are hyporesponsive to lipopolysaccharide: evidence for TLR4 as the Lps gene product. *J Immunol* 1999;162:3749-3752.

43. Miyake K. Innate immune sensing of pathogens and danger signals by cell surface Toll-like receptors. *Semin Immunol* 2007;19:3-10.

44. Piccinini AM, Midwood KS. DAMPening inflammation by modulating TLR signalling. *Mediators Inflamm* 2010;2010.

45. Bhattacharyya S, Kelley K, Melichian DS, et al. Toll-like receptor 4 signaling augments transforming growth factor-beta responses: a novel mechanism for maintaining and amplifying fibrosis in scleroderma. *Am J Pathol* 2013;182:192-205.

46. Seki E, De Minicis S, Osterreicher CH, et al. TLR4 enhances TGF-beta signaling and hepatic fibrosis. *Nat Med* 2007;13:1324-1332.

47. Pulskens WP, Rampanelli E, Teske GJ, et al. TLR4 promotes fibrosis but attenuates tubular damage in progressive renal injury. *J Am Soc Nephrol* 2010;21:1299-1308.

48. Campbell MT, Hile KL, Zhang H, et al. Toll-like receptor 4: a novel signaling pathway during renal fibrogenesis. *J Surg Res* 2011;168:e61-69.

49. Huang H, Shiffman ML, Friedman S, et al. A 7 gene signature identifies the risk of developing cirrhosis in patients with chronic hepatitis C. *Hepatology* 2007;46:297-306.

50. Li Y, Chang M, Abar O, et al. Multiple variants in toll-like receptor 4 gene modulate risk of liver fibrosis in Caucasians with chronic hepatitis C infection. *J Hepatol* 2009;51:750-757.

51. Tovar-Vidales T, Fitzgerald AM, Clark AF, Wordinger RJ. Transforming growth factor-beta2 induces expression of biologically active bone morphogenetic protein-1 in human trabecular meshwork cells. *Invest Ophthalmol Vis Sci* 2013;54:4741-4748.

52. Pang IH, Shade DL, Clark AF, Steely HT, DeSantis L. Preliminary characterization of a transformed cell strain derived from human trabecular meshwork. *Curr Eye Res* 1994;13:51-63.

53. Matsunaga N, Tsuchimori N, Matsumoto T, Ii M. TAK-242 (resatorvid), a small-molecule inhibitor of Toll-like receptor (TLR) 4 signaling, binds selectively to TLR4 and interferes with interactions between TLR4 and its adaptor molecules. *Mol Pharmacol* 2011;79:34-41.

54. Hussain T, Nasreen N, Lai Y, Bellew BF, Antony VB, Mohammed KA. Innate immune responses in murine pleural mesothelial cells: Toll-like receptor-2 dependent induction of beta-defensin-2 by staphylococcal peptidoglycan. *Am J Physiol Lung Cell Mol Physiol* 2008;295:L461-470.

55. MacRedmond RE, Greene CM, Dorscheid DR, McElvaney NG, O'Neill SJ. Epithelial expression of TLR4 is modulated in COPD and by steroids, salmeterol and cigarette smoke. *Respir Res* 2007;8:84.

56. Maglio M, McMahon C, Hoskins D, Alvarado J. Potential artifacts in scanning electron microscopy of the trabecular meshwork in glaucoma. *Am J Ophthalmol* 1980;90:645-653.

57. McDowell CM, Luan T, Zhang Z, et al. Mutant human myocilin induces strain specific differences in ocular hypertension and optic nerve damage in mice. *Exp Eye Res* 2012;100:65-72.

58. Grybauskas A, Koga T, Kuprys PV, et al. ABCB1 transporter and Toll-like receptor 4 in trabecular meshwork cells. *Mol Vis* 2015;21:201-212.

59. Bahler CK, Hann CR, Fjield T, Haffner D, Heitzmann H, Fautsch MP. Second-generation trabecular meshwork bypass stent (iStent inject) increases outflow facility in cultured human anterior segments. *Am J Ophthalmol* 2012;153:1206-1213.

60. Bhattacharyya S, Tamaki Z, Wang W, et al. FibronectinEDA promotes chronic cutaneous fibrosis through Toll-like receptor signaling. *Sci Transl Med* 2014;6:232ra250.

61. Qureshi ST, Lariviere L, Leveque G, et al. Endotoxin-tolerant mice have mutations in Toll-like receptor 4 (Tlr4). *J Exp Med* 1999;189:615-625.

62. Kawai T, Akira S. The role of pattern-recognition receptors in innate immunity: update on Toll-like receptors. *Nat Immunol* 2010;11:373-384.

63. Guo J, Friedman SL. Toll-like receptor 4 signaling in liver injury and hepatic fibrogenesis. *Fibrogenesis Tissue Repair* 2010;3:21.

64. Huang QQ, Pope RM. The role of toll-like receptors in rheumatoid arthritis. *Curr Rheumatol Rep* 2009;11:357-364.

65. Landreth GE, Reed-Geaghan EG. Toll-like receptors in Alzheimer's disease. *Curr Top Microbiol Immunol* 2009;336:137-153.

66. Yang L, Seki E. Toll-like receptors in liver fibrosis: cellular crosstalk and mechanisms. *Front Physiol* 2012;3:138.

67. Tovar-Vidales T, Fitzgerald AM, Clark AF. Human trabecular meshwork cells express BMP antagonist mRNAs and proteins. *Exp Eye Res* 2016;147:156-160.

68. Yan X, Lin Z, Chen F, et al. Human BAMBI cooperates with Smad7 to inhibit transforming growth factor-beta signaling. *J Biol Chem* 2009;284:30097-30104.

69. Lin SJ, Lerch TF, Cook RW, Jardetzky TS, Woodruff TK. The structural basis of TGF-beta, bone morphogenetic protein, and activin ligand binding. *Reproduction* 2006;132:179-190.

70. Yaghoubi M, Moradi-Lakeh M, Mokhtari-Payam M, Fakhraie G, Shokraneh F. Confocal scan laser ophthalmoscope for diagnosing glaucoma: a systematic review and meta-analysis. *Asia Pac J Ophthalmol (Phila)* 2015;4:32-39.

CHAPTER III

BMP and Activin Membrane Bound Inhibitor Regulates the Extracellular Matrix in the Trabecular Meshwork

Humberto Hernandez, J. Cameron Millar, Stacy M. Curry, Abbot F. Clark, Colleen M. McDowell

IOVS November 2017

ABSTRACT

Purpose

The trabecular meshwork (TM) plays an important role in the regulation of aqueous humor outflow and intraocular pressure (IOP). Regulation of the extracellular matrix (ECM) by TGFβ2 been extensively studied. BMP and activin membrane-bound inhibitor (BAMBI) has been shown to inhibit or modulate TGFβ2 signaling. In this study, we investigate the role of TGFβ2 and BAMBI in the regulation of TM ECM and ocular hypertension.

Methods

Mouse TM (MTM) cells were isolated from B6;129S1-Bambi^{tm1Jian}/J flox mice, characterized for TGFβ2 and Dexamethasone (DEX) induced expression of fibronectin, collagen-1, collagen-4, laminin, α-smooth muscle actin, cross-linked actin networks (CLANs) formation and DEX induced myocilin (*MYOC*) expression. MTM cells were transduced with Ad5.GFP to identify transduction efficiency. MTM cells and mouse eyes were transduced with Ad5.Null, Ad5.Cre, Ad5.TGFβ2, or Ad5.TGFβ2 + Ad5.Cre to evaluate the effect on ECM production, IOP, and outflow facility.

Results:

MTM cells express TM markers and respond to DEX and TGFβ2. Ad5.GFP at 100 MOI had the highest transduction efficiency. *Bambi* knockdown by Ad5.Cre and Ad5.TGFβ2 both increased fibronectin, collagen-1, and collagen-4 in TM cells in culture and tissue. Ad5.Cre, Ad5.TGFβ2, and Ad5.TGFβ2 + Ad5.Cre each significantly induced ocular hypertension and lowered aqueous humor outflow facility in transduced eyes.

Conclusions

We show for the first time that knockdown of *Bambi* alters ECM expression in cultured cells and mouse TM, reduces outflow facility, and causes ocular hypertension. These data provide a novel insight into the development of glaucomatous TM damage and identify BAMBI as an important regulator of TM ECM and ocular hypertension.

Keywords: BAMBI, TGFβ2, BMP, trabecular meshwork, ocular hypertension, extracellular matrix

Grant support: Bright Focus Foundation G2014063 (CMM), R01EY026529 (CMM), and Neurobiology of Aging training grant T32AG020494 (HH).

Introduction

Glaucoma is the second leading cause of blindness worldwide[1], affecting approximately 70 million individuals[2]. It is a heterogeneous group of optic neuropathies, characterized by the loss of retinal ganglions cells (RGCs) leading to irreversible vision loss and blindness. Primary open angle glaucoma (POAG) affects the drainage angle of the eye and is associated with elevated intraocular pressure (IOP). Elevated IOP is due to increased outflow resistance at the trabecular meshwork (TM). Glaucomatous changes at the TM include loss of TM cellularity, thickening of the TM beams, and increased extracellular matrix (ECM) production, deposition and remodeling. Current treatment options for POAG patients generally involve reducing IOP with pharmacological drugs that do not target the pathological processes occurring at the TM. The molecular mechanisms responsible for changes to the TM and aqueous humor outflow resistance needs further investigation.

Transforming growth factor beta 2 (TGFβ2) is one of the most studied growth factors and the most common isoform in the eye[3-6]. Studies have shown that aqueous humor levels of TGFβ2 are elevated in POAG patients[3, 7-10]. It is well established that TGFβ2 alters the ECM composition and ECM crosslinking of the TM[11-17]. We and others have previously demonstrated that TGFβ2 elevates IOP in the anterior segment perfusion organ culture models[14, 18] and Ad5.TGFβ2 induces ocular hypertension in mice[19-21]. It is well known that TM cells express and secrete TGFβ2[22]. TGFβ2-induced changes to the TM occur through both the canonical SMAD and non-SMAD signaling pathways, and the canonical SMAD pathway is essential for TGFβ2-induced ocular hypertension in mice[11, 12, 21, 23]. The canonical signaling pathway is initiated when TGFβ2 binds type II receptors (TGFβRII), which assembles, activates, and phosphorylates type I receptors (TGFβRI). Activated TGFβRI subsequently phosphorylates SMAD2/3 and leads to the

association of SMAD4 into a complex. This complex interacts with coactivators or corepressors to regulate gene transcription. To understand the development of ocular hypertension, the homeostatic regulatory molecules of TGFβ2 and signaling molecules must be evaluated.

Bone morphogenetic proteins (BMPs) are a family of growth factors involved in the regulation of the ECM. BMPs can suppress TGFβ2 induced ECM deposition[16, 24], the BMP antagonist gremlin elevates IOP in perfusion cultured anterior segments[24], and over-expression of gremlin in mouse eyes[20] and BMP2 in rats[25] causes ocular hypertension, suggesting that BMP signaling is required for regulating outflow. Similar to TGFβ2, BMP signaling requires 2 types of transmembrane serine/threonine receptors, type I (BMPR-I) and type II (BMPR-II)[26]. BMPR-II is most commonly utilized for BMP signaling and is the target of BMP antagonists[27]. The activated BMPR-I and BMPR-II complex results in phosphorylation of SMAD1, SMAD5, or SMAD8[26, 28-30]. The phosphorylated SMAD1/5/8 complex associates with SMAD4, and the complex translocates to the nucleus and associates with coactivators or corepressors to regulate gene transcription[31]. We have previously shown that TM cells express BMPs and their receptors; BMP2, BMP4, BMP5, BMP7 BMP-RIA, BMP-RIB, and BMP-RII[32]. A better understanding of the regulatory mechanisms involved in BMP and TGFβ2 signaling are necessary for the development of novel disease modifying therapeutic treatments for POAG patients[33].

BMP and activing membrane-bound inhibitor (BAMBI) is a transmembrane glycoprotein related to the TGFβ-family type I receptors, but lacks an intracellular kinase domain[34]. BAMBI has been shown to be important in embryonic development as it is co-expressed with BMP4 and BAMBI expression is induced by BMP4, suggesting a negative mechanistic feedback loop[35]. BAMBI is evolutionarily conserved from fish to humans[34-36], with a mouse and human homology of 85%[34, 37, 38]. BAMBI has been shown to inhibit BMP, activin, and TGFβ

signaling[34]. BAMBI can interact with BMP receptors directly and antagonize BMP signaling[39], as well as interact directly with TGFβ receptors and antagonize TGFβ signaling[40]. BAMBI can also interact with BMP and TGFβ signaling pathways through other different mechanisms. BAMBI can form a ternary complex with SMAD7/ALK5/TGFβRI and inhibit the interaction between ALK5/TGFβRI and SMAD3, thus impairing SMAD3 activation[41]. BAMBI has also been shown to co-translocate with SMAD2/3 into the nucleus upon TGFβ treatment and modulate TGFβ signalling[42]. The human BAMBI promoter contains the elements that directly associate with SMAD3 and SMAD4, and these elements are critical for the TGFβ responsiveness to the BAMBI promoter[43]. BAMBI has been shown to inhibit fibrogenesis through suppression of TGFβ induced collagen-I expression[44]. Knockdown of *Bambi* expression enhances canonical[41] and non-canonical TGFβ signaling[45]. Recently, we have shown that BAMBI is expressed in human TM cells and is downregulated by the presence of TGFβ2 (5ng/ml) at 24 hours[46]. These data suggest that BAMBI is an important molecule in TGFβ signaling regulation.

Toll-like receptor 4 (TLR4) signaling has been identified as a regulator of BAMBI expression. TLR4 activation by lipopolysaccharide (LPS) downregulates BAMBI, which enhances TGFβ signaling leading to increased ECM production via a SMAD-dependent pathway[47, 48]. BAMBI downregulation by TLR4 is regulated by the MyD88-NFκB-dependent pathway[47, 49, 50]. The transcriptional repression of BAMBI by NF-κB p50 enhances TGFβ signaling in hepatic satellate cells[51]. In addition, TLR4 enhances TGFβ signaling and hepatic fibrosis by downregulation of BAMBI[52]. These data suggest that TLR4 is an important regulator of BAMBI expression in the context of TGFβ2-TLR4 signaling crosstalk. Further experiments are needed to determine the exact mechanistic role of BAMBI in TGFβ2-TLR4 signaling;

however, these data suggest that activation of TLR4 downregulates BAMBI leading to TGFβ fibrogenesis.

BAMBI has also been associated with the pathogenesis of several human diseases including colorectoral carcinoma, hepatocellular carcinomas, gastric carcinoma, hepatic fibrosis, and sceleroderma[48, 52-54]. *Bambi* knockdown has been shown to increase TGFβ signaling in a model of diabetic globular disease where overexpression of TGFβ has been correlated with the disease pathology[45]. We have also recently identified TGFβ2-TLR4 signaling crosstalk as an important regulator of the ECM in the TM and ocular hypertension[55]. Here we demonstrate that TGFβ2 regulates BAMBI expression in TM cells, knockdown of *Bambi* induces ECM production in TM cells *in vitro and in vivo*, and knockdown of *Bambi* in the mouse TM induces ocular hypertension and outflow resistance.

MATERIALS AND METHODS

Mouse TM Cell Culture

Mouse TM (MTM) cells were isolated, cultured, and maintained in Dulbecco's modified Eagle's medium (DMEM; Invitrogen-Gibco Life Technologies, Grand Island, NY) containing 15% fetal bovine serum (FBS; Atlas Biologicals Products, Fort Collins, CO) and supplemented with penicillin (100 units/ml), streptomycin (0.1 mg/ml) and L-glutamine (0.292 mg/ml) (Gibco BRL Life Technologies). MTM cells were isolated as described below. All experiments were performed on cells within 10 passages.

B6;129S1-Bambi^{tm1Jian}/J mice

All experiments were conducted in compliance with the ARVO Statement of the Use of Animals in Ophthalmic and Vision Research and the University of North Texas Health Science Center (UNTHSC; Fort Worth, TX, USA) Institutional Animal Care and Use Committee (IACUC) Guidelines and Regulations. B6;129S1-Bambi^{tm1Jian}/J conditional knockout mice were obtained from The Jackson Laboratory and subsequently bred at UNTHSC. All mice were 3-5 months old at the start of the experiment. All animals were housed in the UNTHSC vivarium. MTM cells were isolated from B6;129S1-Bambi^{tm1Jian}/J as stated. Adenovirus serotype 5 (Ad5) viral vector expressing human TGFβ2$^{c226s/c228s}$ (hereafter referred as Ad5.TGFβ2) (University of Iowa, Iowa City, IA) was used to over-express TGFβ2 as previously described[19-21]. Ad5.Cre (Vector Biolabs, Malvern, PA) was used to knockdown *Bambi,* and Ad5.Null vector (Vector Biolabs, Malvern, PA) was used as a negative control. Briefly, 2.5 µl of 2.5 x 10^7 plaque forming units (pfu) was intravitreally injected into one eye, and the contralateral eyes used as negative controls.

Mouse TM Cells Isolation and Characterization

Intracameral injections, anterior segment dissections, and magnetic bead isolation of MTM cells was performed according to our established protocol with modifications[56]. It is well established that TM cells have phagocytic properties[57-70]. Uptake of pigment by TM cells was prevented by its removal during the isolation protocol. Briefly, the dissected TM ring was placed in collagenase at 37C for 2 hours. After digestion, cells were spun down (600g for 10 minutes), resuspended in PBS and passed through a 100 µM cell strainer (Thermo scientific, Worcester, MA). The flow through was transferred to Eppendorf tubes and attracted to a magnet on the tube hinge side for 5 minutes. The non-binding cells were transferred to another Eppendorf and

attracted cells were resuspended in PBS. This process was repeated at least three times until the Eppendorf tubes containing attracted cells had no visible pigment, after which complete medium was added and cells transferred to a 96 well plate. Isolated MTM cells were cultured in 24 well-plates on coverslips and allowed to reach confluency. Cells were treated for 96 hours (protein expression) or 7 days (CLANs characterization) with TGFβ2 (5ng/mL), culture medium (TGFβ2 control), DEX (100 nM) or ETOH (vehicle control) in serum free medium. Culture medium was changed every other day. Cells were processed for immunocytochemistry and CLANs counted as previously described[56]. CLAN formation rate was expressed as the ratio of CLAN-positive cells/total number of DAPI-stained cells. For each treatment, 5 regions in each coverslip and 5 to 6 coverslips were counted.

Adenovirus Transduction

In order to determine the transduction efficiency of Ad5 in MTM cells isolated from B6;129S1-Bambi^{tm1Jian}/J mice, MTM cells were transduced with Ad5.GFP at 25, 50, 100, and 200 MOI (multiplicity of infection) for 12 hours and conditioned medium replaced by serum free medium for 24 hours. Similarly, MTM cells were transduced with Ad5.Cre at 0, 50, 100, and 200 MOI for 12 hours, conditioned medium replaced, and after 48 hours changes in fibronectin and collagen-1 was evaluated using immunocytochemistry. Additionally, MTM cells were transduced with Ad5.Null, Ad5.Cre, or Ad5.TGFβ2 at 100 MOI for 12 hours, conditioned medium replaced for 48 hours, and the expression of BAMBI, fibronectin, and collagen-1 was evaluated using immunocytochemistry.

Immunocytochemistry

Mouse TM cells were seeded in 24 well plates on coverslips. After completing the treatment time course, cells were washed with PBS, fixed with 4% paraformaldehyde (PFA), permeabilized with 0.05% Triton X-100 in PBS and blocked using Superblock Blocking Buffer in PBS (Thermo Fisher Scientific; Rockford, IL, USA) for 60 minutes at room temperature. Cells were labeled overnight at 4°C with rabbit anti-fibronectin (EMD Millipore; Billerica, MA) 1:500 dilution, anti-laminin (Novus Biologicals, LL; Littleton, CO) 1:250 dilution, anti-collagen-1 (Novus Biologicals, LL; Littleton, CO) 1:250 dilution, anti-collagen-4 (Novus Biologicals, LL; Littleton, CO) 1:350 dilution, and α-smooth muscle actin (Abcam; Cambridge, MA, USA) 1:500 dilution in Superblock Blocking Buffer in PBS (Thermo Fisher Scientific; Rockford, IL). Treatment without the primary antibodies was used as negative controls. Coverslips were incubated for 2 hours using Alexa-Fluor-labeled anti-rabbit or anti-mouse antibodies (Life Technologies; Carlsbad, CA) 1:1000 dilution. To label CLANs, MTM cells were probed for filamentous actin (F-actin) using Alexa Fluor 488 phalloidin (Thermo Fisher Scientific; Rockford, IL, USA) 1:250 dilution. Coverslips were mounted onto slides with Prolong Gold mounting medium containing DAPI (Invitrogen-Molecular Probes; Carlsbad, CA). Image acquisition was performed using the Keyence BZ-X700 fluorescence microscope (Keyence Corporation of America; Itasca, IL). Images were taken either at 100x, 200x, 400x, or 600x magnification, with each presented figure containing its corresponding scale bar.

Immunohistochemistry of Mouse Eyes

To evaluate early changes in the TM ECM of mice transduced with viral vectors, mice were harvested 11-days post-injection. IOP was recorded at 10-days post-injection and at 11-days post-injection, eyes were enucleated. Eyes were fixed in 4% PFA overnight, embedded in paraffin, cut into 5 μm sections, and transferred to glass slides. Deparaffinization was performed by washing two times with xylene, 100% ethanol, 95% ethanol, and 50% ethanol for 2 minutes each. Slides were then soaked in PBS for 5 minutes. Tissues were blocked using Superblock Blocking Buffer in PBS (Thermo Fisher Scientific; Rockford, IL) for 60 minutes. Rabbit anti-fibronectin (EMD Millipore; Billerica, MA) 1:500 dilution, rabbit anti-collagen-1 (Novus Biologicals, LL; Littleton, CO) 1:250 dilution, mouse anti-collagen-4 (Sigma-Aldrich; St. Louis, MO) 1:250 dilution, and mouse anti-BAMBI (Abnova; Walnut, CA) 1:250 dilution, were used as primary antibodies, followed by Alexa-Fluor-labeled anti-rabbit or anti-mouse antibodies (Life Technologies; Carlsbad, CA) 1:500 dilution. Prolong Gold mounting medium containing DAPI (Invitrogen-Molecular Probes; Carlsbad, CA) was used to mount the slides, and sections were imaged using the Keyence BZ-X700 fluorescence microscope (Keyence Corporation of America; Itasca, IL). All images were taken at 100x magnification; scale bars represent 100μm.

Western Blot Analysis

Western blot studies were performed as previously described[55]. Briefly, MTM cells were treated as stated above. Conditioned medium samples were prepared as follows: conditioned medium (30μL) and 4x Laemmli Buffer (10μL) (Bio-Rad Laboratories, Hercules, CA) were combined for a total volume of 40 μL. Samples were boiled for 10 minutes followed by separation using 12% SDS-PAGE. To verify equal loading for CM samples, gels were stained with Gel Code Blue

Stain Reagent (Thermo Fisher Scientific Inc., Rockford, IL). Proteins were transferred to PVDF membranes (Millipore, Bedford, MA), and membranes blocked with Superblock Blocking Buffer in TBS (Thermo Fisher Scientific; Rockford, IL). Membranes were immunolabeled overnight at 4°C with rabbit anti-fibronectin antibody (EMD Millipore; Billerica, MA) dilution 1:1000. Blots were incubated for 1 hour with horseradish peroxidase (HRP) conjugated goat anti-rabbit secondary antibody (1:1,000; Pierce Biotechnology, Inc., Rockford, IL) diluted in Superblock Blocking Buffer in TBS. Immunolabeled signals were developed using Clarity™ Western ECL Substrate, and blot images were acquired using ChemiDoc Touch Imaging System (Bio-Rad Laboratories, Hercules, CA). Each experiment was repeated 3 times. Densitometry analysis of western immunoblot images was used to determine changes in protein content after treatment. Band intensity for fibronectin was measured using Image Lab Software (Bio-Rad Laboratories). Fold change was compared to Ad5.Null and represented as the mean ± SEM. Statistical significance was determined by one-way ANOVA and Tukey post-hoc analysis comparing all treatments.

Intraocular Pressure Measurements

After intravitreal injection of 2.5 µl (2.5 x 10^7 pfu) of Ad5.Null (n=7 mice), Ad5.Cre (n=9 mice), Ad5.TGFβ2 (n=10 mice), or Ad5.Cre + Ad5.TGFβ2 (n=10 mice), IOP was measured as previously described[19-21, 71]. Briefly, IOP was measured under isoflurane anesthesia using the Tonolab tonometer (Colonial Medical Supply, Franconia, NH). All IOP measurements were performed during the same time period of the light-on phase. Statistical significance was determined by Student's paired t-test at each time point comparing the injected eye to the contralateral uninjected control eye.

Aqueous Humor Outflow Facility

To evaluate the effect of Ad5.Cre and Ad5.TGFβ2 on aqueous humor outflow rate in B6;129S1-Bambi^{tm1Jian}/J mice, 3 to 5 mice were used for outflow facility determination as previously described[72, 73]. Briefly, eyes of anesthetized mice were cannulated intracamerally with a 30-gauge steel needle inserted through the peripheral cornea approximately 1 to 2 mm from the limbus and pushed toward the region of the opposing chamber angle. The needle was connected by tubing to an in-line pressure transducer for the continuous determination of pressure within the system. The opposing terminal of the pressure transducer was connected by tubing to a 50 µL glass micro syringe loaded into a microdialysis infusion pump. The pump was switched on and set to a flow rate of 0.1 µL/min. The pump remained running until the pressure in the system was stabilized. Flow rates were then increased sequentially to 0.4, and 0.5 µL/min, and stabilized pressure values at each flow rate were recorded. For each eye, aqueous humor outflow facility (µL/min/mm Hg) was calculated as the reciprocal of the slope of the respective pressure-flow rate curves.

RESULTS

Isolation and characterization of Mouse TM cells

Extracellular matrix deposition at the TM is one of the major factors involved in the development of ocular hypertension. TGFβ2 is a major growth factor involved in ECM deposition in the glaucomatous TM. BAMBI has been shown to regulate TGFβ2 signaling in other tissues[41, 45, 51]. We have previously shown that both TM and optic nerve head (ONH) cells and tissues express BAMBI[32]. To better understand the role of BAMBI in ECM deposition in

TM cells, MTM cells were isolated from B6;129S1-Bambi$^{tm1Jian/J}$ mice using magnetic beads (Figure 1A, 1B). We utilized our established protocol[56] and removed the pigment during the isolation process (Figure 1). MTM cells were characterized for the expression of TM markers[74-78]. It is well established that TGFβ2 and DEX induce the expression of ECM proteins in the TM. Here we show that isolated MTM cells express fibronectin, collagen-1, collagen-4, laminin, and α-smooth muscle actin (Figure 2). In addition, TGFβ2 (ng/mL) and DEX (100μM) induce an increase in expression of these markers when compared to their control treatments (Figure 2A – 2T). Recently, we have shown that isolated mouse TM cells in culture respond to DEX treatment by upregulating myocilin expression and inducing the formation of CLANs[56]. Here, DEX (100μM) induced the expression of myocilin at 4 days post treatment when compared to vehicle treated cells (Figure 3A, 3B). Recombinant human TGFβ2 (5ng/mL) and DEX (100μM) each induced the expression of CLANs when compared to their controls (3C – 3H). These data demonstrate that mouse TM cells can be isolated and cultured *in vitro*, express known TM markers, and respond to TGFβ2 and DEX.

Knockdown of *Bambi* Increases ECM Expression

Adenovirus serotype 5 has selective tropism to the TM[79]. Therefore, we evaluated the ability of isolated TM cells in culture to be transduced by Ad5.GFP utilizing different MOI's (Figure 4A). We observed that 200 MOI had the highest transduction efficiency; however, cells were visibly unhealthy and there was evidence of cell death. At 100 MOI, the cells were healthy and the majority of cells were GFP positive. We also evaluated whether knockdown of *Bambi* leads to ECM changes in cultured MTM cells. Knockdown of *Bambi* utilizing Ad5.Cre increased the levels of fibronectin and collagen-1 in an MOI dependent manner (Figure 4B). Further,

Ad5.TGFβ2 (100 MOI) and Ad5.Cre (100 MOI) decreased BAMBI (Figure 5D, G) expression and increased fibronectin (Figure 5E, H) and collagen-1 (Figure 5F, I) expression when compared to Ad5.Null (100 MOI) treated cells (Figure 5A, B, C). Fibronectin expression in the conditioned medium was also quantified by western blot (Figure 5J, K). These data provide evidence that BAMBI is an important regulator of the ECM in mouse TM cells.

Conditional Knockdown of *Bambi* in Mice Increases ECM Expression

BAMBI has been shown to be a regulator of growth factors involved in ECM remodeling[44, 80-85]. To evaluate the effects of BAMBI on ECM regulation *in vivo*, *Bambi* floxed mice were injected intravitreally with Ad5.Cre in one eye, while the contralateral uninjected eye served as a control. Here we show for the first time that the mouse TM expresses BAMBI, and Ad5.Cre transduction is sufficient to knockdown *Bambi* in the TM (n=5) (Figure 6). We have previously shown that Ad5.TGFβ2 is able to increase the expression of fibronectin mRNA and protein in the TM of mice[20, 21, 55]. We evaluated the importance of BAMBI in the regulation of ECM and used Ad5.TGFβ2 as a positive control. In the present study, Ad5.Null (n=7), Ad5.Cre (n=15), and Ad5.TGFβ2 (n=9) were used to transduce the TM of mice. Interesting, knockdown of *Bambi* by Ad5.Cre or by Ad5.TGFβ2 increased the expression of fibronectin, collagen-1, and collagen-4 in the TM when compared to Ad5.Null (Figure 7).

Conditional Knockdown of *Bambi* Induces Ocular Hypertension in Mice

To test the effect of *Bambi* knockdown on ocular hypertension, Ad5.Null, Ad5.Cre, Ad5.TGFβ2, or Ad5.Cre + Ad5.TGFβ2 were injected intravitreally into B6;129S1-Bambi^{tm1Jian}/J mice (Figure 8A – Figure 8D). Our established mouse model of ocular hypertension using Ad5.TGFβ2 was

used as our positive control[19-21] and Ad5.Null was used as a negative control. Ad5.Null, Ad5.Cre, Ad5.TGFβ2, or Ad5.Cre+Ad5.TGFβ2 viral vectors were injected intravitreally into one eye of each animal and the contralateral eye was used as an uninjected control. Ad5.Null did not elevate IOP at any time point (n=7) (Figure 8A). Interestingly, knockdown of *Bambi* by Ad5.Cre significantly elevated IOP at all time points post-injection compared to the uninjected control eyes (Figure 8B) ($p<.001$, n=9). As expected, Ad5.TGFβ2 had significant IOP elevation at all time points post-injection compared to the uninjected control eyes (Figure 8C) ($p<.001$, n=10). Ad5.TGFβ2 + Ad5.Cre also significantly elevated IOP at all time points (Figure 8D) ($p<.001$, n=10). These data suggest that knockdown of *Bambi* is sufficient to cause ocular hypertension in mice to the same degree as overexpression of TGFβ2. Co-treatment of Ad5.TGFβ2 + Ad5.Cre did not produce additional IOP elevation above that of Ad5.Cre or Ad5.TGFβ2 alone, suggesting that we may have reached the maximum IOP elevation for this experimental paradigm. Statistical significance was determined by Student's paired t-test at each time point comparing the transduced eye to the contralateral uninjected control eye.

Outflow Facility

To further understand if the elevated IOP was the result of increased outflow resistance, measurement of outflow facility was performed on transduced (Ad5.Cre, Ad5.TGFβ2, or Ad5.Cre+Ad5.TGFβ2) mouse eyes and control uninjected eyes after the 56-day time point (Figure 9). Aqueous humor outflow facility was significantly lower in Ad5.Cre ($p=0.012$, n=5), Ad5.TGFβ2 ($p=0.011$, n=3), and Ad5.TGFβ2 + Ad5.Cre ($p=0.02$, n=3) transduced eyes compared to their control uninjected eyes. Further, the reduction in outflow facility correlated closely with the observed increase in IOP. Statistical significance was determined by Student's

paired t-test at each time point comparing the transduced eye to the contralateral uninjected control eye.

DISCUSSION

In this study, we demonstrate that BAMBI is a novel regular of the ECM and fibrosis in the TM. Isolated MTM cells from B6;129S1-Bambi^{tm1Jian}/J mice express TM markers and knockdown of *Bambi* in these cells increased ECM protein expression. Interestingly, knockdown of *Bambi* in the TM of mice elevated IOP, reduced outflow facility, and increased ECM proteins in the TM. These findings suggest that BAMBI plays an important role in TM ECM and IOP regulation.

Regulatory mechanisms to control TGFβ signaling have been shown to directly affect the TGFβ receptors and downstream signaling molecules. BAMBI has been identified as an important regulator of TGFβ signaling. The extracellular domain of BAMBI is closely related to type-I TGFβ and BMP receptors[34]. BAMBI can incorporate into complexes with TGFβR I and II[34], thereby preventing their dimerization. The intracellular domain of BAMBI does not encode a serine/threonine-kinase domain, thus inhibiting TGFβ and BMP signaling. TGFβ can directly increase BAMBI protein expression through SMAD3/4 binding to the SMAD binding element of the *hBAMBI* promoter[43]. We have previously reported that TGFβ2 decreases BAMBI mRNA and protein expression in human TM cells[46]. In addition, TLR4 signaling has been shown to downregulate BAMBI expression via a NF-kB dependent pathway[51]. TGFβ2-TLR4 signaling crosstalk has been implicated in several fibrosis diseases including scleroderma, liver cirrhosis, and kidney disease[48, 49, 50, 52].

Recently we have shown TGFβ2-TLR4 signaling in the development of glaucomatous TM damage[55]. TLR4 can be activated by damage-associated molecular patterns (DAMPs) such as cellular fibronectin containing the EDA isoform (cFN-EDA). We demonstrated that activation of TLR4 in TM cells by cFN-EDA induces ECM production[55]. Inhibition of TLR4 signaling by a selective TLR4 inhibitor (TAK-242) blocked ECM production. In addition, *Tlr4* mutant mice were resistant to TGFβ2 induced ocular hypertension. These data suggest that in the TM, TGFβ2-TLR4 signaling crosstalk is important in regulating ECM production. Recent evidence suggests that upon TLR4 activation, NF-kB translocates into the nucleus and serves as a transcription factor to suppress BAMBI expression[52]. Downregulation of BAMBI in the TM could contribute to uninhibited TGFβ2 signaling, resulting in the increase in TM ECM production and ocular hypertension.

Our studies suggest that regulation of the TGFβ2 signaling pathway is important for TM and IOP homeostasis. In addition, TLR4 activation and *Bambi* knockdown has been shown to effect TGFβ signaling[86]. Overexpression of BAMBI suppresses the effect of TGFβ[42, 87, 88]. Here we show for the first time that knockdown of *Bambi* in the TM is sufficient to induce ocular hypertension and glaucoma-like changes to the TM. Future studies are necessary to understand the effect of BAMBI on endogenous levels of TGFβ2, BMPs, activin, and DAMPs in the TM.

In summary, we demonstrate that BAMBI is involved in the production and regulation of the ECM in the TM. These data provide evidence that BAMBI is a critical link molecule in TGFβ2-TLR4 signaling crosstalk. Our data further provide a new insight into the molecular mechanism involved in the development of glaucomatous TM damage.

Figure Legends

Figure 1

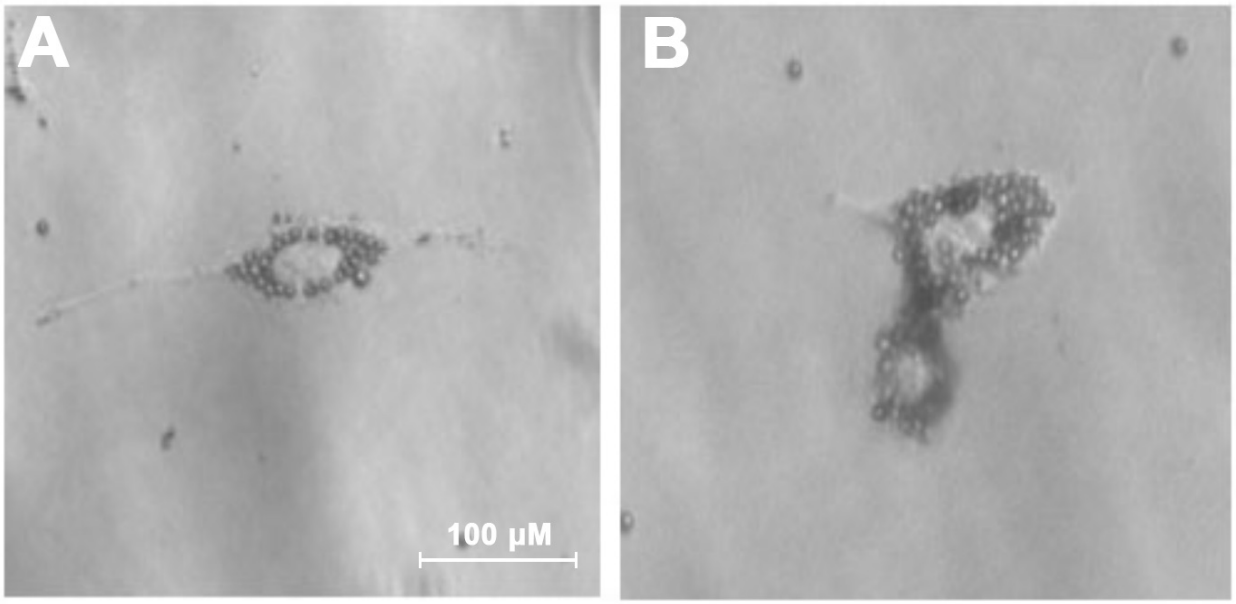

Figure 1. Magnetic bead isolation of MTM cells from B6/129S1-*Bambi*^{tm1Jian}/J mice. Mouse TM cells were isolated from B6;129S1-Bambi^{tm1Jian}/J mice using our established magnetic bead isolation protocol[56]. (A) MTM cells growing in the absence of pigment after 24 hours. (B) MTM cell dividing and containing magnetic beads.

Figure 2

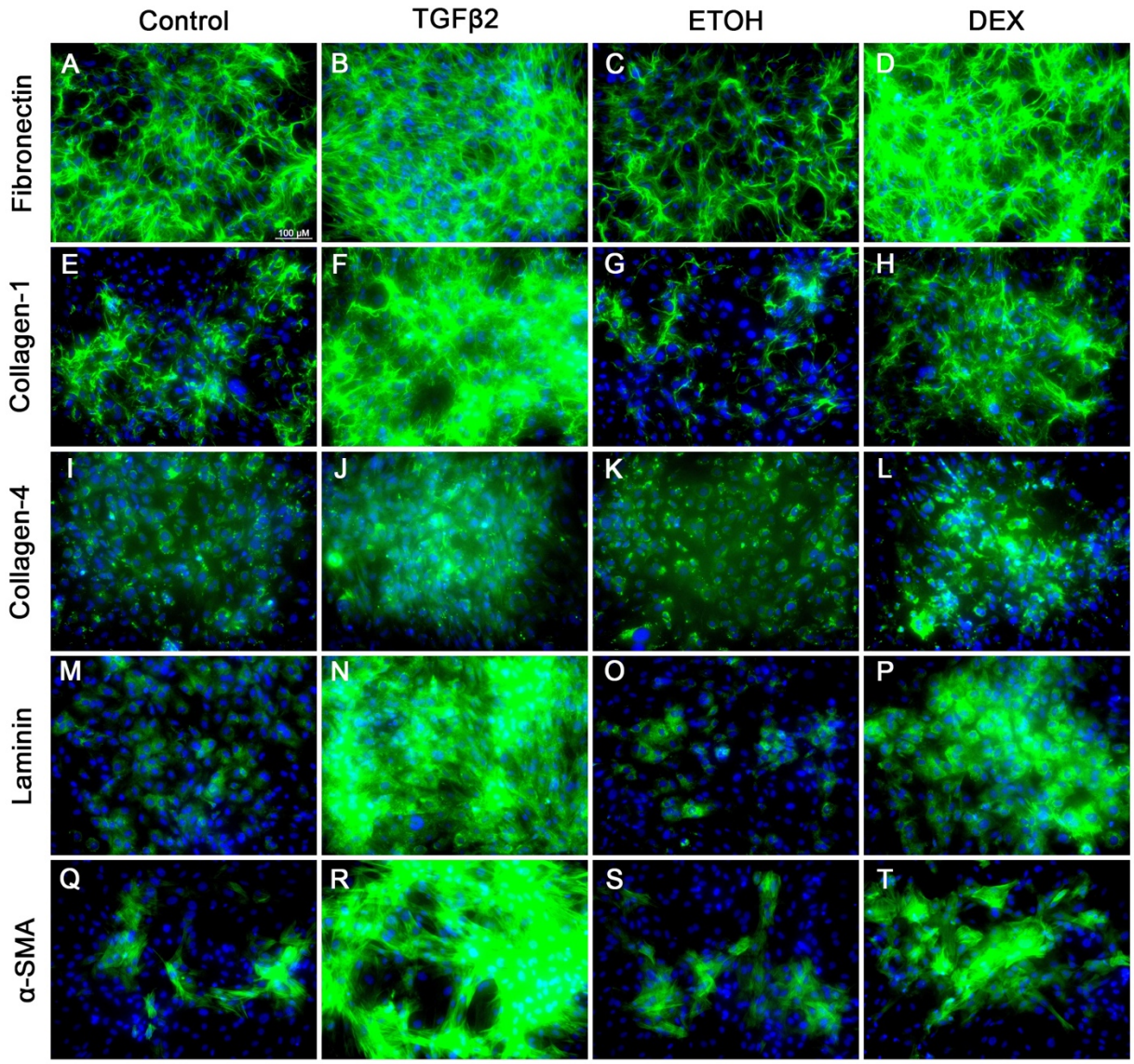
Control
TGFβ2
ETOH
DEX
Fibronectin
Collagen-1
Collagen-4
Laminin
α-SMA
A
B
C
D
E
F
G
H
I
J
K
L
M
N
O
P
Q
R
S
T
100 µM

Figure 2. Characterization of MTM cells for the expression of fibronectin, collagen-1, collagen-4, laminin, and α-smooth muscle actin. MTM cells (n=3 replicates) were grown to confluency, treated for 96 hours with control (serum free medium) (A, E, I, M, Q), TGFβ2 (5ng/mL) (B, F, J, N, R), ETOH (vehicle control for DEX) (C, G, K, O, S), or DEX (100 nM) (D, H, L, P, T). Control treated cells each expressed basal levels of fibronectin (A, C), collagen-1 (E, G), collagen-4 (I, K), laminin (N, P), and α-smooth muscle actin (R, T). TGFβ2 and DEX both induced the expression of fibronectin (B, D), collagen-1 (F, H), collagen-4 (J, L), laminin (N, P), and α-smooth muscle actin (R, T) when compared to control.

Figure 3

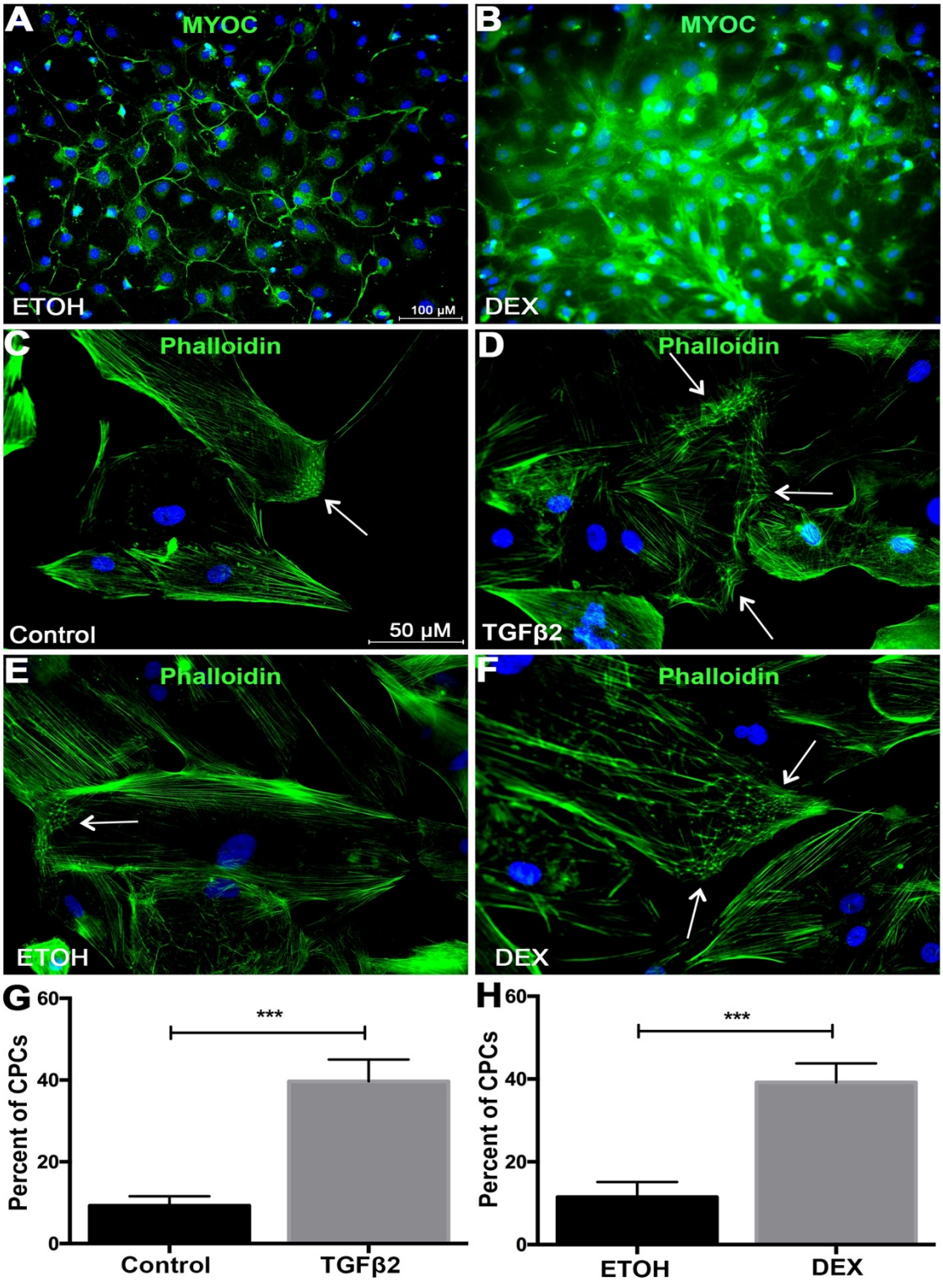
A
MYOC
ETOH
100 μM
B
MYOC
DEX
C
Phalloidin
Control
50 μM
D
Phalloidin
TGFβ2
E
Phalloidin
ETOH
F
Phalloidin
DEX
G
Percent of CPCs
60
40
20
0
***
Control
TGFβ2
H
Percent of CPCs
60
40
20
0
***
ETOH
DEX

Figure 3. Characterization of MTM cells for DEX induced myocilin expression and formation of cross-linked actin networks (CLANs). MTM cells (n=3 replicates) were grown to confluency and treated with (A) ETOH (vehicle control for DEX) or (B) DEX (100 nM) in serum free medium for 4 days for immunostaining of DEX induced myocilin expression. To access CLAN formation, MTM cells were grown to confluency and treated with (C) medium, (D) TGFβ2 (5ng/ml), (E) ETOH, or (F) DEX (100) for 7 days with 1% FBS. (D) TGFβ2 induced the formation of CLANS when compared to (C) control treated MTM cells. (F) DEX induced the expression of CLANs when compared to (E) ETOH (vehicle control) treated MTM cells. Quantification of CLAN positive cells (CPCs) in (G) TGFβ2 and vehicle control, as well as (H) DEX and ETOH treated MTM cells. Statistical significance was determined by Student's unpaired t-test, (*** $p<0.001$).

Figure 4

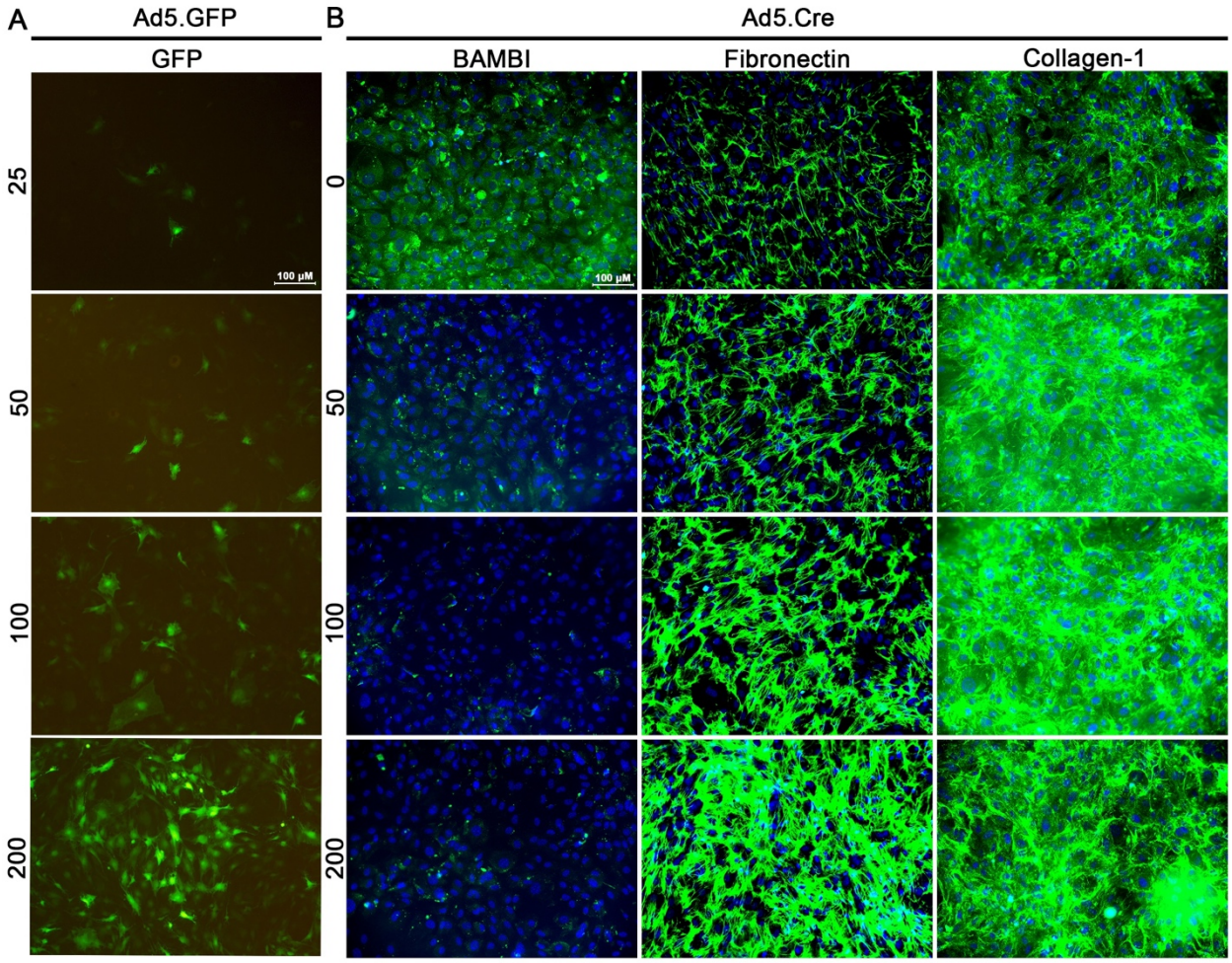
A
Ad5.GFP
B
Ad5.Cre
GFP
BAMBI
Fibronectin
Collagen-1
25
50
100
200
0
50
100
200
100 µM
100 µM

Figure 4. Ad5.GFP transduces primary MTM cells and knockdown of *Bambi* using Ad5.Cre increases fibronectin and collagen-1 expression. (A) MTM cells were transduced for 12 hours with Ad5.GFP at 25, 50, 100, and 200 MOI followed by incubation for 48 hours in serum free medium (n=4 replicates). Ad5.GFP at 200 MOI had the highest transduction efficiency and 100 MOI had the highest cellular health. (B) MTM cells were cultured to confluency and transduced for 12 hours with Ad5.Cre at 50, 100, and 200 MOI. After 12 hours incubation, cells were cultured for 48 hours in serum free medium. Ad5.Cre knockdown of *Bambi* induces the expression of fibronectin and collagen-1 expression at 50, 100, and 200 MOI (n=3 replicates).

Figure 5

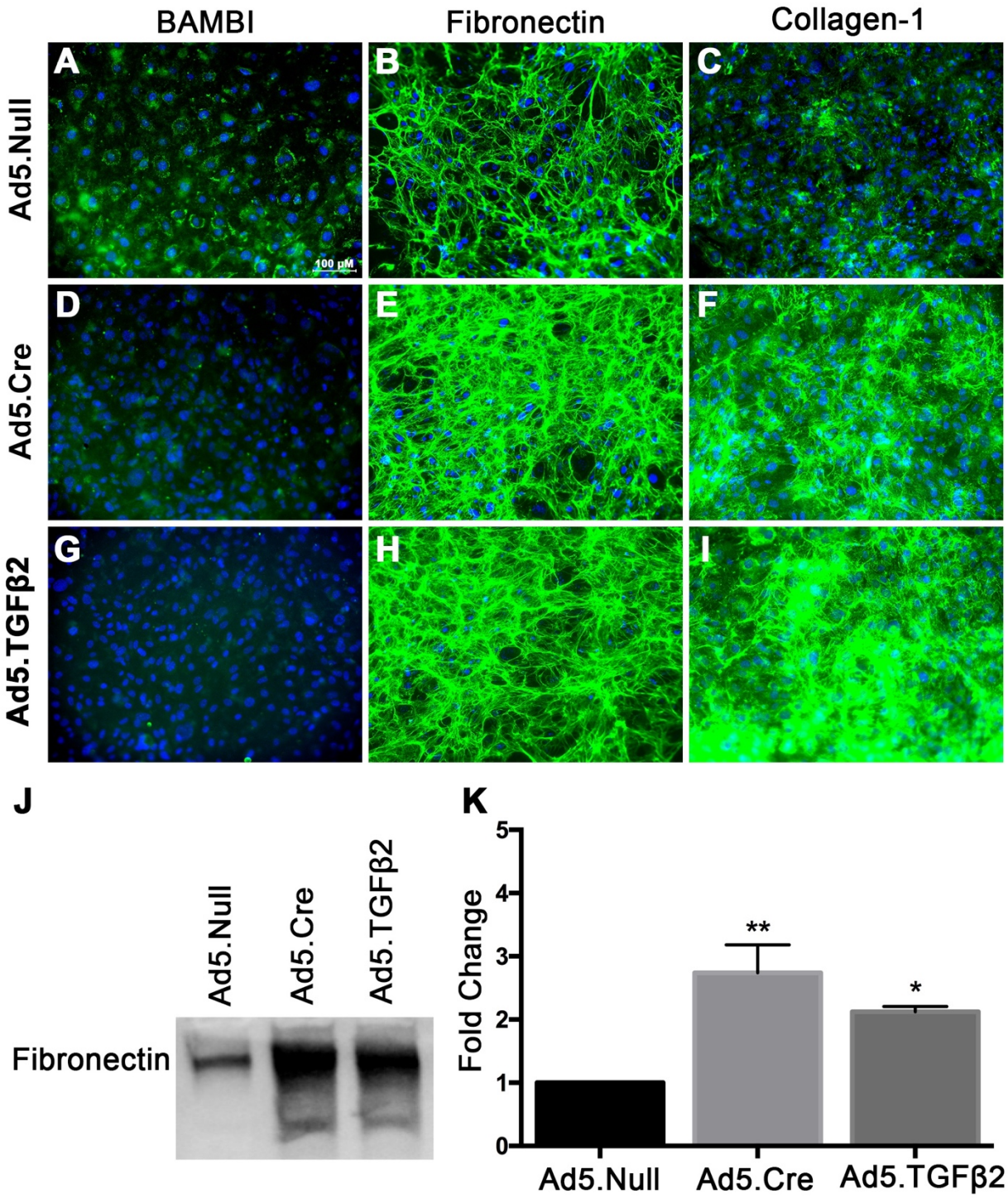
BAMBI
Fibronectin
Collagen-1
Ad5.Null
Ad5.Cre
Ad5.TGFβ2
A
B
C
D
E
F
G
H
I
100 μM
J
Ad5.Null
Ad5.Cre
Ad5.TGFβ2
Fibronectin
K
Fold Change
0
1
2
3
4
5
**
*
Ad5.Null
Ad5.Cre
Ad5.TGFβ2

Figure 5. Ad5.Cre and Ad5.TGFβ2 increases fibronectin and collagen-1 expression in MTM cells. MTM cells (n=3 replicates) were cultured to confluency and transduced overnight with Ad5.Null, Ad5.Cre, or Ad5.TGFβ2 at 100 MOI. After overnight incubation with the adenovirus, cells were cultured for 48 hours in serum free medium. Ad5.Null had no effect on (A) BAMBI, (B) collagen-1, and (C) fibronectin expression. Ad5.Cre and Ad5.TGFβ2 decreased (D, G) BAMBI expression and increased (E, H) fibronectin and (F, I) collagen-1 expression. (J, K) Densitometric analysis of conditioned medium showed that Ad5.Cre and Ad5.TGFβ2 increased fibronectin expression compared to Ad5.Null. Statistical significance was determined by one-way ANOVA and Tukey post-hoc analysis, * $p < 0.05$, ** $p < 0.01$ (* = compared to Ad5.Null).

Figure 6

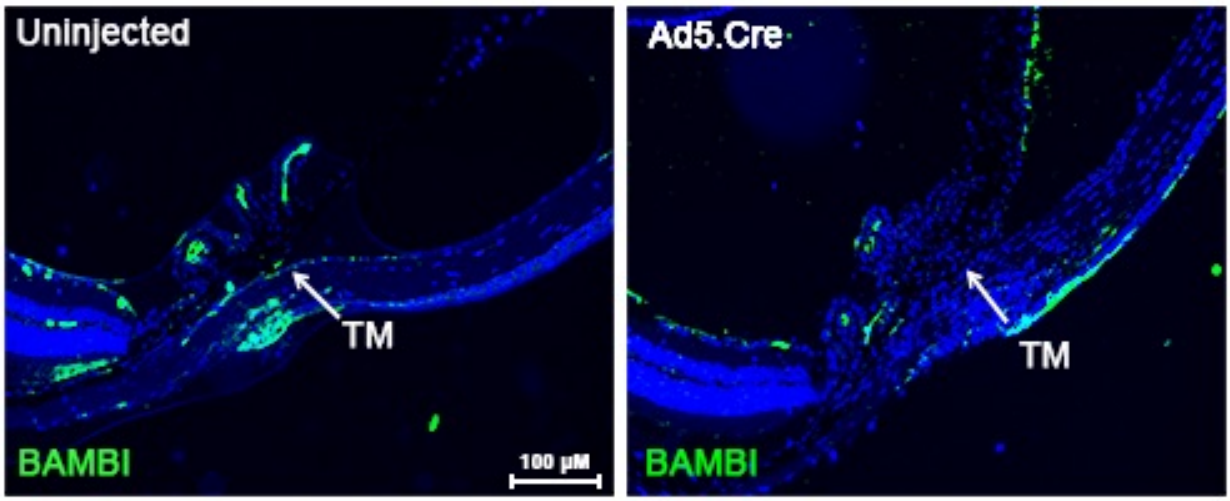

Figure 6. Ad5.Cre knockdown *Bambi* in the TM of B6;129S1-*Bambi*^{tm1Jian}/J mice. Mice were injected with Ad5.Cre ($2.5x10^7$ pfu) intravitreally in one eye of each animal and the contralateral uninjected eyes were used as negative controls (n=5). Mouse eyes were harvested 11 days post-injection and analyzed for the expression of BAMBI by immunohistochemistry. The uninjected eyes express BAMBI in the TM, whereas the eyes injected with Ad5.Cre did not show detectable BAMBI expression.

Figure 7

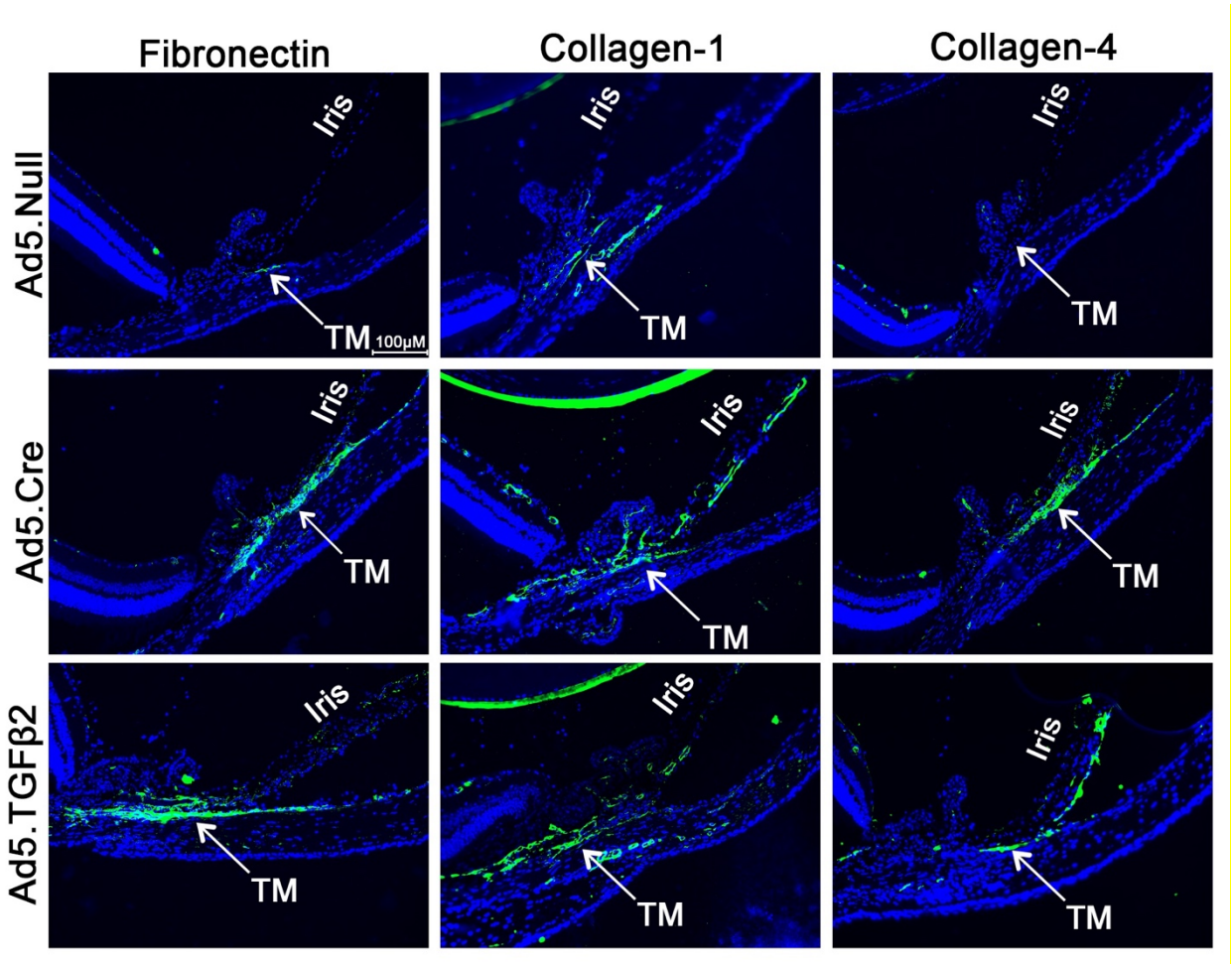
Fibronectin
Collagen-1
Collagen-4
Ad5.Null
Ad5.Cre
Ad5.TGFβ2
Iris
TM
100μM

Figure 7. Fibronectin, collagen-1, and collagen-4 expression in the TM of B6;129S1-*Bambi*^{tm1Jian}/J mice treated with Ad5.TGFβ2 and Ad5.Cre. Mice were injected with Ad5.Null ($2.5x10^7$ pfu), Ad5.TGFβ2 ($2.5x10^7$ pfu), or Ad5.Cre ($2.5x10^7$ pfu) intravitreally in one eye of each animal and the contralateral uninjected eyes were used as controls. Eyes were harvested 11 days post-injection and analyzed for fibronectin, collagen-1, and collagen-4 expression by immunohistochemistry. Both Ad5.Cre (n=15) and Ad5.TGFβ2 (n=9) increased fibronectin, collagen-1, and collagen-4 expression in the TM compared to Ad5.Null (n=7).

Figure 8

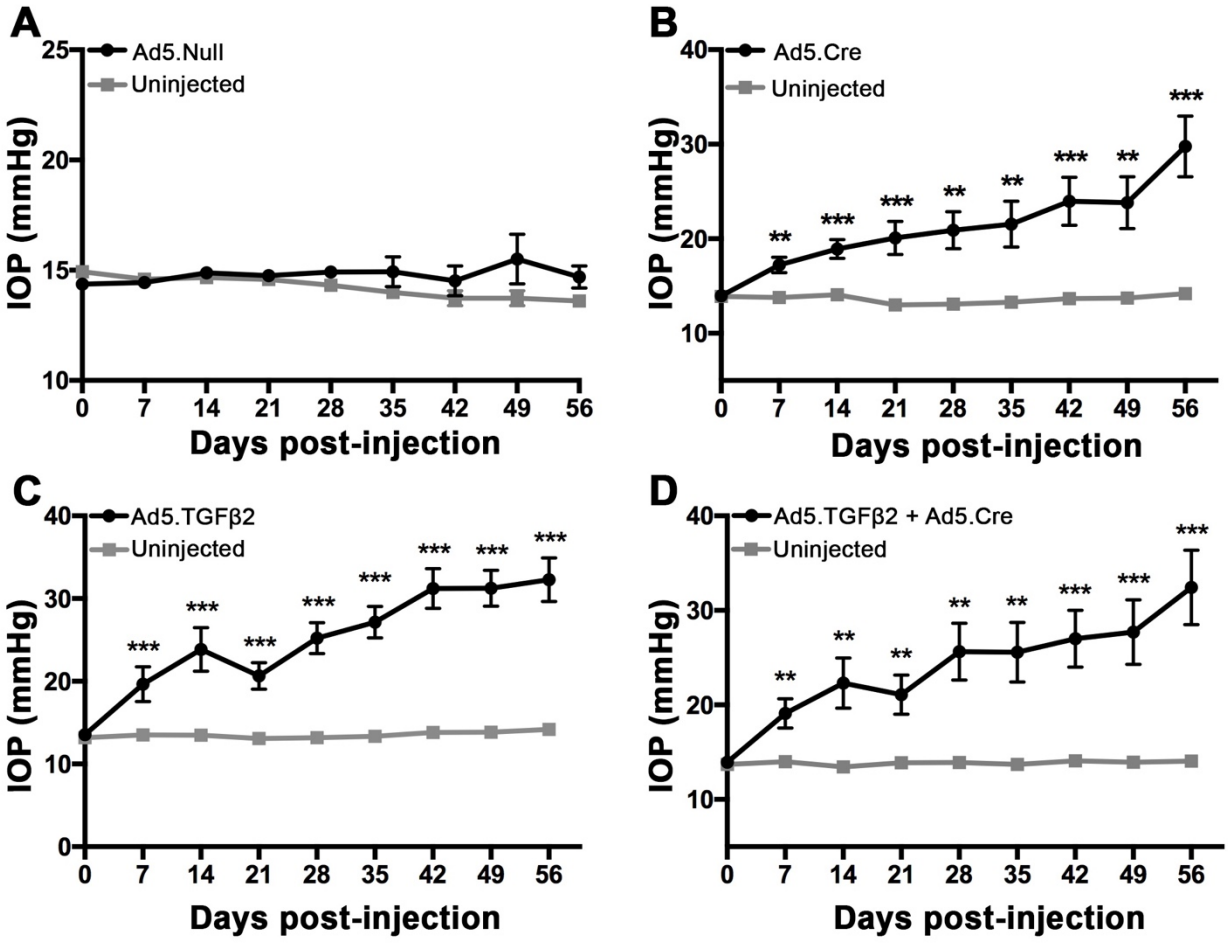
A
Ad5.Null
Uninjected
IOP (mmHg)
Days post-injection
B
Ad5.Cre
Uninjected
IOP (mmHg)
Days post-injection
C
Ad5.TGFβ2
Uninjected
IOP (mmHg)
Days post-injection
D
Ad5.TGFβ2 + Ad5.Cre
Uninjected
IOP (mmHg)
Days post-injection

Figure 8. Effects of Ad5. Null, Ad5.TGFβ2, and Ad5.Cre on IOP in B6/129S1-*Bambi*^{tm1Jian}/J mice. Mice were injected intravitreally with Ad5.Null, Ad5.Cre, Ad5.TGFβ2, or Ad5.TGFβ2 + Ad5.Cre (2.5×10^7 pfu). Day of injection was designated as day 0. The contralateral eye of each mouse was uninjected and served as a paired control. (A) Ad5.Null did not induce ocular hypertension at any time point when compared to the contralateral eye (n=7). (B, C, D) Injection with Ad5.Cre, Ad5.TGFβ2, or Ad5.TGFβ2 + Ad5.Cre each induced ocular hypertension starting at day 7 post-injection and maintained significant IOP elevation throughout the 56 day time course when compared to uninjected control eyes ($p<0.01$, days 7-56). (B) At day 56 post-injection IOP increased to 29.8 +/- 3.2 mmHg in Ad5.Cre injected eyes compared to 14.2 +/- 0.3 mmHg in contralateral uninjected eyes ($p<0.001$, n=9). (C) Ad5.TGFβ2 (32.3 +/- 2.6 mm Hg) had significant IOP elevation at 56 days post-injection compared to 14.2 +/- 0.3 mmHg in uninjected control eyes ($p<0.001$, n=10). (D) Ad5.TGFβ2 + Ad5.Cre (32.4 +/- 3.9 mmHg) had significant IOP elevation at 56 days post-injection compared to uninjected control eyes (14.1 +/- 0.3 mmHg) ($p<0.001$, n=10). Statistical significance was determined by Student's paired t-test at each time point comparing the transduced eye to the contralateral uninjected control eye, ** $p<$ 0.01, *** $p<0.001$ (* = compared to uninjected control).

Figure 9

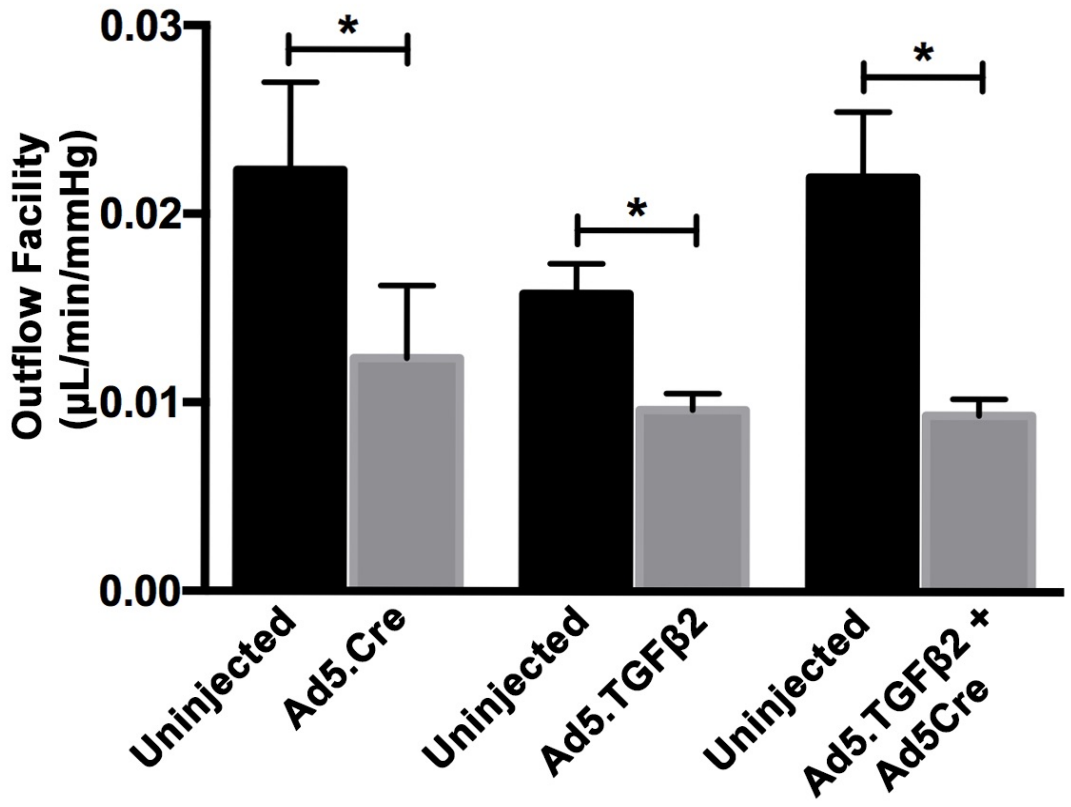
Outflow Facility
(µL/min/mmHg)
0.03
0.02
0.01
0.00
*
*
*
Uninjected
Ad5.Cre
Uninjected
Ad5.TGFβ2
Uninjected
Ad5.TGFβ2 +
Ad5Cre

Figure 9. Effects of Ad5.TGFβ2 and Ad5.Cre on outflow facility. At 56-days post-injection of Ad5.Cre, Ad5.TGFβ2, or Ad5.TGFβ2 + Ad5.Cre, 3 to 5 mice were randomly selected for outflow facility. Aqueous humor outflow facility was significantly lower in transduced eyes compared to control uninjected eyes: Ad5.Cre injected ($p=0.012$, $n=5$), Ad5.TGFβ2 injected ($p=0.011$, $n=3$), and Ad5.TGFβ2 + Ad5.Cre ($p=0.02$, $n=3$). Statistical significance was determined by Student's paired t-test comparing the transduced eye to the contralateral uninjected control eye.

References

1. Kingman S. Glaucoma is second leading cause of blindness globally. *Bulletin of the World Health Organization* 2004;82:887-888.

2. Quigley HA. Number of people with glaucoma worldwide. *Br J Ophthalmol* 1996;80:389-393.

3. Min SH, Lee TI, Chung YS, Kim HK. Transforming growth factor-beta levels in human aqueous humor of glaucomatous, diabetic and uveitic eyes. *Korean J Ophthalmol* 2006;20:162-165.

4. Cousins SW, McCabe MM, Danielpour D, Streilein JW. Identification of transforming growth factor-beta as an immunosuppressive factor in aqueous humor. *Invest Ophthalmol Vis Sci* 1991;32:2201-2211.

5. Jampel HD, Roche N, Stark WJ, Roberts AB. Transforming growth factor-beta in human aqueous humor. *Curr Eye Res* 1990;9:963-969.

6. Granstein RD, Staszewski R, Knisely TL, et al. Aqueous humor contains transforming growth factor-beta and a small (less than 3500 daltons) inhibitor of thymocyte proliferation. *J Immunol* 1990;144:3021-3027.

7. Inatani M, Tanihara H, Katsuta H, Honjo M, Kido N, Honda Y. Transforming growth factor-beta 2 levels in aqueous humor of glaucomatous eyes. *Graefes Arch Clin Exp Ophthalmol* 2001;239:109-113.

8. Ochiai Y, Ochiai H. Higher concentration of transforming growth factor-beta in aqueous humor of glaucomatous eyes and diabetic eyes. *Jpn J Ophthalmol* 2002;46:249-253.

9. Ozcan AA, Ozdemir N, Canataroglu A. The aqueous levels of TGF-beta2 in patients with glaucoma. *Int Ophthalmol* 2004;25:19-22.

10. Tripathi RC, Li J, Chan WF, Tripathi BJ. Aqueous humor in glaucomatous eyes contains an increased level of TGF-beta 2. *Exp Eye Res* 1994;59:723-727.

11. Sethi A, Jain A, Zode GS, Wordinger RJ, Clark AF. Role of TGFbeta/Smad signaling in gremlin induction of human trabecular meshwork extracellular matrix proteins. *IOVS* 2011;52:5251-5259.

12. Tovar-Vidales T, Clark AF, Wordinger RJ. Transforming growth factor-beta2 utilizes the canonical smad-signaling pathway to regulate tissue transglutaminase expression in human trabecular meshwork cells. *Experimental Eye Research* 2011;93:442-451.

13. Welge-Lussen U, May CA, Lütjen-Drecoll E. Induction of tissue transglutaminase in the trabecular meshwork by TGF-beta1 and TGF-beta2. *Invest Ophthalmol Vis Sci* 2000;41:2229-2238.

14. Fleenor DL, Shepard AR, Hellberg PE, Jacobson N, Pang IH, Clark AF. TGFbeta2-induced changes in human trabecular meshwork: implications for intraocular pressure. *Invest Ophthalmol Vis Sci* 2006;47:226-234.

15. Wordinger RJ, Fleenor DL, Hellberg PE, et al. Effects of TGF-beta2, BMP-4, and gremlin in the trabecular meshwork: implications for glaucoma. *IOVS* 2007;48:1191-1200.

16. Fuchshofer R, Yu AH, Welge-Lussen U, Tamm ER. Bone morphogenetic protein-7 is an antagonist of transforming growth factor-beta2 in human trabecular meshwork cells. *Invest Ophthalmol Vis Sci* 2007;48:715-726.

17. Welge-Lüssen U, May CA, Eichhorn M, Bloemendal H, Lütjen-Drecoll E. AlphaB-crystallin in the trabecular meshwork is inducible by transforming growth factor-beta. *Invest Ophthalmol Vis Sci* 1999;40:2235-2241.

18. Gottanka J, Chan D, Eichhorn M, Lütjen-Drecoll E, Ethier CR. Effects of TGF-beta2 in perfused human eyes. *Invest Ophthalmol Vis Sci* 2004;45:153-158.

19. Shepard AR, Millar JC, Pang I-H, Jacobson N, Wang W-H, Clark AF. Adenoviral gene transfer of active human transforming growth factor-beta2 elevates intraocular pressure and reduces outflow facility in rodent eyes. *Invest Ophthalmol Vis Sci* 2010;51:2067-2076.

20. McDowell CM, Hernandez H, Mao W, Clark AF. Gremlin induces ocular hypertension in mice through smad3-dependent signaling. *IOVS* 2015;56:5485-5488.

21. McDowell CM, Tebow HE, Wordinger RJ, Clark AF. Smad3 is necessary for transforming growth factor-beta2 induced ocular hypertension in mice. *Experimental Eye Research* 2013;116:419-423.

22. Tripathi RC, Chan WF, Li J, Tripathi BJ. Trabecular cells express the TGF-beta 2 gene and secrete the cytokine. *Experimental Eye Research* 1994;58:523-528.

23. Zode GS, Sethi A, Brun-Zinkernagel A-M, Chang IF, Clark AF, Wordinger RJ. Transforming growth factor-β2 increases extracellular matrix proteins in optic nerve head cells via activation of the Smad signaling pathway. *Mol Vis* 2011;17:1745-1758.

24. Wordinger RJ, Fleenor DL, Hellberg PE, et al. Effects of TGF-beta2, BMP-4, and gremlin in the trabecular meshwork: implications for glaucoma. *Invest Ophthalmol Vis Sci* 2007;48:1191-1200.

25. Buie LK, Karim MZ, Smith MH, Borras T. Development of a model of elevated intraocular pressure in rats by gene transfer of bone morphogenetic protein 2. *Invest Ophthalmol Vis Sci* 2013;54:5441-5455.

26. Nohe A, Keating E, Knaus P, Petersen NO. Signal transduction of bone morphogenetic protein receptors. *Cell Signal* 2004;16:291-299.

27. Wordinger RJ, Sharma T, Clark AF. The role of TGF-β2 and bone morphogenetic proteins in the trabecular meshwork and glaucoma. *Journal of Ocular Pharmacology and Therapeutics* 2014;30:154-162.

28. Kretzschmar M, Liu F, Hata A, Doody J, Massague J. The TGF-beta family mediator Smad1 is phosphorylated directly and activated functionally by the BMP receptor kinase. *Genes Dev* 1997;11:984-995.

29. Sapkota G, Alarcon C, Spagnoli FM, Brivanlou AH, Massague J. Balancing BMP signaling through integrated inputs into the Smad1 linker. *Mol Cell* 2007;25:441-454.

30. Alarcon C, Zaromytidou AI, Xi Q, et al. Nuclear CDKs drive Smad transcriptional activation and turnover in BMP and TGF-beta pathways. *Cell* 2009;139:757-769.

31. Wang RN, Green J, Wang Z, et al. Bone Morphogenetic Protein (BMP) signaling in development and human diseases. *Genes Dis* 2014;1:87-105.

32. Wordinger RJ, Agarwal R, Talati M, Fuller J, Lambert W, Clark AF. Expression of bone morphogenetic proteins (BMP), BMP receptors, and BMP associated proteins in human trabecular meshwork and optic nerve head cells and tissues. *Mol Vis* 2002;8:241-250.

33. Agarwal R, Agarwal P. Future target molecules in antiglaucoma therapy: TGF-Beta may have a role to play. *Ophthalmic Res* 2010;43:1-10.

34. Onichtchouk D, Chen YG, Dosch R, et al. Silencing of TGF-beta signalling by the pseudoreceptor BAMBI. *Nature* 1999;401:480-485.

35. Grotewold L, Plum M, Dildrop R, Peters T, Ruther U. Bambi is coexpressed with Bmp-4 during mouse embryogenesis. *Mech Dev* 2001;100:327-330.

36. Loveland KL, Bakker M, Meehan T, et al. Expression of Bambi is widespread in juvenile and adult rat tissues and is regulated in male germ cells. *Endocrinology* 2003;144:4180-4186.

37. Knight C, Papagerakis P, Simmons D, Berdal A, MacDougall M. Genomic organization and localization of mouse Nma/BAMBI: possible implications related to ameloblastoma formation. *Connect Tissue Res* 2002;43:359-364.

38. Knight C, Simmons D, Gu TT, et al. Cloning, characterization, and tissue expression pattern of mouse Nma/BAMBI during odontogenesis. *J Dent Res* 2001;80:1895-1902.

39. Borras T, Comes N. Evidence for a calcification process in the trabecular meshwork. *Exp Eye Res* 2009;88:738-746.

40. Lin SJ, Lerch TF, Cook RW, Jardetzky TS, Woodruff TK. The structural basis of TGF-beta, bone morphogenetic protein, and activin ligand binding. *Reproduction* 2006;132:179-190.

41. Yan X, Lin Z, Chen F, et al. Human BAMBI cooperates with smad7 to inhibit TGF-β Signaling. *J Biol Chem* 2009;284:jbc.M109.049304-030104.

42. Pils D, Wittinger M, Petz M, et al. BAMBI is overexpressed in ovarian cancer and co-translocates with smads into the nucleus upon TGF-beta treatment. *Gynecol Oncol* 2010;117:189-197.

43. Sekiya T, Oda T, Matsuura K, Akiyama T. Transcriptional regulation of the TGF-β pseudoreceptor BAMBI by TGF-β signaling. *Biochemical and Biophysical Research Communications* 2004;320:680-684.

44. Lin L, Wang Y, Liu W, Huang Y. BAMBI inhibits skin fibrosis in keloid through suppressing TGF-beta1-induced hypernomic fibroblast cell proliferation and excessive accumulation of collagen I. *Int J Clin Exp Med* 2015;8:13227-13234.

45. Fan Y, Li X, Xiao W, et al. BAMBI elimination enhances alternative TGF-beta signaling and glomerular dysfunction in diabetic mice. *Diabetes* 2015;64:2220-2233.

46. Tovar-Vidales T, Fitzgerald AM, Clark AF. Human trabecular meshwork cells express BMP antagonist mRNAs and proteins. *Exp Eye Res* 2016;147:156-160.

47. Seki E, De Minicis S, Osterreicher CH, et al. TLR4 enhances TGF-beta signaling and hepatic fibrosis. *Nat Med* 2007;13:1324-1332.

48. Bhattacharyya S, Kelley K, Melichian DS, et al. Toll-like receptor 4 signaling augments transforming growth factor-beta responses: a novel mechanism for maintaining and amplifying fibrosis in scleroderma. *Am J Pathol* 2013;182:192-205.

49. Yang L, Seki E. Toll-like receptors in liver fibrosis: cellular crosstalk and mechanisms. *Front Physiol* 2012;3:138.

50. Guo J, Friedman SL. Toll-like receptor 4 signaling in liver injury and hepatic fibrogenesis. *Fibrogenesis Tissue Repair* 2010;3:21.

51. Liu C, Chen X, Yang L, Kisseleva T, Brenner DA, Seki E. Transcriptional repression of the transforming growth factor beta (TGF-beta) pseudoreceptor BMP and activin membrane-bound inhibitor (BAMBI) by Nuclear Factor kappaB (NF-kappaB) p50 enhances TGF-beta signaling in hepatic stellate cells. *J Biol Chem* 2014;289:7082-7091.

52. Seki E, De Minicis S, Osterreicher CH, et al. TLR4 enhances TGF-beta signaling and hepatic fibrosis. *Nat Med* 2007;13:1324-1332.

53. Sasaki T, Sasahira T, Shimura H, Ikeda S, Kuniyasu H. Effect of Nma on growth inhibition by TGF-beta in human gastric carcinoma cell lines. *Oncol Rep* 2004;11:1219-1223.

54. Sekiya T, Adachi S, Kohu K, et al. Identification of BMP and activin membrane-bound inhibitor (BAMBI), an inhibitor of transforming growth factor-beta signaling, as a target of the beta-catenin pathway in colorectal tumor cells. *J Biol Chem* 2004;279:6840-6846.

55. Hernandez H, Medina-Ortiz WE, Luan T, Clark AF, McDowell CM. Crosstalk between transforming growth factor beta-2 and toll-like receptor 4 in the trabecular meshwork. *Invest Ophthalmol Vis Sci* 2017;58:1811-1823.

56. Mao W, Liu Y, Wordinger RJ, Clark AF. A magnetic bead-based method for mouse trabecular meshwork cell isolation. *Invest Ophthalmol Vis Sci* 2013;54:3600-3606.

57. Peotter JL, Phillips J, Tong T, Dimeo K, Gonzalez JM, Jr., Peters DM. Involvement of Tiam1, RhoG and ELMO2/ILK in Rac1-mediated phagocytosis in human trabecular meshwork cells. *Exp Cell Res* 2016;347:301-311.

58. Gagen D, Filla MS, Clark R, Liton P, Peters DM. Activated alphavbeta3 integrin regulates alphavbeta5 integrin-mediated phagocytosis in trabecular meshwork cells. *Invest Ophthalmol Vis Sci* 2013;54:5000-5011.

59. Zhang X, Ognibene CM, Clark AF, Yorio T. Dexamethasone inhibition of trabecular meshwork cell phagocytosis and its modulation by glucocorticoid receptor beta. *Exp Eye Res* 2007;84:275-284.

60. Cao Y, Wei H, Da B, Huang Y. Effect of transforming growth factor-beta 2 on phagocytosis in cultured bovine trabecular meshwork cells. *J Tongji Med Univ* 2001;21:318-320.

61. Matsumoto Y, Johnson DH. Trabecular meshwork phagocytosis in glaucomatous eyes. *Ophthalmologica* 1997;211:147-152.

62. Matsumoto Y, Johnson DH. Dexamethasone decreases phagocytosis by human trabecular meshwork cells in situ. *Invest Ophthalmol Vis Sci* 1997;38:1902-1907.

63. Yang X, Li M. [Establishment of in vitro culture of bovine trabecular meshwork cells and their phagocytosis]. *Zhonghua Yan Ke Za Zhi* 1996;32:136-139.

64. Zhou L, Fukuchi T, Kawa JE, Higginbotham EJ, Yue BY. Loss of cell-matrix cohesiveness after phagocytosis by trabecular meshwork cells. *Invest Ophthalmol Vis Sci* 1995;36:787-795.

65. Park CH, Latina MA. Effects of gamma-interferon on human trabecular meshwork cell phagocytosis. *Invest Ophthalmol Vis Sci* 1993;34:2228-2236.

66. Buller C, Johnson DH, Tschumper RC. Human trabecular meshwork phagocytosis. Observations in an organ culture system. *Invest Ophthalmol Vis Sci* 1990;31:2156-2163.

67. Shirato S, Murphy CG, Bloom E, et al. Kinetics of phagocytosis in trabecular meshwork cells. Flow cytometry and morphometry. *Invest Ophthalmol Vis Sci* 1989;30:2499-2511.

68. Sherwood ME, Richardson TM. Phagocytosis by trabecular meshwork cells: sequence of events in cats and monkeys. *Exp Eye Res* 1988;46:881-895.

69. Chisholm IA, Grierson I. Particulate phagocytosis by trabecular meshwork endothelium. *Can J Ophthalmol* 1977;12:293-299.

70. Grierson I, Lee WR. Erythrocyte phagocytosis in the human trabecular meshwork. *Br J Ophthalmol* 1973;57:400-415.

71. McDowell CM, Luan T, Zhang Z, et al. Mutant human myocilin induces strain specific differences in ocular hypertension and optic nerve damage in mice. *Exp Eye Res* 2012;100:65-72.

72. Millar JC, Clark AF, Pang IH. Assessment of aqueous humor dynamics in the mouse by a novel method of constant-flow infusion. *Invest Ophthalmol Vis Sci* 2011;52:685-694.

73. Millar JC, Phan TN, Pang IH, Clark AF. Strain and age effects on aqueous humor dynamics in the mouse. *Invest Ophthalmol Vis Sci* 2015;56:5764-5776.

74. Lin S, Lee OT, Minasi P, Wong J. Isolation, culture, and characterization of human fetal trabecular meshwork cells. *Curr Eye Res* 2007;32:43-50.

75. Knepper PA, Samples JR, Yue BYJT. Biomarkers of primary open-angle glaucoma. *Expert Rev Ophthalmol* 2010;5:731-742.

76. Pattabiraman PP, Rao PV. Hic-5 regulates actin cytoskeletal reorganization and expression of fibrogenic markers and myocilin in trabecular meshwork cells. *Invest Ophthalmol Vis Sci* 2015;56:5656-5669.

77. Stamer WD, Clark AF. The many faces of the trabecular meshwork cell. *Exp Eye Res* 2016.

78. Mao W, Liu Y, Mody A, Montecchi-Palmer M, Wordinger RJ, Clark AF. Characterization of a spontaneously immortalized bovine trabecular meshwork cell line. *Exp Eye Res* 2012;105:53-59.

79. Ueyama K, Mori K, Shoji T, et al. Ocular localization and transduction by adenoviral vectors are serotype-dependent and can be modified by inclusion of RGD fiber modifications. *PLoS One* 2014;9:e108071.

80. Mai Y, Zhang Z, Yang H, et al. BMP and activin membrane-bound inhibitor (BAMBI) inhibits the adipogenesis of porcine preadipocytes through Wnt/beta-catenin signaling pathway. *Biochem Cell Biol* 2014;92:172-182.

81. Villar AV, Garcia R, Llano M, et al. BAMBI (BMP and activin membrane-bound inhibitor) protects the murine heart from pressure-overload biomechanical stress by restraining TGF-beta signaling. *Biochim Biophys Acta* 2013;1832:323-335.

82. Luo X, Hutley LJ, Webster JA, et al. Identification of BMP and activin membrane-bound inhibitor (BAMBI) as a potent negative regulator of adipogenesis and modulator of autocrine/paracrine adipogenic factors. *Diabetes* 2012;61:124-136.

83. Wanninger J, Neumeier M, Bauer S, et al. Adiponectin induces the transforming growth factor decoy receptor BAMBI in human hepatocytes. *FEBS Lett* 2011;585:1338-1344.

84. Tramullas M, Lantero A, Diaz A, et al. BAMBI (bone morphogenetic protein and activin membrane-bound inhibitor) reveals the involvement of the transforming growth factor-beta family in pain modulation. *J Neurosci* 2010;30:1502-1511.

85. Tsuchida K, Nakatani M, Hitachi K, et al. Activin signaling as an emerging target for therapeutic interventions. *Cell Commun Signal* 2009;7:15.

86. He Y, Ou Z, Chen X, et al. LPS/TLR4 signaling enhances TGF-beta response through downregulating BAMBI during prostatic hyperplasia. *Sci Rep* 2016;6:27051.

87. Zhang Y, Yu Z, Xiao Q, et al. Expression of BAMBI and its combination with smad7 correlates with tumor invasion and poor prognosis in gastric cancer. *Tumour Biol* 2014;35:7047-7056.

88. Zhou L, Park J, Jang KY, et al. The overexpression of BAMBI and its involvement in the growth and invasion of human osteosarcoma cells. *Oncol Rep* 2013;30:1315-1322.

CHAPTER IV

Discussion and Future Direction

Contribution of TLR4 to glaucomatous TM damage has not been evaluated. Analysis of TLR4 SNPs in POAG and NTG patients indicate that TLR4 may be a risk factor contributing to glaucomatous damage. It is now widely accepted that in the glaucomatous TM, TGFβ2 is contributing to changes in the TM which increases outflow resistance. Recently, Paul Knepper and colleagues first identified the expression of TLR4 in TM cells[1]. TLR4 was also shown to contribute to the activity of ATP-binding cassette transporter (ABC). However, the expression of ECM in relation to TLR4 has not been evaluated. Recent evidence has linked DAMP activated TLR4 signaling to fibrosis and the regulation and production of ECM proteins. DAMPs (cFN-EDA, low molecular weight hyaluronan, tenascin C, amongst others) have been shown to activate TLR4 and augment TGFβ signaling and downstream fibrotic responses in other diseases such as hepatic fibrosis, renal fibrosis, lesional skin and lung in scleroderma patients, as well as in *Tlr4* mutant mice[2-6]. In chapter II, we revealed a TGFβ2-TLR4 crosstalk in the TM. We confirmed the expression of *TLR4* in TM cells and protein expression of TLR4 in the mouse and human TM tissues. TGFβ2 induced the expression of ECM proteins in primary human TM cells. Pretreated transformed and primary human TM cells with TLR4 inhibitor, TAK-242, did not induce the expression of ECM to the same degree as TGFβ2 alone. These studies suggest that TGFβ2 induces the expression of endogenous DAMPs capable of activating TLR4 and amplifying the effects of TGFβ2. As mentioned in chapter II, TAK-242 selectively inhibits the interaction between TLR4 and its adaptor molecules, TIRAP and TRAM, via the TLR4 intracellular Cys747 residue, thereby inhibiting TLR4 downstream signaling events[7]. Beutler and

colleagues first discovered the specificity of LPS to TLR4 and showed that mutations in TLR4 selectively impede lipopolysaccharide (LPS) signal transduction in the C3H/HeJ and C57BL/10ScCr mice[8]. In our studies, activation of TLR4 via LPS and endogenous DAMP, cFN-EDA, was capable inducing the expression of fibronectin, collagen-1, and laminin, suggesting that TLR4 contributes to ECM production in TM cells. These findings were consistent with a previously report by Bhattacharyya and colleagues where fibronectin-EDA stimulated the expression of ECM[9]. To test the hypothesis that TLR4 activation enhances TGFβ2 signaling, TM cells were treated with LPS + TGFβ2 and cFN-EDA + TGFβ2. This treatment amplified the expression of ECM as compared to TGFβ2 alone. Pretreatment with TAK-242 inhibited the effect of LPS + TGFβ2 or cFN-EDA + TGFβ2, suggesting a TGFβ2-TLR4 crosstalk in the TM. Interestingly, *Tlr4* mutant mice (C3H/HeJ) did not induce ocular hypertension using our established ocular hypertensive model. This finding was consistent with previous studies performed by Souza and colleagues were TLR4 mutant (C3H/HeJ) mice were protected against fibrosis and disease progression[10]. The wild-type C3H/OuJ induced ocular hypertension and ECM deposition in our studies, supporting our hypothesis that TLR4 contributes to TGFβ2 induction of ECM and ocular hypertension. In summary, we demonstrated that the ECM composition in the TM is regulated by the TGFβ2 and the TLR4 signaling pathways.

Recent findings suggest that TLR4 activation downregulates the TGFβ pseudoreceptor BAMBI, which enhances TGFβ signaling leading to increased ECM production[2, 3]. In chapter III, we aimed to determine the mechanistic role of BAMBI in TGFβ2-TLR4 signaling in the TM. We hypothesized that conditional knockdown of *Bambi* in the TM would lead to increased TGFβ2 signaling, leading to increased ECM production in the TM and increased IOP. Using the magnetic bead isolation protocol developed by Mao and colleagues[11], we isolated mouse TM

(MTM) cells from B6;129S1-*Bambi*^{tm1Jian}/J (mice harbor *loxP* sites flanking exon 1 of the *Bambi* locus) conditional knockout mice. MTM cells were characterized for the basal expression and induction of TM markers with TGFβ2 and dexamethasone.

We showed for the first time that conditional knockdown of *Bambi* with Ad5.Cre induces the expression of fibronectin, collagen-1, and collagen-4 in MTM cells in culture and the TM of mice *in vivo*. Ad5.Cre also induced ocular hypertension by reducing aqueous humor outflow facility. These studies provided evidence that in the TM, BAMBI is a critical molecule involved in the TGFβ2-TLR4 crosstalk.

Future studies: *In vitro*

The mechanism behind the TGFβ2-TLR4 crosstalk is beginning to be elucidated. We have shown that TLR4 activation is mediated by endogenous DAMP, cFN-EDA, in the TM. Activation of TLR4 by other endogenous DAMPs in the glaucomatous TM is very likely. Known DAMP activators of TLR4 include high mobility group box 1(HMGB1), surfactant proteins A and D, β-defensin 2, HSP60, HSP70, HSP72, HSP22, Gp96, S100A8, S100A9, neutrophil elastase, antiphospholipid antibodies, lactoferrin, serum amyloid A, oxidized LDL, saturated fatty acids, resistin, pancreatic adenocarcinoma upregulated factor (PAUF), monosodium urate crystals, biglycan, fibronectin-EDA, fibrinogen, tenascin-C, heparin sulphate fragments, and hyaluronic acid fragments[12]. All of these have the capacity to activate TLR4, however, the most likely activators are HMGB1, fibronectin-EDA, and hyaluronic acid fragments. Indeed, Knepper and colleagues have formulated a hypothesis in which low molecular hyaluronic acid activates TLR4 via CD44 and MD2[13]. As depicted in Figure 1, low-molecular hyaluronic acid leads to downstream signaling pathways to activate NF-κB, p38, and

JNK. These signaling molecules have to potential to modulate the expression of MMPs, growth factors, and cytokines.

To test the hypothesis that NF-κB plays a role in the TGFβ2-TLR4 crosstalk, transactivation studies of were carried out on NF-κB (Figure 2). Interesting, cFN-EDA, LPS, and TGFβ2 increased the activity of NF-κB. Pretreatment with TLR4 inhibitor, TAK-242, blocked the effect of each individual treatment. These data suggested that; cFN-EDA, LPS, and TGFβ2 activate NF-κB expression, NF-κB transactivation is mediated by the TLR4 pathway, and TGFβ2 signaling leads to the expression of TLR4 ligands which transactivate NF-κB. In summary, upregulation of NF-κB maybe the critical step involved in generating the TGFβ2-TLR4 crosstalk. Further studies are needed to confirm the activity assay by western blotting techniques.

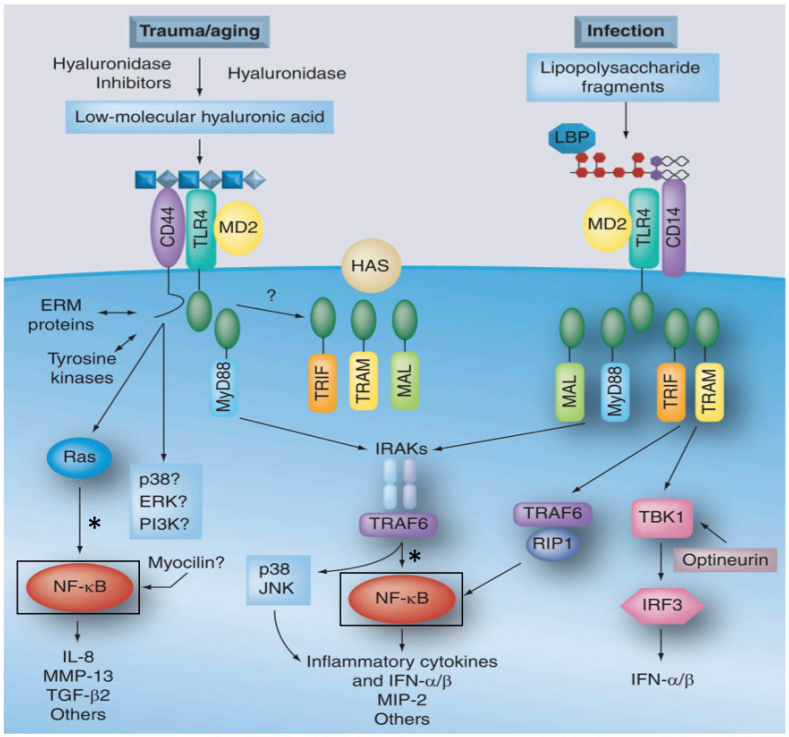

Figure 1. Putative activation of Toll-like receptor 4 occurs by trauma/aging to the extracellular matrix trabecular meshwork or by mechanical deformation, that is, cupping of the optic nerve,

leading to breakdown of hyaluronic acid into hyaluronic acid oligosaccharides. Low-molecular-weight hyaluronic acid oligosaccharides are released from the ECM as a result of trauma and are regulated by the balance of hyaluronidase inhibitors and hyaluronidase. These oligosaccharides bind to TLR4 along with MD2 and the CD44 receptor. This receptor complex utilizes ERM proteins and MyD88. Ras and NF-κB are upregulated, which leads to downstream production of effectors including MMP-13, TGFβ2, SOCS3 and inflammatory cytokines. By contrast, Gram-negative bacteria release membrane fragments containing LPS. The fragments bind to LBP, which bind to TLR4 requiring CD14 and MD2. Ligand binding to TLR4 and activates certain protein kinases (e.g., IRAK, TRAFs and TBK1) that amplify the signal, leading to the inflammatory response and its modulation of the ECM, cell signaling molecules, stress response and immunity related changes. **Adapted from Knepper et al., 2010.**

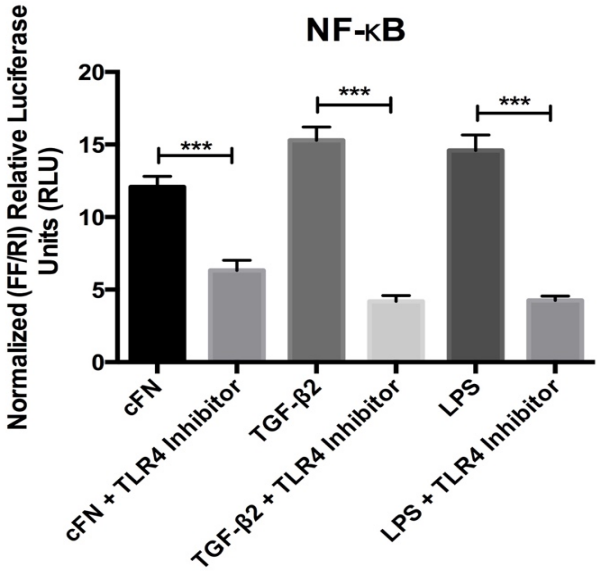

Figure 2. Transactivation of NF-κB in TM cells. Immortalized glaucomatous TM cells (GTM3) cells were transfected with 100ng of NF-κB dual-luciferase reporter or negative control (Qiagen), using Lipofectamine 3000 transfection reagent (Invitrogen). Cells were pre-treated with selective TLR4 inhibitor (TAK-242, 15μM) for 60 minutes, followed by TGFβ2 (5ng/ml),

TLR4 ligand (Fibronectin-EDA isoform 10μg/ml) or LPS(100ng/ml) for 24 hours. Luciferase activity was determined using the Dual-Glo Luciferase Assay System (Promega) and the Infinite M200 (Tecan). Transfection efficiency was normalized to Renilla luciferase activity. Data are represented as normalized relative light units,*** = P<.001.

We proposed that activation of NF-κB is a critical step in downregulating BAMBI, leading to the TGFβ2-TLR4 crosstalk in the TM. To test this hypothesis, we performed phosphorylation studies using cFN-EDA, LPS, and TGFβ2 as our ligands (Figure 3). As expected, TGFβ2 induced the phosphorylation of SMAD2 in a time dependent manner (Figure 3A). Interestingly, TGFβ2 also induced the phosphorylation of NF-κB in a time dependent manner. This data suggests that TGFβ2 signaling can lead to the phosphorylation of NF-κB independently of TLR4. To test the effect of TLR4 ligands on phosphorylation of SMAD3 and NF-κB, TM cells were treated with cFN-EDA and LPS. Interestingly, cFN-EDA induced the phosphorylation of NF-κB and SMAD3 in a concentration dependent manner. Inhibition of TLR4 signaling with TAK-242 inhibited the phosphorylation of SMAD3 and NF-κB. LPS treatment at 4 hours induce the phosphorylation of NF-κB, however, phosphorylation occurred very rapidly. These data suggest that TLR4 signaling utilizes the SMAD signaling pathway.

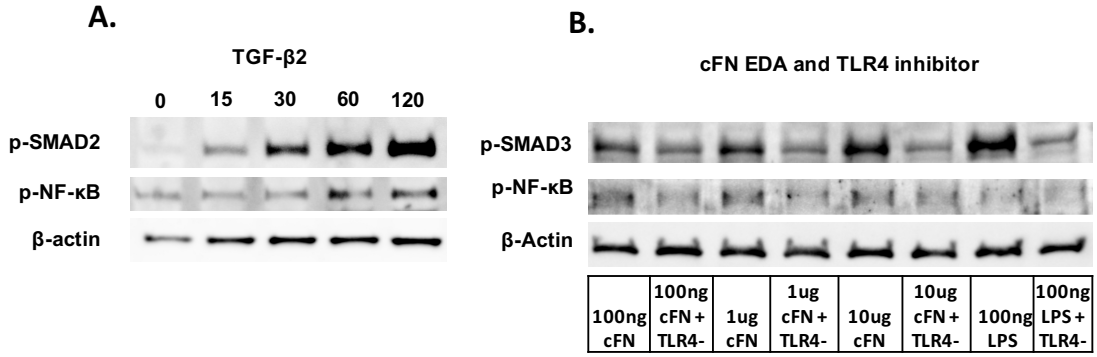

Figure 3. Time dependent phosphorylation of SMAD2 and NF-κB. TLR4 signaling inhibitor blocked phosphorylation of SMAD3 and NF-κB. A) Time dependent phosphorylation

of SMAD3 and NF-κB after treatment with recombinant TGFβ2 (5ng/mL). B) Dose response of primary human TM following treatment with cFN, TLR4, and LPS. A representative western blot shown for pSMAD2 and pNF-κB. Cells were pre-treated with TLR-4 inhibitor or PBS for 2 hours followed by treatment with cFN at 100ng/ml, 1μg/ml, 10μg/ml /ml, or 100ng of LPS for 4 hours.

The signaling pathways of the TGFβ2-TLR4 crosstalk can be very complex. However, our preliminary data suggests that SMADs and NF-κB play a major role. NF-κB can be activated by SMAD-dependent and SMAD-independent signaling. SMAD3 can directly interact with NF-κB or IKKα [14-16]. Interestingly, Lopez-Rovira and colleagues demonstrated that the kappaB sites alone are sufficient to mediate immediate transcriptional activation by TGFβ, requiring an intact NF-κB pathway[14]. In response to TGFβ, IKKα can associate with SMAD3 and undergo nuclear translocation[16]. Nuclear translocation of the IKKα/ SMAD3 would lead to transcriptional regulation of TGFβ signaling inhibitors.

TGFβ can induce acetylation of p65 and enhance the transcription activity of NF-κB, a mechanism dependent on SMAD3 and SMAD4[17]. In a SMAD independent manner, TGFβ can induce NF-κB activation by TAK-1[18-22]. Once TRAF6 or TRAF4 activate TAK-1 by polyubiquitination at Lys158[20, 22-25], TAK-1 phosphorylates and activates IKKα, leading to NF-κB signaling[23, 25]. The SMAD independent pathway is probably the signaling pathway responsible for TGFβ2 phosphorylation of NF-κB. Interestingly, RhoA-Rho-associated kinase (ROCK) can be activated by TGFβ induced TAK1 polyubiquitylation[26]. TAK-1 would then phosphorylate and activate IKKβ, leading to NF-κB activation. This evidence suggests that the TGFβ and the TLR4 signaling molecules can interact and modulate downstream signaling

pathways. Future studies will elucidate the effect of cFN-EDA on downstream signaling molecules of the TGFβ2-TLR4 crosstalk (Table 1).

Protein	TGF-β2	TLR4 Inhibitor	TGF-β2 + TLR4 Inhibitor	cFN	cFN + TGF-β2	cFN + TLR4 Inhibitor	cFN + TGF-β2 + TLR4 Inhibitor
p-NF-κB	↑	-	↑	↑	↑↑	-	↑
NF-κB	↑	-	↑	↑	↑↑	-	↑
p-SMAD2	↑	-	↑	↑	↑↑	-	↑
p-SMAD3	↑	-	↑	↑	↑↑	-	↑
SMAD2	↑	-	↑	↑	↑↑	-	↑
SMAD3	↑	-	↑	↑	↑↑	-	↑
p-TAK1	↑	-	↑	↑	↑↑	-	↑
p-TAB2	↑	-	↑	↑	↑↑	-	↑
TAK1	↑	-	↑	↑	↑↑	-	↑
TAB2	↑	-	↑	↑	↑↑	-	↑
BAMBI	↓	-	↓	↓	↓↓	-	↓
Collagen-1	↑	-	↑	↑	↑↑	-	↑
Fibronectin	↑	-	↑	↑	↑↑	-	↑

Legend

-	Decrease
↑	Moderate Increase
↑	Increase
↑↑	Greatly Increase

Table 1. Expected protein and gene expression changes in the TGFβ2 - TLR4 crosstalk.

Future directions: *In vivo*

To evaluate the role of DAMP activation on TLR4 and development of ocular hypertension, Ad5.TGFβ2 injections will be performed on FN-EDA$^{-/-}$, FN-EDA$^{+/+}$, FN-EDA$^{+/+}$/TLR4$^{-/-}$, and FN-EDA$^{-/-}$/ TLR4$^{-/-}$ mice. We hypothesize that Ad5.TGFβ2 will induce the expression of FN-EDA isoform and other DAMP molecules. These DAMPs will activate TLR4 and augment TGFβ2 signaling. The FN-EDA$^{-/-}$/ TLR4$^{-/-}$ mice will not induce IOP and ECM deposition. Using our ocular hypertension model of intravitreal injections of Ad5.TGFβ2, the TLR4 mutant (C3H/HeJ) mice did not induce ocular hypertension and fibronectin expression. Therefore, the TLR4$^{-/-}$ should not induce ocular hypertension and ECM deposition. FN-EDA$^{-/-}$ single knockouts are not expected to develop ocular hypertension to the same degree as wild-

type. If so, this would indicate that FN-EDA is necessary for the development of ocular hypertension. To evaluate downstream signaling molecules of TLR4 activation, Myd88 flox mice and NF-κB mutant mice will be used to evaluate the development of ocular hypertension and ECM deposition at the TM. We hypothesize that the development of ocular hypertension is through the Myd88-dependent TLR4 pathway. We do not expect conditional knockout of *Myd88* to develop ocular hypertension and ECM deposition, however, Ad5.TGFβ2 injected mice should develop ocular hypertension more rapidly and robustly than Ad5.Cre + Ad5.TGFβ2. If transduced eyes injected with Ad5.Cre + Ad5.TGFβ2 do not develop ocular hypertension to the same degree as Ad5.TGFβ2, this would suggest that TLR4 signaling is through the Myd88-dependent pathway. As previously described in Figure 2 and Figure 3, cFN-EDA and TGFβ2 both activate and phosphorylate NF-κB. This indicates that NF-κB might be a convergent signaling pathway required for ECM deposition. To test the effect of mutant NF-κB on the development of ocular hypertension, we will use our model of ocular hypertension. We expect NF-κB mutant mice to not develop ocular hypertension, whereas NF-κB wildtype mice should develop ocular hypertension and ECM deposition at the TM. If NF-κB mutant mice do not develop ocular hypertension using our stablished ocular hypertensive model, this would indicate that NF-κB is important for the TGFβ2-TLR4 crosstalk. Table 2 summarizes the expected outcomes of the current and future experiments.

Mouse Strain	No injection	Ad5.null	Ad5.TGFβ2	Ad5.Cre	Ad5.TGFβ2 + Ad5.Cre
C3H/HeJ (TLR4 mutant)	–	–	–	N/A	N/A
C3H/HeOuJ (TLR4 wild-type)	–	–	↑	N/A	N/A
FN-EDA$^{-/-}$	–	–	–	N/A	N/A
FN-EDA$^{+/+}$	–	–	↑	N/A	N/A
Fn-EDA$^{+/+}$/TLR4$^{-/-}$	–	–	–	N/A	N/A
Fn-EDA$^{-/-}$/ TLR4$^{-/-}$	–	–	–	N/A	N/A
B6;129S1-*Bambi*^{tm1Jian}/J (BAMBI flox)	–	–	↑	– or ↑	↑↑
B6.129P2(SJL)-*Myd88*^{tm1Defr}/J (Myd88 flox)	–	–	↑	–	–
B6.Cg-*Nfkb1*^{tm1Bal}/J (NFkb mutant)	–	–	–	N/A	N/A

Table 2. Summary of expected *in vivo* experiments

Future directions: *ex vivo*

We have previously demonstrated the capacity of TAK-242 to block the effects of TGFβ2. Our *in vivo* data suggests that TLR4 mutant mice do not induce ocular hypertension in response to Ad5.TGFβ2. To test the hypothesis that TLR4 plays a major role in inducing ocular hypertension, we will utilize the organ culture system. Similar to the studies performed in chapter II, anterior segments will be perfused with TGFβ2. IOP will be compared to eyes treated with TAK-242 and TGFβ2. To evaluate the effect of Myd88, inhibitors to Myd88 such as ST2825 can be used. ST2825 interferes with recruitment of IRAK1 and IRAK4 by MyD88, causing inhibition of IL-1-mediated activation of NF-κB transcriptional activity[27]. To evaluate the effects of NF-κB on TGFβ2 induction of IOP, inhibitors to NF-κB such as digitoxin and ouabain can be used[28]. These drugs are very potent and do not induce cell death.

Conclusion

We identified the TGFβ2 –TLR4 signaling crosstalk as an important pathway involved in the development of ocular hypertension and glaucomatous TM damage. Using *in vitro*, *in vivo*, and *ex vivo* approaches, we expect to elucidate the molecular pathways of the glaucomatous TM. Future studies will evaluate associated DAMPs to glaucomatous TM damage. Our studies provide potential new targets to lower IOP and ECM deposition in POAG patients.

References

1. Grybauskas A, Koga T, Kuprys PV, et al. ABCB1 transporter and Toll-like receptor 4 in trabecular meshwork cells. *Mol Vis* 2015;21:201-212.

2. Bhattacharyya S, Kelley K, Melichian DS, et al. Toll-like receptor 4 signaling augments transforming growth factor-beta responses: a novel mechanism for maintaining and amplifying fibrosis in scleroderma. *Am J Pathol* 2013;182:192-205.

3. Seki E, De Minicis S, Osterreicher CH, et al. TLR4 enhances TGF-beta signaling and hepatic fibrosis. *Nat Med* 2007;13:1324-1332.

4. Pulskens WP, Rampanelli E, Teske GJ, et al. TLR4 promotes fibrosis but attenuates tubular damage in progressive renal injury. *J Am Soc Nephrol* 2010;21:1299-1308.

5. Campbell MT, Hile KL, Zhang H, et al. Toll-like receptor 4: a novel signaling pathway during renal fibrogenesis. *J Surg Res* 2011;168:e61-69.

6. Poltorak A, He X, Smirnova I, et al. Defective LPS signaling in C3H/HeJ and C57BL/10ScCr mice: mutations in Tlr4 gene. *Science* 1998;282:2085-2088.

7. Matsunaga N, Tsuchimori N, Matsumoto T, Ii M. TAK-242 (resatorvid), a small-molecule inhibitor of Toll-like receptor (TLR) 4 signaling, binds selectively to TLR4 and interferes with interactions between TLR4 and its adaptor molecules. *Mol Pharmacol* 2011;79:34-41.

8. Poltorak A, He X, Smirnova I, et al. Defective LPS signaling in C3H/HeJ and C57BL/10ScCr mice: mutations in Tlr4 gene. *Science* 1998;282:2085-2088.

9. Bhattacharyya S, Tamaki Z, Wang W, et al. FibronectinEDA promotes chronic cutaneous fibrosis through Toll-like receptor signaling. *Sci Transl Med* 2014;6:232ra250-232ra250.

10. Souza AC, Tsuji T, Baranova IN, et al. TLR4 mutant mice are protected from renal fibrosis and chronic kidney disease progression. *Physiol Rep* 2015;3.

11. Mao W, Liu Y, Wordinger RJ, Clark AF. A magnetic bead-based method for mouse trabecular meshwork cell isolation. *Invest Ophthalmol Vis Sci* 2013;54:3600-3606.

12. Theresa H. Page KSM. Targeting DAMP activation of toll-like receptors: novel pathways to treat rheumatoid arthritis? In: Lemmey A (ed), *Rheumatoid Arthritis - Treatment*: InTech; 2012:211 - 232.

13. Knepper PA, Samples JR, Yue BYJT. Biomarkers of primary open-angle glaucoma. *Expert Rev Ophthalmol* 2010;5:731-742.

14. Lopez-Rovira T, Chalaux E, Rosa JL, Bartrons R, Ventura F. Interaction and functional cooperation of NF-kappa B with Smads. Transcriptional regulation of the junB promoter. *J Biol Chem* 2000;275:28937-28946.

15. Descargues P, Sil AK, Sano Y, et al. IKKalpha is a critical coregulator of a Smad4-independent TGFbeta-Smad2/3 signaling pathway that controls keratinocyte differentiation. *Proc Natl Acad Sci U S A* 2008;105:2487-2492.

16. Brandl M, Seidler B, Haller F, et al. IKK(alpha) controls canonical TGF(ss)-SMAD signaling to regulate genes expressing SNAIL and SLUG during EMT in panc1 cells. *J Cell Sci* 2010;123:4231-4239.

17. Ishinaga H, Jono H, Lim JH, et al. TGF-beta induces p65 acetylation to enhance bacteria-induced NF-kappaB activation. *EMBO J* 2007;26:1150-1162.

18. Arsura M, Panta GR, Bilyeu JD, et al. Transient activation of NF-kappaB through a TAK1/IKK kinase pathway by TGF-beta1 inhibits AP-1/SMAD signaling and apoptosis: implications in liver tumor formation. *Oncogene* 2003;22:412-425.

19. Gingery A, Bradley EW, Pederson L, Ruan M, Horwood NJ, Oursler MJ. TGF-beta coordinately activates TAK1/MEK/AKT/NFkB and SMAD pathways to promote osteoclast survival. *Exp Cell Res* 2008;314:2725-2738.

20. Mao R, Fan Y, Mou Y, Zhang H, Fu S, Yang J. TAK1 lysine 158 is required for TGF-beta-induced TRAF6-mediated Smad-independent IKK/NF-kappaB and JNK/AP-1 activation. *Cell Signal* 2011;23:222-227.

21. Freudlsperger C, Bian Y, Contag Wise S, et al. TGF-beta and NF-kappaB signal pathway cross-talk is mediated through TAK1 and SMAD7 in a subset of head and neck cancers. *Oncogene* 2013;32:1549-1559.

22. Zhang L, Zhou F, Garcia de Vinuesa A, et al. TRAF4 promotes TGF-beta receptor signaling and drives breast cancer metastasis. *Mol Cell* 2013;51:559-572.

23. Wang C, Deng L, Hong M, Akkaraju GR, Inoue J, Chen ZJ. TAK1 is a ubiquitin-dependent kinase of MKK and IKK. *Nature* 2001;412:346-351.

24. Sorrentino A, Thakur N, Grimsby S, et al. The type I TGF-beta receptor engages TRAF6 to activate TAK1 in a receptor kinase-independent manner. *Nat Cell Biol* 2008;10:1199-1207.

25. Xia ZP, Sun L, Chen X, et al. Direct activation of protein kinases by unanchored polyubiquitin chains. *Nature* 2009;461:114-119.

26. Kim HJ, Kim JG, Moon MY, Park SH, Park JB. IkappaB kinase gamma/nuclear factor-kappaB-essential modulator (IKKgamma/NEMO) facilitates RhoA GTPase activation, which, in

turn, activates Rho-associated KINASE (ROCK) to phosphorylate IKKbeta in response to transforming growth factor (TGF)-beta1. *J Biol Chem* 2014;289:1429-1440.

27. Loiarro M, Capolunghi F, Fanto N, et al. Pivotal Advance: Inhibition of MyD88 dimerization and recruitment of IRAK1 and IRAK4 by a novel peptidomimetic compound. *J Leukoc Biol* 2007;82:801-810.

28. Miller SC, Huang R, Sakamuru S, et al. Identification of known drugs that act as inhibitors of NF-kappaB signaling and their mechanism of action. *Biochem Pharmacol* 2010;79:1272-1280.

LIST OF PUBLICATIONS

Humberto Hernandez, J. Cameron Millar, Stacy Curry, Abbot F. Clark, Colleen M. McDowell. BMP and Activin Membrane Bound Inhibitor Regulates the Extracellular Matrix in the Trabecular Meshwork. Submitted: Investigative Ophthalmology & Visual Science (IOVS), submitted 11/2017.

Humberto Hernandez, Wanda Medina-Ortiz, Tomi Luan, Abbot F. Clark, Colleen M. McDowell. "Crosstalk Between Transforming Growth Factor Beta-2 and Toll-Like Receptor 4 in the Trabecular Meshwork". Investigative Ophthalmology & Visual Science March 2017, Vol.58, 1811-1823. doi:10.1167/iovs.16-21331

McDowell CM, **Hernandez H**, Mao W, Clark AF. Gremlin induces ocular hypertension in mice through Smad3-dependent signaling. Investigative Ophthalmology & Visual Science, August 2015, Vol.56, 5485-5492. doi:10.1167/iovs.15-16993

Humberto Hernandez, Caleb Marceau, Hailey Halliday, Julie Callison, Viktoriya Borisevich, Olivier Escaffre, Jeffrey Creech, Heinz Feldmann and Barry Rockx. Development and Characterization of Broadly Cross-reactive Monoclonal Antibodies Against All Known *Ebolavirus* Species. *The Journal of Infectious Diseases*, *212*(Suppl 2), S410–S413. http://doi.org/10.1093/infdis/jiv209

Caleb D. Marceau, Surenga S. Negi, **Humberto Hernandez**, Julie Callison, Andrea Marzi, Viktoria Borisevich, Werner Braun, Jody Berry, Heinz Feldmann, Barry Rockx. Novel

Neutralizing Monoclonal Antibodies Protect Rodents Against Lethal Filovirus Challenges, *Trials in Vaccinology*, 2014, volume 3, 89 – 94. https://doi.org/10.1016/j.trivac.2014.04.002